National Park Service
U.S. Department of the Interior

Natural Resource Stewardship and Science

# Impacts of Fire Management on Carbon Stocks in Yosemite and Sequoia & Kings Canyon National Parks

Natural Resource Technical Report NPS/XXXX/NRTR—20XX/XXX

**ON THIS PAGE**
High severity postfire landscape within Yosemite National Park
Photograph by: Leeland Tarnay

**ON THE COVER**
High elevation vegetation as viewed from Mt Hoffman in Yosemite National Park
Photograph by: Leeland Tarnay

# Impacts of Fire Management on Carbon Stocks in Yosemite and Sequoia & Kings Canyon National Parks

Natural Resource Technical Report NPS/XXXX/NRTR—20XX/XXX

John R. Matchett[1], Jamea A. Lutz[2], Leland W. Tarnay[3], Douglas G. Smith[3], Kendall M.L. Becker[2], and Matthew L. Brooks[1]

[1] U.S. Geological Survey
Western Ecological Research Center
Yosemite Field Station
40298 Junction Dr, Suite A
Oakhurst, CA 93644

[2] Utah State University
Wildland Resources
5230 Old Main Hill
Logan, UT 84322-5230

[3]National Park Service
Yosemite National Park
5083 Foresta Road
El Portal, CA 95318

December 2013

U.S. Department of the Interior
National Park Service
Natural Resource Stewardship and Science
Fort Collins, Colorado

The National Park Service, Natural Resource Stewardship and Science office in Fort Collins, Colorado, publishes a range of reports that address natural resource topics. These reports are of interest and applicability to a broad audience in the National Park Service and others in natural resource management, including scientists, conservation and environmental constituencies, and the public.

The Natural Resource Technical Report Series is used to disseminate results of scientific studies in the physical, biological, and social sciences for both the advancement of science and the achievement of the National Park Service mission. The series provides contributors with a forum for displaying comprehensive data that are often deleted from journals because of page limitations.

All manuscripts in the series receive the appropriate level of peer review to ensure that the information is scientifically credible, technically accurate, appropriately written for the intended audience, and designed and published in a professional manner.

Views, statements, findings, conclusions, recommendations, and data in this report do not necessarily reflect views and policies of the National Park Service, U.S. Department of the Interior. Mention of trade names or commercial products does not constitute endorsement or recommendation for use by the U.S. Government.

This report is available in digital format from Yosemite and Sequoia & Kings Canyon National Parks, and the Natural Resource Publications Management website (http://www.nature.nps.gov/publications/nrpm/). To receive this report in a format optimized for screen readers, please email irma@nps.gov.

Please cite this publication as: Matchett, J.R., J.A. Lutz, L.W. Tarnay, D.G. Smith, K.M.L. Becker, and M.L. Brooks. 2013. Impacts of Fire Management on Carbon Stocks in Yosemite and Sequoia & Kings Canyon National Parks. Natural Resource Technical Report NPS/XXXX/NRTR—20XX/XXX. National Park Service, Fort Collins, Colorado.

# Contents

# Figures

Page

# Tables

Page

# Appendices

Page

# Abstract/Executive Summary

Forest biomass on Sierra Nevada landscapes constitutes one of the largest carbon stocks in the state of California and the stability of that carbon stock is tightly linked to fire and the ecological factors that drive the fire regime. Recent research suggests that over a century of fire suppression, fuel accumulation, and the reintroduction of fire in Sierra Nevada forests have reduced the amount of carbon that such suppressed landscapes store, while increasing the likelihood of catastrophic, stand-replacing fire. For over 30 years, fire management at Yosemite (YOSE) and Sequoia & Kings Canyon (SEKI) National Parks has led the nation in restoring fire to park landscapes, however the impacts of that restoration on the stability and magnitude of carbon stocks are not yet known.

The purpose of this project was to examine the effects of fire on carbon stocks in these two parks. Our approach to this question was focused on evaluating the effect of fire on the: 1) amount of above-ground carbon on the landscape (limited to trees and standing snags); and 2) rate of carbon accumulation by individual trees. In 2010, we were successful in designing and planning the plot work, and building the foundational database for this analysis through an interagency agreement with U.S. Geological Survey and through a CESU agreement with University of Washington. In 2011, we hired and trained the field crew and acquired the plot data, including tree core specimens, from the 117 out of 200 target plots. In 2012, we completed the interpretive component and began the analyses of the plot data. In 2013, processing of tree cores began (at Utah State University, due to the move of investigators Lutz and Becker). In 2014, final processing of tree cores, data analyses, and manuscript preparation will be completed for objectives 1 and 2. This final report addresses and maps the quantitative amount and stability of tree carbon stocks relative to fire for both YOSE and SEKI. This research became the seed for a much larger effort that will continue to lead to results beyond those outlined in the original proposal.

Examining carbon densities across the landscape in burned vs. unburned areas, our analysis of the effect of fire history on carbon densities showed no significant difference (at the 95% confidence level) between burned and unburned plots in the areas sampled (15-16 years post-fire in most plots), though there was a non-significant tendency toward lower carbon in some vegetation types, especially red fir.

In order to quantify carbon and the potential difference between burned and unburned areas in these parks, we had to account for all sources of error and propagate that error as we summed carbon densities across various landscape strata. Using Monte Carlo simulation methods, we found that mapping uncertainty was the largest source of uncertainty, while measurement uncertainties arising from using general allometry were relatively small. For managers, this report presents a map of carbon that incorporates these uncertainties, and a recommended method for propagating these uncertainties across selected areas of management interest.

To illustrate the utility of this map for looking at areas of management interest, our report uses this tool to look not only the total amount of tree carbon in YOSE (25 Tg C) and SEKI (19 Tg C), but also look at the amount of carbon in different vegetation types (red fir and sugar pine –white fir dominated forest comprise the bulk of the carbon stocks in both parks) and (in YOSE only) how

much carbon is in areas of varying degrees of "departure" from historic fire return intervals as a proxy for the stability of our carbon stocks. For YOSE, about 10 out of the 25 Tg C (mostly red fir, Jeffrey pine, and western white pine) is relatively "secure" in low risk areas, another ~10 Tg (mostly red fir and western white pine) lies in areas that have missed two fire return intervals, with the rest of the C (largely ponderosa pine and white fir – sugar pine) in higher risk areas that have missed 9 or more fire return intervals.

Finally, we compare these results to remotely sensed carbon (NASA-CASA, http://geo.arc.nasa.gov/sge/casa/) and find that, accounting for likely biases and uncertainties in our plot-based estimates, the two methods roughly agree. Our analysis and intercomparisons clearly show however that accounting for fire severity within fire perimeters should be part of any future effort to map and quantify the effects of fire across landscapes. We illustrate the potential importance of this with an example using the 2013 Rim Fire, which burned an area containing over 5 Tg C, but likely left a large fraction of that C on the landscape if one accounts for fire severity.

## Acknowledgments

Funding was provided by the National Park Service, Climate Change Adaptation Program, the National Park Service Fire and Aviation Management Research Fund, and the U.S. Geological Survey, Terrestrial, Freshwater, and Marine Ecosystems Program. Remotely sensed data on carbon stocks was provided by Chris Potter with the NASA-CASA program (http://geo.arc.nasa.gov/sge/casa/). Any use of trade, product, or firm names is for descriptive purposes only and does not imply endorsement by the U.S. Government.

# Introduction

The distribution and abundance of carbon sequestered on the landscapes of western North America is of crucial importance to land management issues relating to fire (Hurteau and Brooks 2011) and climate (Swann et al. 2012). Rates of carbon sequestration are also fundamental to global gradients of productivity (Chisholm et al. 2013). However, detailed estimates of carbon have many sources of variation that are difficult to quantify for any particular landscape. In the Sierra Nevada, the heterogeneity of carbon across landscapes arises from virtually every ecological process: the species present (Lutz et al. 2010), the productivity gradient (Larson et al. 2008), the history and magnitude of fire and wind (van Wagtendonk and Lutz 2007, Lutz and Halpern 2006, Lutz et al. 2011, North et al. 2007), fuels treatment and management (Hurteau and North 2009), dispersal and post-disturbance forest development (Halpern and Lutz 2013), and the effects of insects and pathogens. Of these processes, fire is perhaps the most fundamental and defining ecosystem process in the Sierra Nevada.

Fire, whether ignited naturally or by fire managers, is indispensable to park managers seeking to promote desirable composition, structure, and function of forests within Yosemite (YOSE) and Sequoia and Kings Canyon (SEKI) National Parks. Fire exclusion, starting 150 years ago, and becoming very effective since the early 1900s (van Wagtendonk 2007), has altered fuel structure, fire behavior, and fire regimes in ways that increase risk to human life and infrastructure, natural and cultural resources, watershed function, tourism, and local economies. The specific changes at the heart of the problem is a shift from low- to mixed-severity fires with short return intervals (Scholl and Taylor 2010) to altered fire regimes in which high severity catastrophic crown fires are more common (either with greater areas burned at high severity or larger size of high-severity patches). During the past three decades fire has been systematically reintroduced into the fire-adapted forests of YOSE and SEKI, either by allowing naturally-ignited fires to burn under prescribed conditions (i.e. wildand fire use fires) or by management-ignited fires (i.e. prescribed fires). The general objectives of these managed fires are to: (1) reduce surface and ladder fuels, (2) minimize the risk of crown fire, and (3) restore historic pre-suppression era fire regimes, and thereby (4) increase the resilience of forests to projected climate changes (e.g. Miller et al. 2012). In the lower montane forests of the Sierra Nevada where much of the carbon is sequestered, the focus in the National Parks has been on increasing fire frequency, increasing overall landscape heterogeneity in burned areas (Hessburg et al. 2005) and restoring other pre-suppression era fuels and fire regime characteristics.

Although fire is an important factor in the carbon dynamics of forests, the effect of restored versus altered fire regimes on carbon stocks has not been previously evaluated. Although fires release large amounts of greenhouse gases from forest biomass – either immediately through combustion or over time, as dead trees decompose – there is always some degree of postfire vegetation regrowth that assimilates carbon back into sequestered biomass (Hurteau and Brooks 2011). The net change of carbon contained in vegetation on the landscape relative to pre-fire levels depends on the time since burning, fire severity, and the type of vegetation that grows back (Hurteau 2013). The time it takes for a forest to develop following a high severity wildfire can be several centuries, but fires that burn at lower severities may be able to replace biomass lost to fire in decadal timescales. The differing productivities of forests and their attendant regrowth rates (Larson et al. 2008), coupled with the

characteristic fire return interval of each forest type, make it difficult to determine the conditions under which fires result in a net emission or assimilation of carbon at decadal and sub-decadal timescales. At broader spatial scales and multidecadal timescales, recent research has shown that frequent fire appears to select for forest stands that are less dense, and contain larger diameter trees that store a greater volume of carbon per unit land area than the stands they replace (Fellows and Goulden, 2008). In the lower elevation forests of YOSE, higher severity fire may be associated with the loss of large-diameter trees, whereas low- and moderate-severity fires do not cause noticeable declines in large-diameter tree density (Collins et al. 2011, Lutz et al. 2009). In addition, forests with larger diameter trees of fire resistant species have complex structure which often includes a high height-to-live-crown, making them less susceptible to catastrophic stand replacing crown fires, and thus promoting long-term carbon storage (Hurteau et al. 2008).

In 2006, California passed the Global Warming Solutions Act (AB 32), mandating that emissions of statewide greenhouse gases be reduced to 1990 emission levels. The California Air Resources Board was charged with developing and implementing a methodology for quantifying and monitoring these greenhouse gas emissions from the different emission "sectors" in California, including the forestry sector. The immediate contribution of emissions from individual fire events to this sector can approach magnitudes equivalent to total annual emissions of medium to large cities in the case of the largest wildfires, leading to the perception that they are significant threats to the carbon sequestration capacity of the landscape. Even though this view only accounts for immediate and short-term fire effects, it still leads to the possibility that the use of fire as a management tool to restore fire regimes may be significantly curtailed in the future if regulations are implemented to limit the conversion of carbon from terrestrial to atmospheric pools during fire events. However, if limiting the use of fire to restore pre-suppression era fire regimes leads to lower and/or more unstable forest carbon stocks, such regulations may be ultimately counterproductive for carbon management.

A more comprehensive and realistic view of fire effects on carbon in the forestry sector requires that the initial loss from the forest must be balanced with longer-term dynamics which could actually result in net gains in carbon stocks depending on if the same amounts and types of biomass grow back post-fire (Hurteau and Brooks 2011, Hurteau 2013). Because forest regrowth can take decades to centuries, it is difficult to determine whether fires cause a net loss or gain of carbon in terrestrial pools over these longer timescales. Ultimately, the energy balance of the planet depends on how much carbon dioxide accumulates in the atmosphere over time. Year-to-year variations in annual emission budgets at small spatial scales (relative to the vegetated area of the planet) thus matter less than net accumulation of CO2 and other greenhouse gases over decades, and any permanent diminishment of the amount and stability of carbons stocks in fire-adapted forest ecosystems in the Sierra Nevada has the potential to exceed sequestration gains made in other sectors by orders of magnitude. Protection of characteristic ecosystem composition, structure, and carbon sequestration, to the extent possible, of these potentially volatile and sensitive carbon pools must therefore be a high priority for and comprehensive strategy to lessen the accumulation of greenhouse gas emissions in the atmosphere.

## Objectives

The objectives of this project were to evaluate the effects of four decades of restored fire on the: 1) amount and stability of above-ground carbon on the landscape (limited to trees and standing snags); and 2) rate of carbon assimilation by individual burned and unburned trees.

## Approach and Scope/Limitations

This work focuses on standing live and dead tree carbon exclusively. Shrubs were excluded because there are very few allometric equations available in the literature and most are relate biomass to cover (e.g. McGinnis et al. 2010) which are much weaker biomass indicators than other metrics such as basal stem diameter (e.g. Halpern and Lutz 2013, Lutz et al submitted). Existing allometric equations relating shrub cover to biomass are also predominantly from lower elevation chaparral ecosystems (McGinnis et al. 2010), which are not characteristic of the predominantly forested systems examined in this study. Since cover rather than basal stem diameter was included in the existing datasets used in this study, we could not estimate shrub carbon. However, shrub carbon usually accounts for a relatively small fraction of total aboveground carbon on landscapes dominated by trees – in intact late successional forests of the Sierra Nevada lower mixed conifer, shrub biomass is approximately 1% of ecosystem biomass (Lutz et al. 2012), and in early seral systems (those responding to catastrophic disturbance – a rarity in the study area), shrub biomass declines from about 1/3 of total biomass 20 years after stand-initiating disturbance to about 6% of total biomass 40 years after stand-initiating disturbance (Halpern and Lutz 2013)

Belowground carbon was excluded primarily because there are insufficient studies of total carbon in late-successional systems, especially those with large-diameter trees. And, although fire removes large roots from previously dead trees and volatilizes some surface carbon, below-ground stores of carbon are less changeable in response to fire than aboveground carbon. We acknowledge the importance of below-ground carbon stocks and the need for further research in this area.

We determined that the first step to understanding carbon dynamics and the interaction of fire was to evaluate above-ground dynamics. We plan to then leverage our existing plots associated with above-ground carbon estimates and pair them with below-ground carbon measurements as part of a future study.

We addressed objective 1 using existing and new vegetation plot data and precise vegetation mapping data combined with a comprehensive review and selection of allometric equations to estimate carbon amounts. We also quantified the uncertainty in carbon estimates that remain after applying the best available science to the carbon estimation, and to suggest areas of further research that would minimize the uncertainty in carbon estimates. After creating a carbon map for YOSE and SEKI, we overlaid fire return interval departure (FRID) maps to evaluate the current stability of the carbons stocks. Data collection and initial analyses are completed for objective 1, and the methods and initial results are presented and discussed in this report. Additional analyses were in progress at the time of this report and will be included in one of the journal manuscripts that will be created for this objective.

We are addressing objective 2 using tree cores and dendrochronological methods to document tree growth patterns and rates of carbon assimilation for the five years before and after fires of low- to moderate-severity. Data collection is complete but some cores still remain to be analyzed. Thus, the methods and results for the Objective 2 will be presented and discussed in a future manuscript for this objective.

# Methods

### Dataset for Objective 1

We compiled a dataset of ground-based tree measurements using existing vegetation project databases throughout the parks. These projects included data collected for natural resource inventories (Peggy Moore, Ecologist, USGS Yosemite Field Station and Sylvia Haultain, Plant Ecologist, Sequoia/Kings Canyon National Park personal communications), vegetation mapping (Keeler-Wolf and Moore 2012; Sylvia Haultain, Plant Ecologist, Sequoia/Kings Canyon National Park personal communication), fire effects monitoring (Gus Smith, Fire Ecologist, Yosemite National Park and Tony Caprio, Fire Ecologist, Sequoia/Kings Canyon National Park personal communications), fuels studies (van Wagtendonk and Moore 2010), one 25.6 ha Smithsonian-affiliated demography plot (Lutz et al. 2012, 2013) and plots established for this project. Plots within forested vegetation types were primarily 0.1 ha in size, within which tree species and diameter at breast height (DBH) were recorded. Our compiled dataset consisted of 2590 total plots, with 1646 plots within forested vegetation types that were used in our analysis (Table 1). The years of plot measurements ranged from 1982 to 2011.

Plots were assigned forest types developed based on a combination of fire regime and tree morphology. Although the number of plots in the study was large (2,231), the number of individually mapped vegetation polygons and community types were many times higher (Aerial Information Systems 2007, Keeler-Wolf et al. 2012). Therefore, we combined named community types so that there would be sufficient numbers of plots in each type to develop meaningful carbon densities for each vegetation type. For example, high elevation woodlands comprise a considerable area of both parks, but have a generally low carbon density, very infrequent fire return interval, and characteristic tree morphology (short, conic boles). Based on the similarity of tree morphology (i.e., Sierra Juniper, whitebark pine, mountain hemlock), and therefore carbon content, and infrequent fire return interval, we used a single “carbon/fire type” for these vegetation communities (Appendix A). These forest types are an aggregation of more specific vegetation types developed by the park vegetation mapping efforts, so we consolidated the originally mapped types to our summary forest types and assigned plots forest types by spatially intersecting their locations with the vegetation maps. We inspected the assigned forest types and species composition of the plots, and it was clear that in some cases there were incorrect assignments, presumably because plot geographic coordinates were incorrect or the map polygon was incorrectly classified. In these cases, we conducted a k-means clustering of plots using their tree species composition, and then assigned the resulting clusters to our summary forest types. We looked for mismatches between the mapped-based and cluster-based forest types, and when found, manually assessed the species composition of those plots and assigned them to the appropriate forest type.

## Allometric Equations for Objective 1

For calculating tree biomass, we compiled a set of allometric equations developed by prior studies (see Jenkins et al. 2004 and references therein)). For each tree species, we examined all the allometric equations listed by Jenkins et al. (2004). We consulted the original source manuscripts for the equations and when selecting the most appropriate equation(s), we considered the geography of the original study, tree age range (where reported), tree diameter range, site productivity, site climate, and sample size. When available, we used species-specific equations from studies geographically closest to our study region (e.g. Westman 1998 for Abies). None of the allometric equations were developed from trees within the parks. If a species-specific equation wasn't available, we chose an equation from a species with a similar growth form or used one of the generalized equations developed by Jenkins et al. (2003). However, in many cases, particularly the high elevation woodlands (above), the Jenkins et al. (2003) generalized equations were not appropriate because of the reduced morphology of high elevation individuals of Pinus and Tsuga. In many cases, the diameter range of trees used to develop an equation did not extend throughout the diameter range of trees in our dataset. Yosemite and Sequoia & Kings Canyon National Parks contain the largest (or nearly so) individuals of Pinus ponderosa, Pinus lambertiana, Abies concolor, Abies magnifica, and Sequoiadendron giganteum (Van Pelt 2001), and because destructive sampling is generally enjoined in the parks, allometric equations of large enough diameter do not exist. Additionally, because of the high productivity of portions of the parks, many other individual trees found in the study plots exceed the diameters for their species-specific equation in Jenkins et al. (2004). For these situations we created blended equations using the species-specific equations over the diameter range of trees from which the equation was developed and equations from similar species and growth forms that covered the necessary diameter range. Appendix B provides a detailed listing of equations used for each species.

All equations were of the form ln(biomass) = a + b * ln(DBH), with biomass expressed in kg, DBH in cm, and ln being the natural logarithm. Each equation included the standard error of the estimate (SEE), which is the standard deviation of the normally-distributed error around the predicted biomass while expressed on a log scale, and can be used to calculate a bias correction factor, which can be used when exponentiating the log-scaled biomass to an arithmetic value. Tree carbon mass was assumed to be 50% of biomass based on the proportion of carbon found in cellulose, hemicellulose, and lignin, but without regard for the various proportions of carbon present in species-specific complex organic compounds (e.g. polyphenols and extractives).

## Field Data Collection for Objective 1

To supplement the pre-existing plot data, we established 105, 0.1 ha circular plots (Figure 1.) in YOSE (67 plots) and SEKI (48 plots). These plots were stratified by five different vegetation cover types (Abies concolor-Pinus lambertiana; ABCO, Abies magnifica; ABMA, Pinus contorta; PICO, Pinus Jeffreyi; PIJE, Pinus ponderosa; PIPO) and fire history (burned or unburned in recorded history; Table 2). Plots were selected from adjacent portions of the forests that had been burned and unburned in an attempt to control for local variation more systematically than was possible with the existing database of plots. Additionally, plots were positioned within at least 50 m inside the mapped boundary of the intended forest type and burn patch, on slopes between 0° and 35°, and were situated at least 100 m from roads, streams, and trails. Upon arriving at site, field crews assessed intended

forest type and burn status, and relocated the plot if it did not meet the intended specifications. Plots were also relocated if a minimum of 10 trees > 8 cm diameter at breast height (dbh, 1.37 m) were not contained with 46.5 m of plot center.

Field crews visited plots between June and September 2011. Position of the plot center (GPS, NAD 83, taken with consumer-grade Garmin receivers), slope, aspect, topographic position (slope position: null, low, mid, upper slope; Level position: null, low, mid, or high level; Hydrology: null, interfluvial, channel, wall, basin floor) and slope configuration (convex vs. concave) were recorded for each plot for later fire behavior analysis. Additionally, two plot photos (north and south view) and panoramic video were taken from plot center of the view surrounding the plot by rotating a video camera on a monopod.

To verify forest type of each plot field crews recorded percentage of canopy cover by species for each quadrant of the plot based on ocular estimates. Field crews also recorded percentage cover by shrub species that occupied ≥ 1% of one quadrant of the plot. The percentages of tree and shrub cover were averaged for the four quadrants to produce one value of percent cover by each species. Overlapping canopies were counted as if there was no overlap so percent cover values could exceed 100%.

To measure species composition and structure of each plot, field crews recorded species and dbh of all live trees and snags > 15.0 cm at breast height. Species and dbh were recorded for live trees and snags with dbh values between 2.5 cm and 15.0 cm in at least one quadrant of the plot. Slope-corrected, species specific estimates of live tree and snag basal area and stems/ha were generated from these data.

## Analyses for Objective 1

### *Density and Total Carbon*

We estimated tree carbon density (kg C / m2) and total carbon (Tg C) for each forest type within each park. Our definition of trees included living trees and standing snags. In addition to the typical uncertainty in estimated statistical parameters arising from sampling a population, we also explored the influence of various other measurement errors on carbon estimates and their uncertainties. These measurements errors included repeatability in tree diameter measurements, uncertainties in allometric equation diameter–biomass relationships, and classification accuracies in vegetation maps. We developed a Monte Carlo simulation which repeatedly calculated carbon densities and total carbon while taking into account those uncertainties. For tree diameter, a normally-distributed error with mean 0 and standard deviation 0.027 (based on the RMSE of duplicated tree diameter measurements reported by Gonzalez et al. [2010]) was added to each tree DBH measurement. Tree biomass was calculated using the assigned allometric equations and a normally-distributed error with mean 0 and standard deviation equal to the equation's standard error of the estimate (SEE) was added (while biomass was on a log scale). Typically, when making a single prediction using a log-log equation, a bias correction is added to the value so that when it is exponentiated it is closer the arithmetic mean (the arithmetic values tend to be log-normally distributed and exponentiating the log value without bias correction will place the prediction closer to the distribution's median; Baskerville 1971). However, during a Monte Carlo simulation, the distribution of multiple arithmetic predictions will realize the log-normal distribution, so a bias correction is not needed. Log-scaled tree biomass values

were exponentiated, summed within a plot, and divided by the plot area to produce a carbon density value (kg C / m2). A bootstrapped sample (a random sample with replacement equal in size to the original sample) of all plots was taken in order to incorporate uncertainty from statistical sampling. We then fit a linear regression model to predict carbon density (log + 1 transformed) using forest type, forest canopy cover class, and their interaction as explanatory variables. Forest canopy cover classes were taken from the forest type maps, where each mapped polygon had been assigned a canopy cover class during photo interpretation. Three forest types (Douglas-fir Forest, Foothill Pine Woodland, and Western White Pine Woodland) did not have enough plots across a range of canopy covers, so their carbon estimates are a simple mean. These steps for predicting carbon densities utilized plots pooled across all parks.

We used the park vegetation maps to calculate the total areas for each combination of forest type and canopy cover class. To take into account uncertainties in vegetation mapping, we used the accuracy assessment matrices to generate uncertainties in forest type areas. The assigned to each polygon was randomly assigned using the numbers of ground-based truthing plots as weights. For example, if a particular vegetation type had 100 ground-based accuracy assessment plots with 70 determined to be the correctly classified type, 20 determined to be another type, and 10 determined to be a third type, , then the probabilities of vegetation type assignment for that polygon were randomly assigned to the three types base on the proportions 0.7, 0.2, and 0.1, respectively. If a vegetation type had four or fewer accuracy assessment plots, we did not randomly reassign types. We then cross-walked the polygon vegetation types to our forest types, summed the total areas for each combination of forest type and canopy cover class, and multiplied by the predicted carbon densities to produce estimates of total carbon (Tg C). These steps were done separately for each park, including using the park-specific accuracy assessment matrix (Keeler-Wolf and Moore 2012, Aerial Information Systems 2007), in order to produce park-specific carbon estimates. Estimates of mean carbon densities for individual forest types (without regards to canopy cover) were calculated by taking a weighted average of the canopy cover class-specific estimates, with the weights equal to the total area of each canopy cover class.

We also explored simplifying the incorporation of allometric equation errors. Since individual trees within a plot are summed together to calculate carbon density, individual tree errors can also be summed together to produce a plot-level error. However, tree biomass errors are expressed, and normally distributed about the prediction, while on a log-scale, however the following equation (Baskerville 1971) can be used for approximating the error on an arithmetic scale: sqrt(exp(2 * SEE ^ 2 + 2 * ln(biomass)) - exp(SEE ^ 2 + 2 * log(biomass))), where SEE is the standard error of the estimate for the log-log allometric equation and biomass is the computed biomass in arithmetic units. There are then two options for summing the resulting tree errors: a simple sum and a sum in quadrature (the square root of the sum of squared errors). If errors are assumed to be random and independent of each other, then summing in quadrature is appropriate, whereas the simple sum is a more conservative approach if independence cannot be assumed. Tree errors within a plot are likely dependent, for example a tree with a smaller-than-predicted bole biomass likely has smaller-than-predicted branch and leaf biomasses; or, tree biomasses in a plot might be higher than predicted if wood density tends to be greater due to slower growth at a low-productivity site. More importantly,

the allometric equations we used were developed from tree sub-populations outside the parks (sometimes a from a considerable distance away), and it is very likely that the tree morphologies differ between the sample location and the parks, forming a consistent (but unknown) bias in the allometric equations. In these situations, tree biomass was calculated using a bias correction factor since only a single prediction is being made. The benefit of using plot-level errors is that in each Monte Carlo realization random errors need only be generated for thousands of plots as opposed to hundreds of thousands, greatly reducing computation time.

Carbon density and total carbon estimates, plus their standard errors and 95% confidence intervals, were based on the means, standard deviations, and 2.5 and 97.5 percentiles of the distributions from a Monte Carlo simulation of 10,000 realizations. The simulations were programmed in R (R Core Team 2013, http://www.R-project.org), graphs developed using ggplot (Wickham 2009) and base R graphics packages, spatial data managed using PostGIS (PostGIS Development Team 2013, http://postgis.net), and maps produced using Quantum GIS (Quantum GIS Development Team 2013, http://qgis.osgeo.org).

### *Fire History and Carbon Density*

We investigated the influence of fire history on carbon density for those forest types that experience regular, natural wildfire and for which we had sufficient sample sizes—specifically, red fir, white fir – sugar pine, ponderosa pine, Jeffrey pine, and lodgepole pine forests. As an initial analysis, we intersected plots within those forest types with fire history polygon data (ca. 1920 to present) from each park and derived three fire history metrics for each plot: 1) burned vs. unburned, 2) years since the last fire, and 3) number of times burned. For plots without a recorded history of fire, we set years since last fire to 100. We assessed if any of those burn metrics were related to forest type carbon density by developing a set of statistical models and comparing them using an information-theoretic approach. We defined seven candidate models: one model having just forest type as an explanatory variable, and six others that included one of the three burn history metrics either in addition to or interacting with forest type as explanatory variables (see Table 3 in Results and Discusssion). Carbon density (log + 1 transformed) was the response variable. Model AIC scores (adjusted for sample size) were used to compare the predictive performances of the candidate models. A summary of plots, by vegetation type for this dataset is in Table 1.

Burn severity has been examined as both an independent predictor and a co-variate, but at the time of this report, those analyses were still in progress (to be published in Becker, K.M.L., Smith, D.G., and Lutz, J.A. In prep. Trends and variability in the effects of fire on forest structure in the Sierra Nevada). Given the limited number of plots and range of fire severity within each vegetation type, preliminary results do not point to a large and statistically significant effect of low- to moderate-severity fire. Although current fire policy is based just on acres burned, the objectives for individual fires often include details regarding severity. The results presented in the current report therefore focus on the burned/unburned alternatives on which policy is currently based, and whether that metric provides any useful information on the effects of fire on carbon stocks. The work still in progress will help bound the effects of lower severity fire on forest composition and structure.

To evaluate the relative stability of the carbon stock in the two parks we overlaid the carbon density map with FRID maps. We then calculated the amount of carbon within each forest type occurring within various FRID levels (number of fire return intervals missed).

#### *Comparison with Other Carbon Accounting Efforts*

Carbon estimation has been examined with a multitude of techniques. Most however focus on larger scales (tens of thousands of square km) and lower resolution (e.g., USGS Carbon Map (Matt/JR?); CEC, 2007) than is useful at the scale of most fires and for decision support by fire/land managers; while other studies focus on the local environment, providing data on specific forest types local to the area (1-10 ha) measured at the site in question (e.g., Lutz et al., 2012, Gonzalez et al., 2010)[c] , but limited applicability at larger scales without an elaborate mapping analysis to reconcile mapping uncertainty. Both types of studies represent static estimates of carbon, and so become less accurate as trees sequester more carbon or die, releasing carbon. Temporal reconciliation accounting for the effects of subsequent disturbance and carbon accumulation can be problematic as well. Since our work was targeted exactly at the scale of most interest to National Park land managers spatially, we would need to reconcile plot estimates ranging from very recent (1-2 years old) to older (10-15 years old) with current conditions to fully support management decisions across polygons 100s of hectares in size.

Recently the NASA-CASA (http://geo.arc.nasa.gov/sge/casa/) program has developed a 250m resolution, California-wide product that applies remotely sensed (MODIS-based) NPP values to baseline stocks set for regional values (Pan et al., beginning in 2000), and brings those carbon values forward temporally to the present day, using a regional scheme for carbon accumulation rates tied to MODIS-observed greenness (Potter, 2010). We used and evaluated these statewide carbon estimates and also compared carbon values over the area of the Yosemite landscape. Further, we use our plot based carbon estimates to evaluate the potential inaccuracies of the CASA method for accounting for carbon stock reductions caused by fires. Finally, we plan to incorporate future results related to carbon accumulation stemming from the tree core collected during this project, so that carbon accumulation rates can be refined more precisely based on measurements from the ground.

# Results and Discussion

### Error Propagation and Sources of Uncertainty

Estimates of carbon rely on plot-based tree allometries linking dbh (diameter at breast height) to biomass measurements and scaling them up the landscape level. There are uncertainties associated with every step in these measurement and scaling processes. Tree inventories are converted to areal estimates of carbon using allometric equations for a given forest type, and landscape level values are calculated based on the distribution of those forest types. It is therefore just as important to understand the aggregate uncertainties involved with the estimates of carbon as it is to understand their “mean” values. Specifically, there are five potentially large sources of error associated with this process of estimating carbon on large landscapes.

1. Uncertainty embedded within allometric equations

The existing tree allometric equations themselves have error associated with them because they are typically derived from a small number of trees (usually <25, but often <10; Jenkins et al. 2004). These small sample sizes relative to the variation in dbh/biomass relationships result in considerable standard errors of typically 10% to 30% through the range of tree diameters used to develop them.

2. Site-specific tree morphology

Site-specific tree morphologies are not constant and trees sampled for allometric equations are usually gathered from one limited portion of the species range. When equations generated within one biophysical context are applied elsewhere, differences in site productivity, disturbances, climate, and land use histories can yield errors due to different morphologies of the sampled and target populations.

3. Lack of equations for large-diameter trees

Growth rates of trees vary over time and the range of tree sizes used to develop allometric equations should conservatively define the range of tree sizes they are applied to. The paucity of large diameter trees in the development of most allometric equations (very few contain trees > 100 cm dbh) is especially problematic since most carbon Sierra Nevada forests is contained in these large trees (Lutz et al. 2012). As a result, the biomass of large-diameter trees must be estimated from those few proxy species that have been sampled at large diameters. The problem of accurately calculating the biomass of large-diameter trees is magnified by their more complex and variable crown architecture compared to smaller trees (Sillett and Van Pelt 2007, Van Pelt and Sillett 2008). In areas where large-diameter trees constitute a large proportion of the tree population (for example where smaller trees are routinely eliminated by fire), or in areas where species reach maximum sizes much greater than any previously dissected, biomass estimates could potentially have large uncertainties.

4. Landscape heterogeneity

Landscapes are heterogeneous containing gradients of biophysical conditions (particularly relating to the site water balance) that can affect dbh/biomass relationships. To be accurate, landscape level estimates of carbon must be based on a sufficient number and distribution of plots to capture the range of these conditions.

5. Vegetation type mapping error

The vegetation maps used to scale up carbon estimates for forest types contain their own degree of error associated with vegetation cover assignment. Georeferencing uncertainties between plot locations (e.g. poor plot location information from older GPS units, difficult topography, or multipath GPS reception cause by high tree density) and vegetation cover polygons (e.g. from poor aerial photograph georectification, incorrect vegetation type identification, or polygon edge error during data input) can add further error.

We evaluated the relative contribution of these five sources of error, and found that in general uncertainties associated with repeated measurements of tree diameters and choice of diameter–

biomass allometric relationships had very little effect on the standard errors and confidence intervals of tree carbon density and total carbon estimates (however, better allometric equations constructed from dissections of large numbers of individual trees would improve uncertainties considerably). The widths of the 95% confidence intervals for total carbon in several major forest types within both parks differed only slightly among the different methods of accounting for allometry error (Figure 2). The typical uncertainty arising from sampling a population—especially a very heterogeneous one—appears much more important for our dataset.

Forest type classification uncertainties, however, were the most important determinant of carbon uncertainty. We observed that Monte Carlo-estimated areas differed from observed mapped-based areas for several forest types. For example, a single summation of red fir forest polygons from Yosemite's vegetation map yields 41,315 ha, while the Monte Carlo estimate is ~13% lower at 36,052 ha (95% confidence interval: 34,655 – 37,723), suggesting that this forest type is currently over-mapped. Other forest types appear to be under-mapped, for example the high woodland type, which occurs on 26,602 ha in Yosemite according to the vegetation map, while the Monte Carlo estimate is ~9% higher at 28,995 ha (95% confidence interval: 28,307 – 29,953). These differences in area estimates noticeably affected total carbon estimates for some forest types, and usually widened the total carbon confidence intervals (Figure 2), although can also narrow the confidence intervals in some types—for example red fir—because the reduction in total area of the type leads to lower total carbon and confidence intervals generally become more narrow as the estimate gets smaller.

Given these responses, the Monte Carlo simulation used to produce the carbon estimates throughout the remainder of this report used the 'plot error simple sum' method to propagate error and incorporate allometric uncertainty (mainly as a conservative approach, because this method tended to produce the widest 95% confidence intervals) and incorporated the vegetation mapping uncertainty. A bootstrapped sample of plots was taken in each Monte Carlo realization to incorporate sampling uncertainty.

### Total Tree Carbon on the YOSE and SEKI Landscapes

Accounting for the uncertainty as described above, we calculate that the amount of tree carbon for the YOSE landscape total was 25 Tg (95% CI, 23-27 Tg) and for SEKI was 20 Tg C (95% CI, 18-21 Tg) (Figure 3), which is about 4.1% of the total standing carbon estimated in the Sierra Nevada (Potter, 2010). Over the area (YOSE has an area of 3,052 km2 and SEKI has an area 3,503 km2) of both parks, the range of aboveground tree carbon is at least 41-48 Tg C (mean of 45 Tg C), which is nearly 10% of the total standing wood in the Sierra Nevada, in about the same percentage of the total area of the Sierra Nevada (the carbon density of forested area is therefore higher in the parks owing to the very large areas of high-elevation with little to no carbon). Carbon densities for tree carbon varied from a low of nearly 0 kg C / m2 in shrub vegetation types to over 55 kg C m2 in the Giant Sequoia vegetation type (Figure 4).

Though the carbon densities for the respective vegetation types were very similar between parks (Figure 4), one of the biggest differences between the respective parks was the spatial extent of these vegetation types, which leads to these vegetation types accounting for different proportions of the total park carbon stock. For example, in SEKI, the namesake giant sequoias alone account for 1.8-3.5

Tg C, or 10-17% of the total park tree carbon. In YOSE, the Sequoia vegetation type only accounts for 0.2-0.4% of the total park tree carbon. The Red Fir forest type accounted for nearly ⅓ of the total tree carbon in both parks (32-36% in SEKI; 37-42% in YOSE), with YOSE (8.8-11.5 Tg C) having nearly double the amount of carbon in its Red Fir than SEKI (5.7-7.6 Tg C). White Fir - Sugar Pine Forest for both parks accounted for about 19-22% of their respective tree carbon (3.5-4.7 Tg C for SEKI; 4.4-5.7 Tg C for YOSE).

Here we should note a fundamental uncertainty and decision point in the estimation of carbon stocks over the area of our Park landscapes: the plot C values that underpin the estimates for total C within each vegetation type aren't normally distributed. A small proportion of plots have very high C, probably because of large-diameter trees, and it makes the estimation of total carbon sensitive to the method of "mean" chosen. For example, Figure 5 shows the cumulative distribution of carbon densities for the 116 red fir plots in YOSE: the red line is the simple mean, the blue line is the median, and the green line is the mean calculated using log-transformed values then exponentiated back to an arithmetic value. The value of the calculated mean for this extremely important vegetation type (Figure 3) can vary by ~7 kg C /m2, depending on how the "mean" is calculated. Taken over the area of YOSE covered by red fir (Figure 6a), this small difference in carbon density, due just to the method chosen for calculating the mean, can result in a ~4 Tg C swing in the carbon estimate for the park. The same principle applies to other vegetation types with large, old-growth trees (e.g., White Fir - Sugar Pine and Giant Sequoia Forest)(Figure 6b), though they cover less area and therefore contribute less to potential differences in the areal total tree C.

Though problematic from a computational/statistical standpoint, there is a growing body of literature suggesting that this skewed distribution toward large trees is a valuable and desired forest characteristic (e.g., Hurteau et al. 2012, Lutz et al. 2012, 2013), from a carbon, fire management, and a forest function perspective. For example, Lutz et al. (2012) found that although large diameter live trees (≥100 cm dbh) only account for 1.4% of the individuals, they account for 49.4% of the biomass, and white fir and sugar pine comprise 93% of the large diameter trees within that forest type. Kane et al. (2013) demonstrate that fires "thin from below" by removing much of the canopy area in the 2-8 m canopy strata. Thus, while fire removes biomass from forests, it disproportionately removes the understory at lower severity leaving the large diameter trees with the greatest proportion of carbon. These large-diameter trees are perhaps the defining feature of these two parks. They are uniquely able to withstand all but the highest severity fires, and are of considerable ecological and social interest (including giving rise to the name of Sequoia National Park itself). Dendrochronological evidence confirms that these large trees developed under frequent fire regimes, with high severity patches that were limited in extent (Scholl and Taylor 2010). The demonstrated resilience of large-diameter trees to characteristic fire suggests that their preservation is important to overall forest composition and structure, and most probably will continue to be so even under projected scenarios of climate change (e.g. Lutz et al. 2010).

### Fire History and Tree Carbon Density

With this carbon map in hand we now have the tools to evaluate the central question of the proposed work, which was to look at whether there was a difference in the amount of carbon on burned vs.

unburned plots on the Yosemite landscape. The statistical model containing forest type, whether a plot was burned or unburned, and its interaction with forest type as explanatory variables had the greatest support (lowest AIC value) out of our seven candidate models (Table 3). The support for that model was slight however, with it's AIC value only being ~3 less than the model having just forest type as an explanatory variable. The other candidate models using the other burn history metrics (number of times burned and years since most recent fire), either alone or interacting with forest type, did not have much support, with AIC values only 2 or less smaller than the model with just forest type.

Tree carbon density estimates using the best model (forest type + burned + forest type × burned) indicated the effect of burn history was inconsistent across forest types (Figure 7a). The largest absolute difference was in red fir forest, where estimated tree carbon density was ~8 kg/m2 (~29%) lower if burned. Carbon densities in ponderosa pine and white fir – sugar pine forests were ~15% lower in burned vs. unburned, while Jeffrey pine forests had ~ 2 kg/m2 (~40%) higher density within burned areas. Burned lodgepole pine forests also appeared to have slightly higher carbon density, but there was substantial uncertainty around the burned estimate, primarily because of small sample size.

Thus, the answer to the most basic question of this work overall is that there is very little difference between burned and unburned plots, although there is a slight tendency for burned to be lower than unburned in some vegetation types, most pronounced in the Red Fir vegetation type (Figure 7a; ~29%). A more sophisticated view of fire and its effects on carbon stock however has to account for fire severity and its effect on carbon accumulation rates (e.g., Hurteau and North, 2012). In addition, it should be noted that the context of our burned vs unburned contrast was for plots that were sampled with a modal range of 14-16 years since last fire (Figure 7b; 50$^{th}$ percentile for each vegetation type). General effects of fire with shorter or longer time since burning are not addressed using our analytical approach.

## Map Applications for Land and Fire managers

### *Quantifying Total Carbon and Uncertainty within an Area/Polygon of Interest*

Following peer review of the associated manuscripts, our GIS maps of park carbon will be available to managers. Total carbon and its uncertainty within a specific area of interest can be readily calculated using our carbon density map layers by the following procedure:

1. Clip the carbon map polygons to the area of interest.
2. Calculate total C within each polygon (polygon_c_total) by multiplying carbon_density (kg/m2) by the polygon area (m2).
3. Calculate the standard error of total polygon C (polygon_c_se) by multiplying se by the polygon area.
4. Sum the total polygon C across all polygons (c_total).
5. Sum the standard errors across all polygons (se_total).

6. The bounds of a 95% confidence interval for the total C can be calculated using c_total ± 1.96 × se_total

#### *Carbon Stability Using Fire Return Interval Departure*

How much of the Yosemite carbon stock is at risk? One metric is the departure from fire return interval (FRID), which is a measure of how far "departed" a given stand is from the naturally occurring cycle of fires, and can be an indicator of the degree to which small ladder fuels are accumulating under large trees. We used the carbon map to estimate the amount of carbon sequestered in areas with various FRID vales (Figure 8). FRID values of less than two probably do not represent a risk of a fire of much higher than characteristic severity. However, FRID values of 3 or higher would indicate a risk of substantial high severity patches within fire perimeters.

#### *Relevance to Current Conditions: Carbon Dynamics*

All this work quantifies tree carbon as of the time most of the plots were measured, 16 years ago in 1998. Obviously there is a need to determine how to move from this baseline map to a current map, governed by the dynamics of carbon accumulation, in burned and unburned areas, pre and post fire.

### Intercomparison with CASA Remotely Sensed Biomass Estimates

#### *Overall YOSE Totals*

Overall, our mean estimate of total YOSE Tree C (25 Tg C), was lower than the amount generated from the 2009 CASA estimate (30 Tg C) by about 17%, and outside the bounds of our upper 95% confidence interval (27 Tg C; Figure 9). One potential underestimation in our methods relates to shrub biomass, as we were focused on tree carbon. In older forests (500 yr) that have experienced a frequent fire regime (e.g. Lutz et al. 2012), shrubs constitute approximately 1% of aboveground biomass, but in stands that have experienced high-severity fire, and that therefore have few large-diameter trees, shrub biomass can be a much higher proportion of total biomass. When broken down by vegetation type across the landscape, this difference is evident in the shrub and woodland vegetation categories where shrubs are an important component, which might explain at least 2 Tg C of the difference between the estimate and brings an estimate without shrubs (e.g., 28 Tg C) very close to the upper 95% CI from our plot-based method (27 Tg C). Shrub biomass is poorly understood, and many estimates are based on cover (e.g. McGinnis et al. 2010). However, due to irregular allometries and ages, cover is often a poor predictor of shrub biomass (e.g. Halpern and Lutz 2013). Realizing the importance of shrubs to carbon, particularly because they are often fully consumed by fire (or nearly so), we developed allometric equations for three shrub species, and encourage other researchers to extend the number of Sierra Nevada shrub species for which high quality (i.e., sample size >25) allometric equations exist (Lutz et al. submitted). Of course, there is currently unknown level of uncertainty associated with the CASA estimates, so it may be that if we had those estimates, the error bars would overlap.

#### *Allometry Bias Toward Tall Pine Growth Forms in High Elevation Vegetation Types*

However, a missing shrub component is not the only issue that might explain the difference between estimates, especially in the higher elevation woodland areas where the CASA estimates fall well above our error bars and shrubs are a less important component of total C (see carbon summaries.pdf

for a statistical breakdown of the components in each vegetation type). In our exploration of the allometric equations commonly used for high elevation pine species in this region of the US (Jenkins et al., 2004), we found distinctly unrealistic equations that generated very tall growing trees, especially at the upper range of DBH values that occurred in YOSE plots. High elevation pines, especially the larger diameter pines, are much more limited in their height at higher elevations, and their growth form at the larger DBHs is much more conical than the columnar boles possessed by tall pines of the lower elevation mixed conifer vegetation types. It is not uncommon for high elevation junipers and whitebark pines to have a dbh of 100 cm and a height less than 10 m as compared to more 'conformal' pines such as ponderosa pine and sugar pine which have heights of >40 m at that diameter (pers. obs.). Thus, if the baseline values (Pan et al, 2011) ascribed to these forest stands were influenced by the Jenkins allometric equations, there is likely a bias toward overestimation of carbon in these vegetation types. Our plot-based estimates attempt to account for this bias by using a hybrid allometric equation that applies a more conical growth form based on juniper (Miller et al. 1981) at the higher end of the DBH range (Appendix B).

### *Temporal Disjunctions and Outdated Plot-based Estimates*

Our carbon map estimates are based on the aerial photography from 1998, which is the most representative year for this map (Aerial Information Systems 2007, Keeler-Wolf et al. 2012). Unfortunately, we only have the CASA data downscaled for YOSE for 2009, though eventually maps going back to 2000 will be available (Potter, 2010) for comparison. Clearly, 11 years vegetation growth between 1998 and 2009 a 2009 map constitutes a "temporal bias" that would lead the CASA estimates to also be higher than our plot-based carbon map. Reconciling the two will require the use of established succession schemes (Davis, 2009), and the development of a downscaled CASA raster developed for the YOSE (and potentially SEKI) areas for the year 2000.

### *Carbon "Reset" Values and Fire History "Bias" in CASA Estimates*

Large fires can have a substantial impact on the amount of carbon on the landscape, exceeding that of incremental growth, especially in the mixed conifer and lower elevation fuel types where fire is more frequent. This is especially true with the current CASA scheme for accounting for the effect of fire, which basically assumes a "reset" carbon values back to a low shrub-based value post-fire. The effect of fire, and impact of using this method is visually evident in the 2009 CASA map, especially when compared to an overlay of Yosemite fire history (Figure 10).

In the Sierra Nevada, fires do not uniformly reduce carbon over the area defined by the fire perimeter except in the most extreme fire high severity scenarios (or in chaparral vegetation types). Even then, only a fraction of the landscape burns at high enough severity to warrant full, eventual reduction of the carbon stock (Kane et al. in press). Rather, there is a range of severities that produce a range of loss both of carbon to the atmosphere and the standing dead C pools (e.g., van Wagtendonk and Lutz 2007, Lutz et al. 2009, Hurteau et a. 2010, Carlson et al. 2012, Kolden et al. 2012). Figure 11 illustrates a hypothetical (and hopefully reasonable) example of how this works from a computational standpoint for reducing carbon stocks using severity, rather than perimeter mapping across a landscape. Results from our carbon mapping (Figure 7a), which show only tendencies toward lower carbon in vs. outside of fire perimeters, also support this notion of a mixed severity regime, where

fire doesn't result in significant overall tree mortality, but rather produces a heterogeneous mix of carbon reductions, much of which (at least in the low to moderate severity areas) is returned to the landscape by tree or shrub regeneration within a decade or two (Hurteau et al., 2010). Visually comparing the CASA maps to our maps (Figure 12) shows how substantially this reduction scheme can impact overall carbon estimates for a landscape. It is more likely that a statistical design that looks for differences, even thresholds for changes in carbon density, as it varies with continuous fire severity variables (e.g., dNBR) is the best approach for quantifying both the effect of fire on landscapes, and the benefits of proactively substituting Rx and resource benefit tactics for the more intense wildfire scenarios. We recommend this severity-based approach and illustrate its potential bias in the next section as a way to better quantify actual stock changes in fire-prone landscapes like YOSE, and reconcile those changes with CASA remote sensing.

### *Potential for Overestimating Losses Due to Fire: the Rim Fire of 2013*

Assuming the above carbon loss percentages by severity scheme (Figure 11) and using initial fire severity (Figure 13), live biomass in the Rim fire footprint was likely somewhere above 5 Tg C pre-fire (Figure 14a), and was reduced to a value of between 1-2 Tg C by the fire (Figure 14b), with about the same amount having been immediately lost to emissions and the atmosphere. Under this carbon loss by severity scheme, the remaining fraction of C is still on the ground as standing dead snags. These values are based on a hypothetical carbon loss by severity scheme, and we use this only as a means to illustrate the utility of this map and the potential difference in estimated losses, not to provide definitive numbers for actual Rim fire carbon losses. Post-fire plots and remote sensing of severity one year post-fire (the dNBR extended assessment instead of the immediate assessment illustrated here) will be needed to get a definitive estimate of the losses to the atmospheric and dead biomass C pools.

# Conclusions

- In this work, we have developed a framework that SEKI and YOSE land and fire managers can use to calculate the amount of carbon in a given area, along with an assessment of the likely uncertainty. We used the most comprehensive plot data and the most applicable allometry for the parks, married to a statistical analysis that allows for the quantification of uncertainty to 95% confidence intervals.

- Our aggregate analysis of burned versus unburned areas and time since the last fire is not sufficient for determining if fire has reduced the carbon stock. A more detailed analysis, including a history of burn severity over decades may be required to examine the effects of fire on carbon stocks. There was no significant difference between the carbon contained in burned and unburned areas, as defined by fire perimeters, at the 95% confidence interval, though there was a tendency for mean carbon density (live biomass only) to be lower in burned areas within some vegetation types.

- With allowances for likely biases of the plot-based techniques, our results are comparable to independent estimates of carbon biomass from remotely sensed data (Potter et al. 2010 ), and

our efforts have the potential to refine the way carbon stocks are calculated based on the effects of fire for the California greenhouse gas inventory.

## Next Steps with the Project Data

- A simple classification of forest portions that were burned vs. unburned is not sufficient to differentiate the effects of fire. It is more likely that explicitly accounting for severity (with either ground-based or satellite-derived metrics) will yield more meaningful estimates of immediate carbon loss due to fire.
- Split out the high severity pixels from moderate and low severity pixels as a way to look for differences in carbon stocks, or use the continuous dNBR values as a means of looking for relationships to carbon stocks in order to quantify severity thresholds at which carbon stocks are substantially changed. It may be that there are an insufficient number of plots placed within areas of recent high-severity fire because most of the plots used in this study were established for other objectives, i.e., vegetation type mapping.
- Explore a severity-based scheme for updating CASA maps that quantify the effect of fire on park carbon stocks.

## Recommendations for Future Carbon Accounting Based on Objective 1

This work has shown that even with thousands of calibration plots, there is still substantial uncertainty associated with quantifying carbon over the area of large landscapes, especially at the operational scale. Tracking fire severity, not just fire history, is key to understanding impacts of fire on carbon stocks on park landscapes.

No one method (including this one) that will completely and definitively quantify tree carbon. However, given the current state of vegetation mapping and allometric equations, we can and have bounded the uncertainty in carbon, and have provided a means for comparison with remote sensing techniques that can help update the map as carbon continues to accumulate and disturbances like fire alter baseline carbon densities. Combining these plot based methods for baselines and the tree coring work to calibrate pre- and post-fire recovery rates with remotely sensed C estimates is likely to provide the best way forward for managers to update carbon inventory maps.

As discussed above, this map and the tools it provides can also be used for planning managed fires, assessing vulnerability of the park carbon stock to future fires, and even calculating tradeoffs between managed fire severity regimes and wildfire severity regimes with respect to carbon stocks.

## Deliverables and Project Completion Plan

### Deliverables Listed in the Project Proposal

The original proposal that was funded by the National Park Service, Climate Change Adaptation Program listed the following deliverables:

1) One peer-reviewed journal article and an accompanying 1-page publication brief summarizing its management implications for each of the two project objectives.

2) Presentation of results in at least one workshop for NPS staff and in at least one national conference. 3) An interpretive component focused on educating the public about the value the YOSE and SEKI carbon stocks, and the impact of fire on them as a "Parks as Classrooms" module.

## Manuscript Delivery Plan

### *Objective 1 Manuscripts*

Lutz, J. A., K. A. Schwindt‡, T. J. Furniss, J. A. Freund, M. E. Swanson, K. I. Hogan‡, G. E. Kenagy‡, and A. J. Larson. Submitted. Community composition and allometry of Leucothoe davisiae, Cornus sericea, and Chrysolepis sempervirens. Canadian Journal of Forest Research.

Lutz, J. A., J. R. Matchett, L.W. Tarnay, D.G. Smith, K.M.L. Becker†, and M.L. Brooks. In prep. The uncertainty of carbon sequestered in forest ecosystems of Yosemite and Sequoia & Kings Canyon National Parks, California, USA. To be submitted to Forest Ecology and Management.

Becker†, K.M.L., Smith, D.G., and Lutz, J.A. In prep. Effects of fire severity, time since fire, and climatic water balance on species composition in Yosemite and Sequoia & Kings Canyon National Parks, California, USA. This manuscript will detail the compositional analysis from the paired (burned and unburned) plots established during this study.

Becker†, K.M.L., Smith, D.G., and Lutz, J.A. In prep. Trends and variability in the effects of fire on forest structure in the Sierra Nevada This manuscript will detail the structural differences found in the paired (burned and unburned) plots established during this study.

### *Objective 2 Manuscripts*

Lutz, J. A., J. R. Matchett, L.W. Tarnay, D.G. Smith, K.M.L. Becker†, and M.L. Brooks. In prep. Pre-fire and post-fire carbon assimilation rates in montane forests of Yosemite and Sequoia & Kings Canyon National Park differs by severity, time since fire, and site water balance.

‡Undergraduate advisee who participated in the research as part of outreach and training.

†Graduate advisee who participated in the research as part of outreach and training.

## Presentation Delivery Plan

Effect of fire on carbon stocks at YOSE and SEKI, JR Matchett et al., Southern Sierra Nevada Fire Science Workshop, May 2014

Carbon sequestration and fire, Matt Brooks and Matt Hurteau, Southern Sierra Nevada Fire Science Workshop, May 2014

Wilson‡, J. 2013. Effects of low-severity fire on structural attributes and radial tree growth in Abies concolor-dominated forests, Yosemite National Park, California Senior Capstone Presentation, Program on the Environment, University of Washington. May 22, 2013

Becker†, K.M.L. 2014. Effects of fire on Abies concolor and Abies magnifica vegetation communities, forest structure, and carbon sequestration in Yosemite and Sequoia & Kings Canyon National Parks. Masters Thesis Defense public presentation. University of Washington, Seattle. March 12, 2014.

### Interpretive Delivery Plan

Two educational products have been developed as a result of this project. The Yosemite National Park's educational team has developed a "Parks as Classrooms" program focused on fire ecology which includes curriculum based educational content and activities focused on impacts of fire on the carbon cycle. Although these products are not complete because all the analyses for interpretation are not complete, the products with grow in depth and breadth as more results are available.

The other product that resulted from this study was a video "Carbon: Forests and Fire" that Kevin Song shot during his summer as a Yosemite Leadership Intern at Yosemite National Park funded by this grant. Kevin was a first year student at University of California – Merced and was an intern on the field crew that collected data for this project. Kevin recorded and presented this video as his completion requirement of his internship in the Park. The link to the video is http://www.youtube.com/watch?v=HIN8iY40Hl8.

The data from the project has also been used in four undergraduate student senior projects at the University of Washington, and one MS thesis, also at the University of Washington.

The Education Branch at Yosemite National Park has many student groups interested in fire and therefore the educational materials produced from this project will be presented to a large audience.

As we complete analyses from this study, the educational team will continue to integrate information into the Parks As Classrooms Fire Ecology curriculum.

## Literature Cited

Aerial Information Systems. 2007. Spatial vegetation data for Sequoia & Kings Canyon National Parks vegetation mapping project. National Park Service, Denver, Colorado.

Chisholm, R. A., H. C. Muller-Landau, K. Abd. Rahman, D. P. Bebber, Y. Bin, S. A. Bohlman, N. A. Bourg, J. Brinks, N. Brokaw, S. Bunyavejchewin, N. Butt, H. Cao, M. Cao, D. Cárdenas, L. W. Chang, J. M. Chiang, G. Chuyong, R. Condit, H. S. Dattaraja, S. Davies, A. Duque, C. Fletcher, C. V. S. Gunatilleke, I. A. U. N. Gunatilleke, Z. Hao, R. D. Harrison, R. Howe, C. F. Hsieh, S. Hubbell, A. Itoh, D. Kenfack, S. Kiratiprayoon, A. J. Larson, J. Lian, D. Lin, H. Liu, J. A. Lutz, K. Ma, Y. Malhi, S. McMahon, W. McShea, M. Meegaskumbura, S. M. Razman, M. D. Morecroft, C. Nytch, A. Oliveira, G. R. Parker, S. Pulla, R. Punchi-Manage, H. Romero, W. Sang, J. Schurman, S. H. Su, R. Sukumar, I. F. Sun, H. S. Suresh, S. Tan, D. Thomas, S. Thomas, J. Thompson, R. Valencia, A. Vicentini, A. Wolf, S. Yap, W. Ye, Z. Yuan, J. Zimmerma. 2013. Scale-dependent relationships between species richness and ecosystem function in forests. Journal of Ecology 101: 1214-1224.

Collins, B. M., R. G. Everett, and S. L. Stephens. 2011. Impacts of fire exclusion and recent managed fire on forest structure in old-growth Sierra Nevada mixed-conifer forests. Ecosphere 2: article 51.

Fellows, A.W., and M.L. Goulden. 2008. Has fire suppression increased the amount of carbon stored in western U.S. forests? Geophysical Research Letters 35(12): L12404.

Halpern, C. B., and J. A. Lutz. 2013. Canopy closure exerts weak controls on understory dynamics: a 30-year study of overstory-understory interactions. Ecological Monographs 83: 19-35.

Hessburg, P.F., J.K. Agee, and J.F. Franklin. 2005. Dry forests and wildland fires of the inland Northwest USA: contracsting the landscape ecology of the pre-settlement and modern eras. Forest Ecology and Management 211: 117-139.

Hurteau, M. D. 2013. Effects of wildland fire management on forest carbon stores. Pages 359-380 in D. G. Brown, D. T. Robinson, N. H. F. French, and B. C. Reed, editors. Land use and the carbon cycle: science applications in human environment interactions. Cambridge University Press, Cambridge UK.

Hurteau, M. D., and M. L. Brooks. 2011. Short- and long-term effects of fire on carbon in US dry temperate forest ecosystems. BioScience 61: 139-146.

Hurteau, M. D., and M. P. North. 2009. Fuel treatment effects on tree-based forest carbon storage and emissions under modeled wildfire scenarios. Frontiers in Ecology and the Environment 7:409-414.

Jenkins, J. C., D. C. Chojnacky, L. S. Heath, L.S., and R. A. Birdsey. 2003. National-Scale Biomass Estimators for United States Tree Species. Forest Science 49:12-35.

Jenkins, J.C., Chojnacky, D.C., Heath, L.S., Birdsey, R.A., 2004. Comprehensive database of diameter-based biomass regressions for North American tree species USDA Forest Service, Northeastern Research Station, General Technical Report NE-319, Newton Square, PA.

Kane, V. R., J. A. Lutz, S. L. Roberts, D. F. Smith, R. J. McGaughey, N. A. Povak, and M. L. Brooks. 2013. Landscape-scale effects of fire severity on mixed-conifer and red fir forest structure in Yosemite National Park. Forest Ecology and Management 287: 17-31.

Kane, V. R., M. North, J. A. Lutz, D. Churchill, S. L. Roberts, D. F. Smith, R. J. McGaughey, J. T. Kane, and M. L. Brooks. In press. Assessing fire-mediated change to forest spatial structure using a fusion of Landsat and airborne LiDAR data in Yosemite National Park. Remote Sensing of Environment.

Kolden, C. A., J. A. Lutz, C. H. Key, J. T. Kane, and J. W. van Wagtendonk. 2012. Mapped versus actual burned area within wildfire perimeters: characterizing the unburned. Forest Ecology and Management 286:38-47.

Larson, A. J., J. A. Lutz, R. F. Gersonde, J. F. Franklin, and F. F. Hietpas. 2008. Productivity influences the rate of forest structural development. Ecological Applications 18: 899-910.

Lutz, J. A., K. A. Schwindt, T. J. Furniss, J. A. Freund, M. E. Swanson, K. I. Hogan, G. E. Kenagy, and A. J. Larson. Submitted. Community composition and allometry of Leucothoe davisiae, Cornus sericea, and Chrysolepis sempervirens. Canadian Journal of Forest Research.

Lutz, J.A., and C. B. Halpern. 2006. Tree mortality during early forest development: a long-term study of rates, causes, and consequences. Ecological Monographs 76:257-275.

Lutz, J. A., C. H. Key, C. A. Kolden, J. T. Kane, and J. W. van Wagtendonk. 2011. Fire frequency, area burned, and severity: A quantitative approach to defining a normal fire year. Fire Ecology 7: 51-65.

Lutz, J. A., A. J. Larson, M. E. Swanson, and J. A. Freund. 2012. Ecological Importance of Large-Diameter Trees in a Temperate Mixed-Conifer Forest. PLoS ONE 7:e36131.

Lutz, J. A, A. J. Larson, J. A. Freund, M. E. Swanson, and K. J. Bible. 2013. The ecological importance of large-diameter trees to forest structural heterogeneity. PLoS ONE 8: e82784.

Lutz, J. A., J. W. van Wagtendonk, A. E. Thode, J. D. Miller, and J. F. Franklin. 2009. Climate, lightning ignitions, and fire severity in Yosemite National Park, California, USA. International Journal of Wildland Fire 18: 765-774.

Lutz, J. A., J. W. van Wagtendonk, and J. F. Franklin. 2009. Twentieth-century decline of large-diameter trees in Yosemite National Park, California, USA. Forest Ecology and Management 257: 2296-2307.

Lutz, J. A., J. W. van Wagtendonk, J. F. Franklin. 2010. Climatic water deficit, tree species ranges, and climate change in Yosemite National Park. Journal of Biogeography 37: 936-950.

McGinnis, T. W., C. D. Shook, and J. E. Keeley. 2010. Estimating aboveground biomass for broadleaf woody plants and young conifers in Sierra Nevada, California, Forests. Western Journal of Applied Forestry 25: 203- 209.

Miller, J. D., B. M. Collins, J. A. Lutz, S. L. Stephens, J.W. van Wagtendonk, and D. A. Yasuda. 2012. Differences in wildfires among ecoregions and land management agencies in the Sierra Nevada region, California, USA. Ecosphere 3(9):80.

Miller, L.M., R.O. Meeuwig, and J.D. Budy. 1981. Biomass of singleleaf pinyon and Utah juniper. USDA Forest Service, Intermountain Forest and Range Experimental Station Research Paper INT-273. Ogden, Utah.

North, M. J., J. Innes, and H. Zald. 2007. Comparison of thinning and prescribed fire restoration treatments to Sierran mixed-conifer historic conditions. Canadian Journal of Forest Research 37: 331-342.

Scholl A. E, and A. H. Taylor. 2010. Fire regimes, forest change, and self-organization in an old-growth mixed-conifer forest, Yosemite National Park, USA. Ecological Applications 20: 362–380.

Sillett, S.C., Van Pelt, R. 2007. Trunk reiteration promotes epiphytes and water storage in an old-growth redwood forest canopy. Ecological Monographs 77: 335-359.

Swann, A. L. S, I. Y. Fung, J. C. H. Chiang. 2012. Mid-latitude afforestation shifts general circulation and tropical precipitation. Proceedings of the National Academy of Sciences of the USA 109: 712-716.

Van Pelt, R. 2001. Forest giants of the Pacific coast. University of Washington Press, Seattle, Washington.

Van Pelt, R., and S. C. Sillett. 2008. Crown development throughout the lifespan of coastal Pseudotsuga menziesii, including a conceptual model for tall conifers. Ecological Monographs 78: 283–311.

van Wagtendonk, J. W. 2007. The history and evolution of Wildland fire use. Fire Ecology 3: 3-17.

van Wagtendonk, J. W., and J. A. Lutz. 2007. Fire regime attributes of wildland fires in Yosemite National Park, USA. Fire Ecology 3: 34-52.

Westman, W. E. 1998. Aboveground biomass, surface area, and production relations of red fir (Abies magnifica) and white fir (A. concolor). Canadian Journal of Forest Research 17: 311-319.

**Table 1.** Number of sampling plots located within each vegetation type.

| Forested Vegetation Type | Number of Plots |
|---|---|
| Deciduous Oak Forest and Woodland | 88 |
| Douglas-fir Forest | 7 |
| Evergreen Oak Forest and Woodland | 110 |
| Foothill Pine Woodland | 11 |
| Foxtail Pine Forest | 58 |
| Giant Sequoia Forest | 42 |
| High Woodland | 89 |
| Jeffrey Pine Forest | 111 |
| Lodgepole Pine Forest | 190 |
| Mountain Hemlock Forest | 38 |
| Pinyon Pine Woodland | 27 |
| Ponderosa Pine Forest | 123 |
| Ponderosa Pine Woodland | 13 |
| Red Fir Forest | 116 |
| Riparian Forest | 87 |
| Riparian Shrub | 23 |
| Shrub | 258 |
| Western White Pine Forest | 27 |
| Western White Pine Woodland | 4 |
| White Fir - Sugar Pine Forest | 224 |
| Total | 1646 |

**Table 2.** Distribution of sampling plot locations by park, vegetation type, and burn status.

| Park | ABCO | | ABMA | | PICO | | PIJE | | PIPO | | Total |
|---|---|---|---|---|---|---|---|---|---|---|---|
| | B[1] | U[2] | B | U | B | U | B | U | B | U | |
| **YOSE** | 11 | 15 | 4 | 4 | 4 | 0 | 4 | 5 | 9 | 11 | 67 |
| **SEKI** | 1 | 0 | 10 | 8 | 3 | 1 | 10 | 2 | 2 | 1 | 38 |
| **Total** | 12 | 15 | 14 | 12 | 7 | 1 | 14 | 7 | 11 | 12 | 105 |

[1]B = burned

[2]U = unburned

**Table 3.** Modelling results.

| Model Effects | AIC | AIC – Minimum AIC |
|---|---|---|
| forest type | 1698.6 | 2.97 |
| forest type + burned | 1699.6 | 3.93 |
| forest type + burned + forest type x burned | 1695.7 | 0.00 |
| forest type + times burned | 1700.6 | 4.96 |
| forest type + times burned + forest type x times burned | 1698.7 | 2.98 |
| forest type + years since fire | 1699.9 | 4.26 |
| forest type + years since fire + forest type x years since fire | 1696.7 | 1.01 |

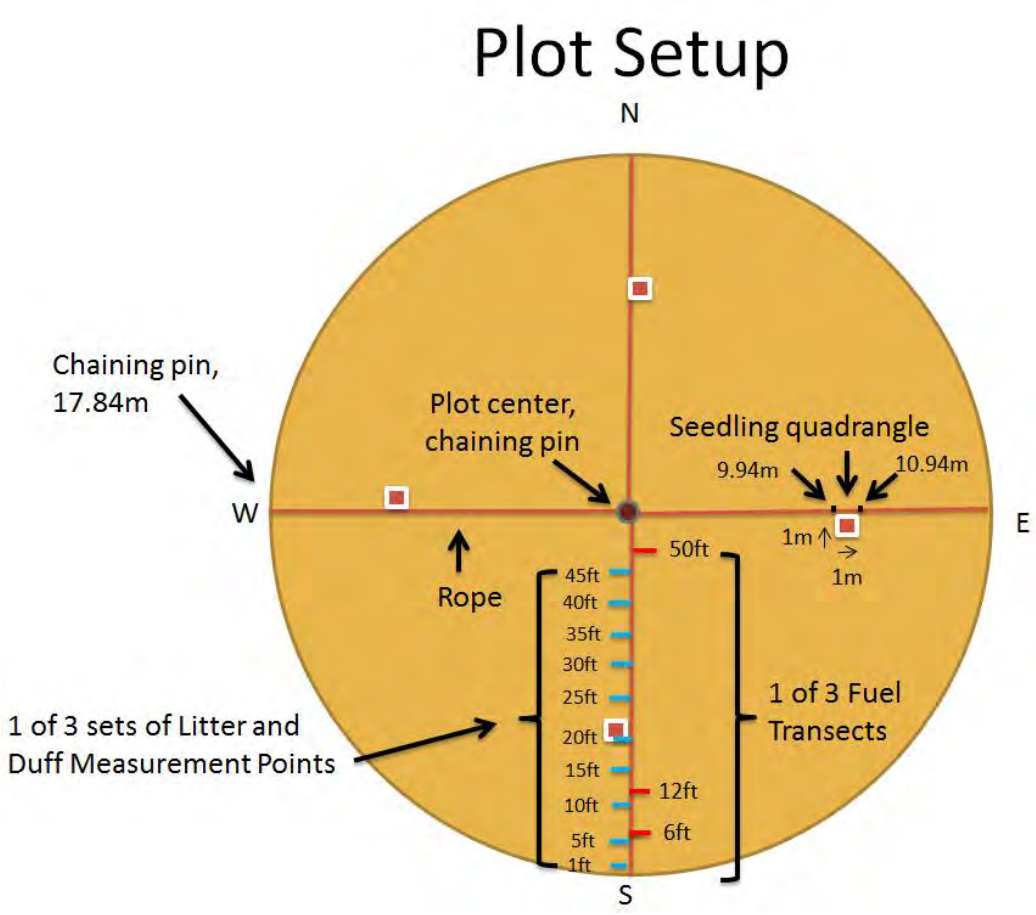


**Figure 1**. Plot layout.

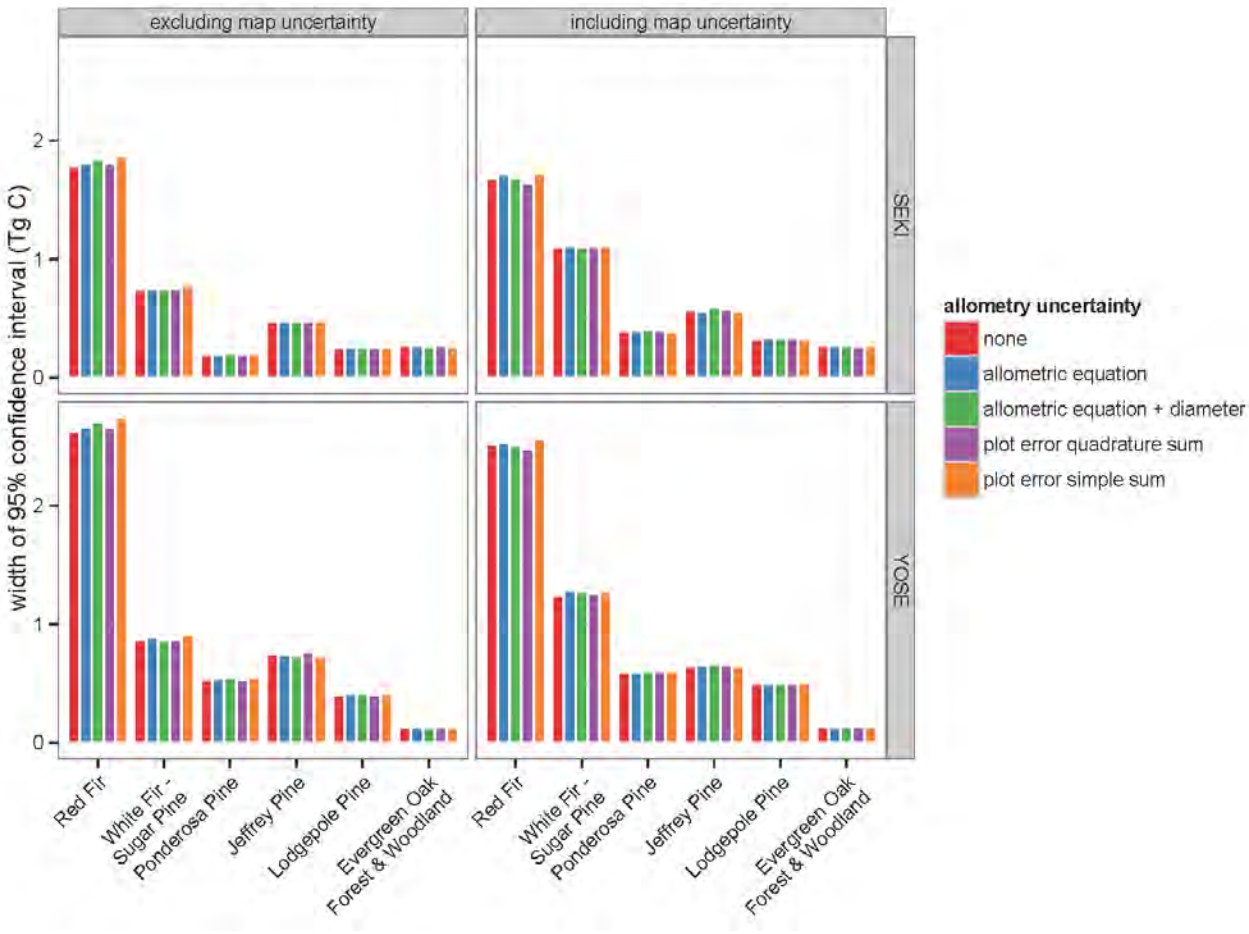


**Figure 2.** Allometry uncertainty comparisons.

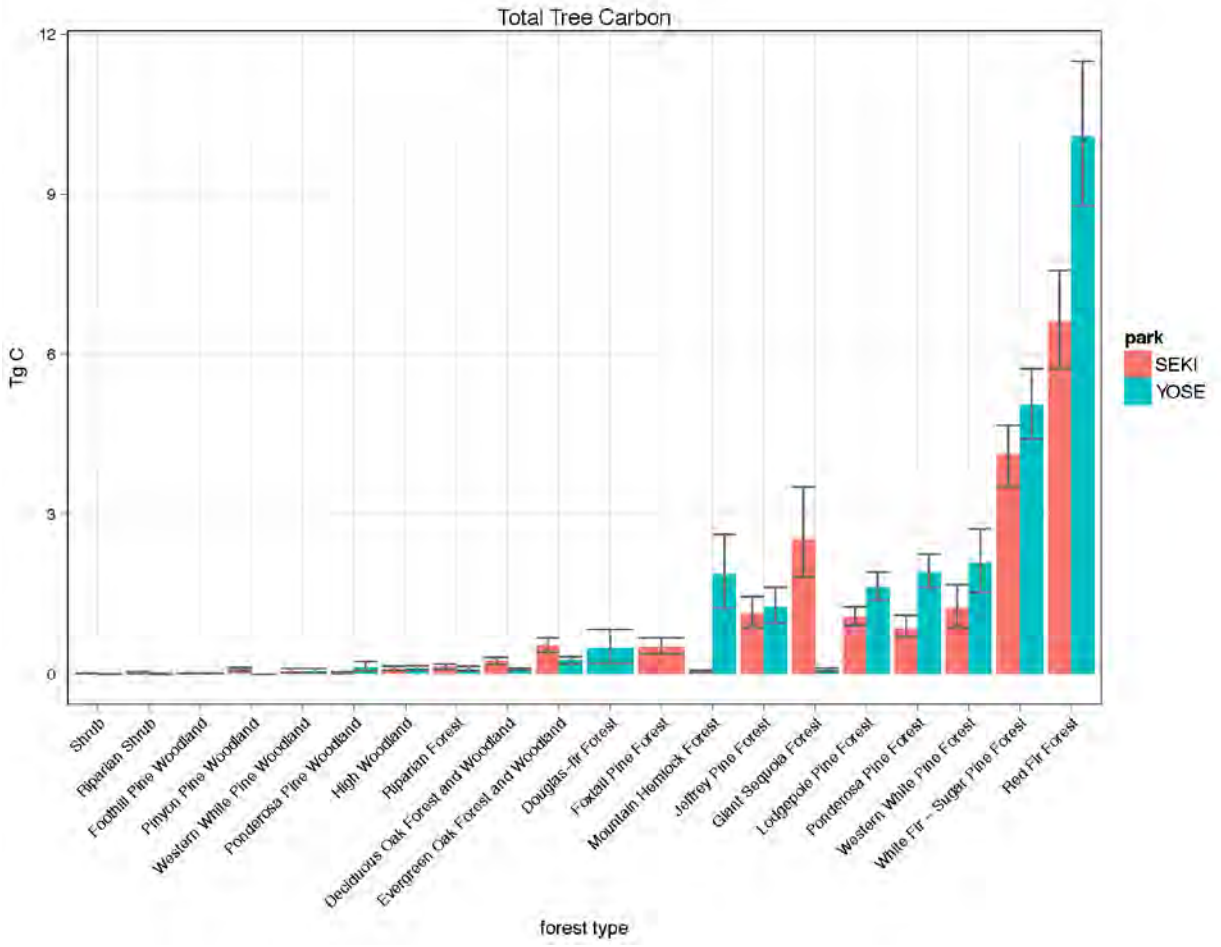


**Figure 3.** Total tree carbon (95% CI) in Sequoia & Kings Canyon National Park (SEKI) and Yosemite National Park.(YOSE).

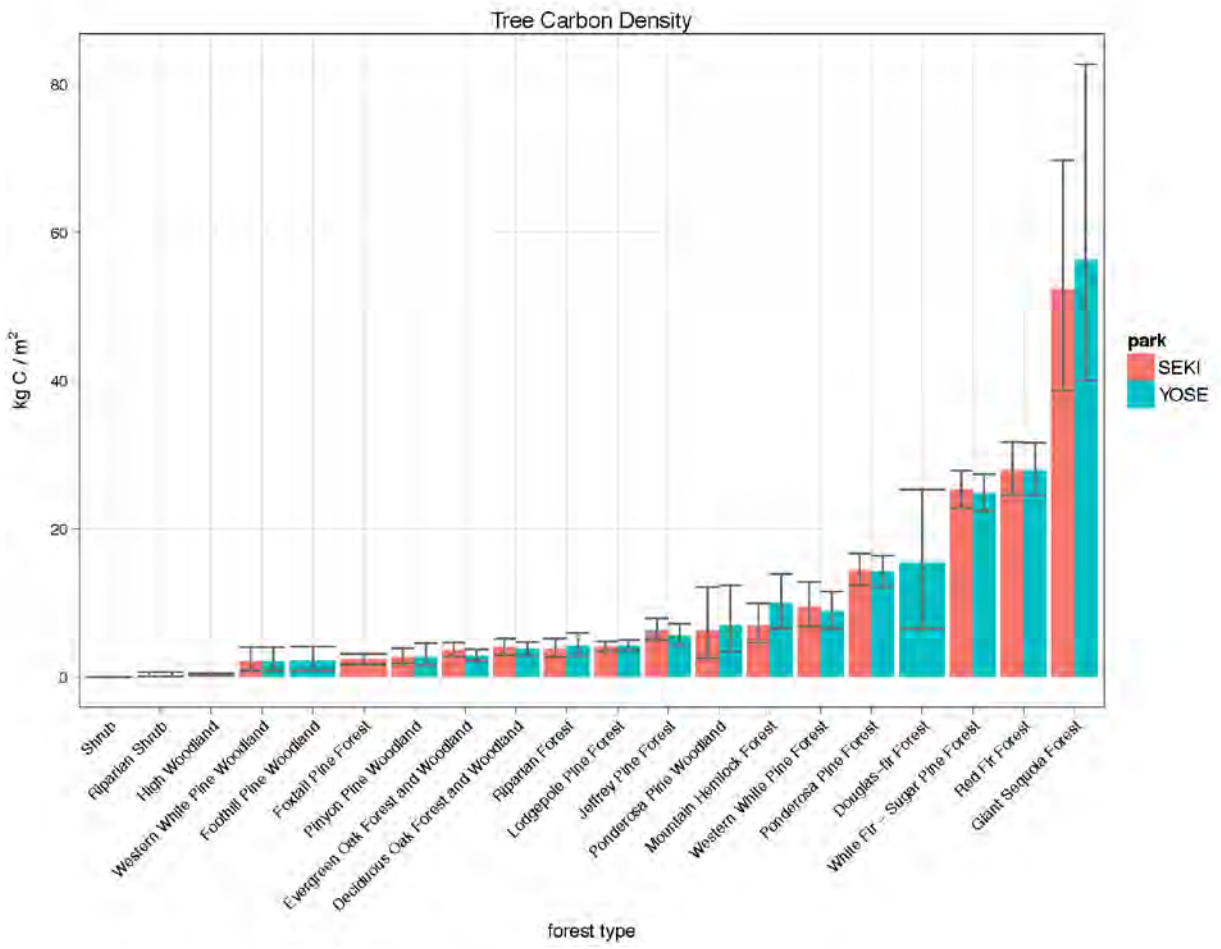


**Figure 4.** Total tree carbon density (95% CI) in Sequoia & Kings Canyon National Park (SEKI) and Yosemite National Park.(YOSE).

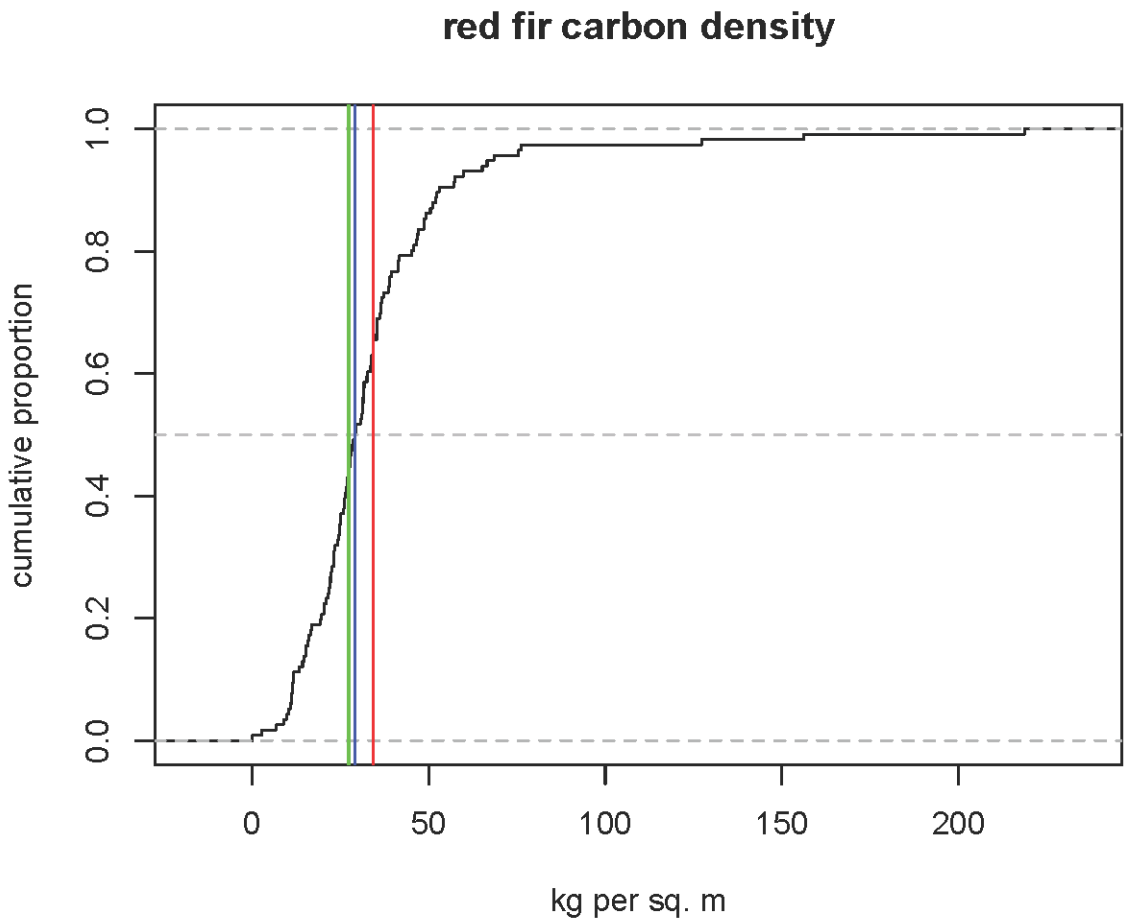


**Figure 5.** Effects of different methods for calculating mean: red fir carbon density distribution example.

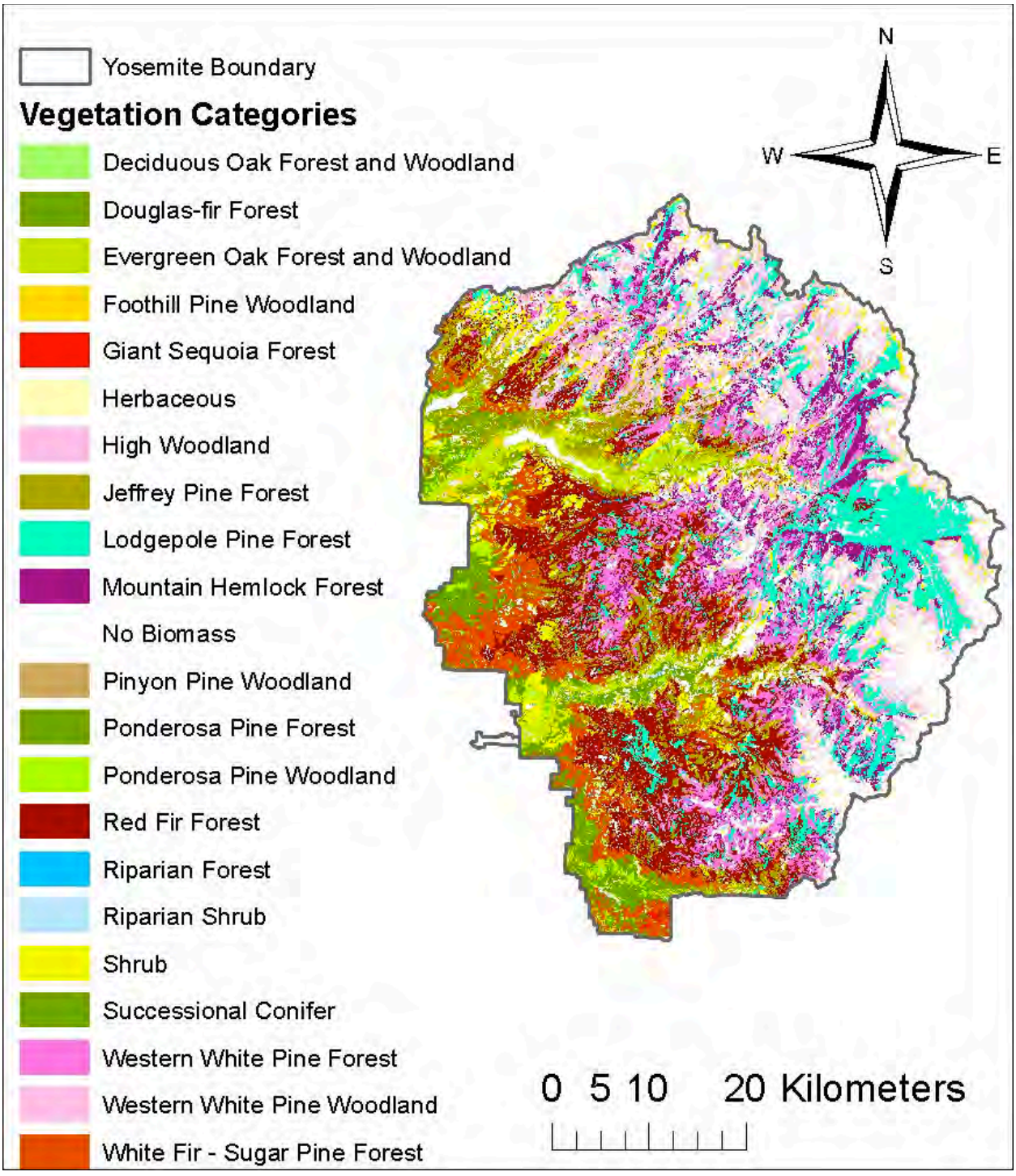


**Figure 6a**. Map of vegetation categories in Yosemite National Park that were used in the analysis for this report.

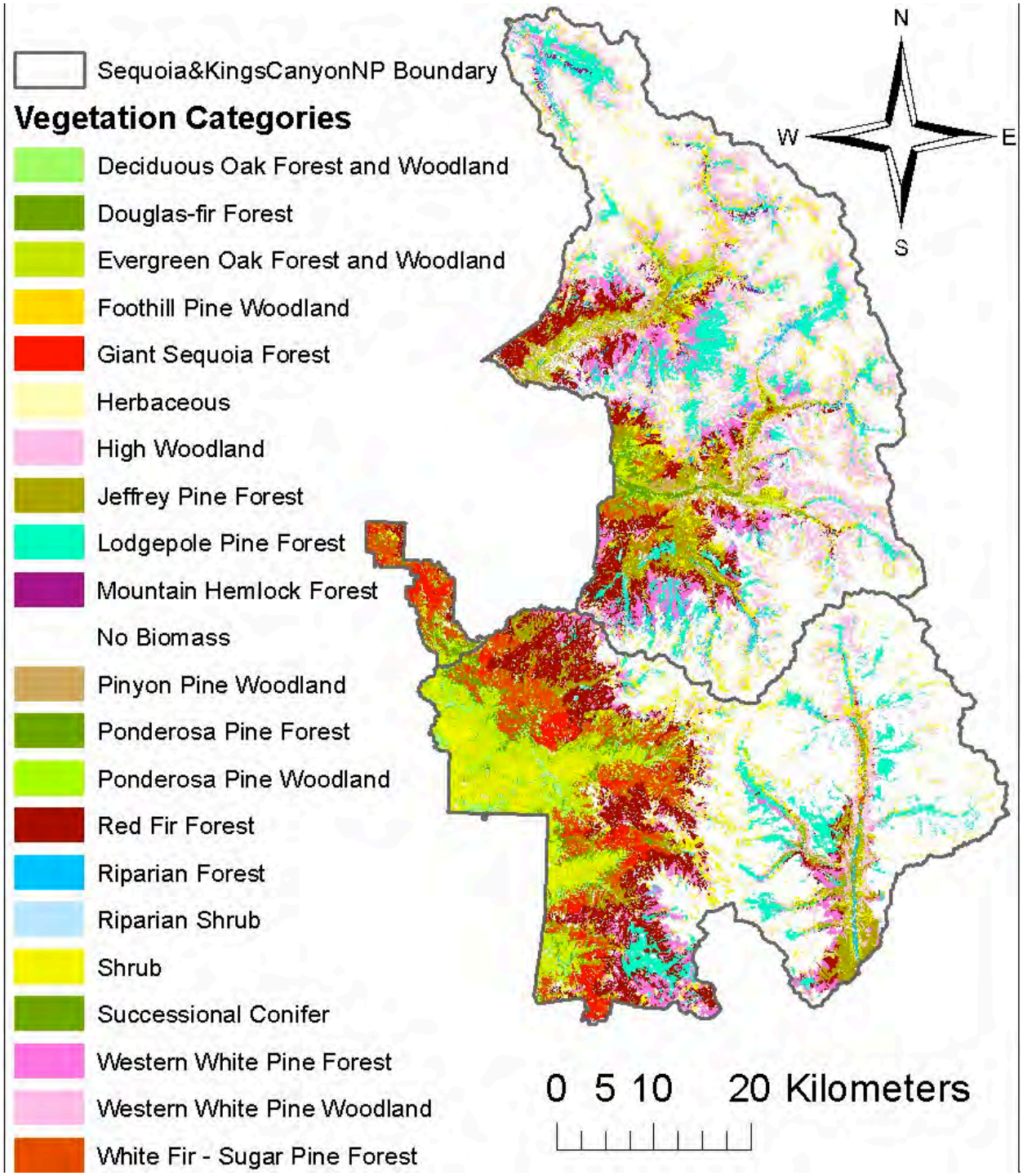


**Figure 6b**. Map of vegetation categories in Yosemite National Park that were used in the analysis for this report

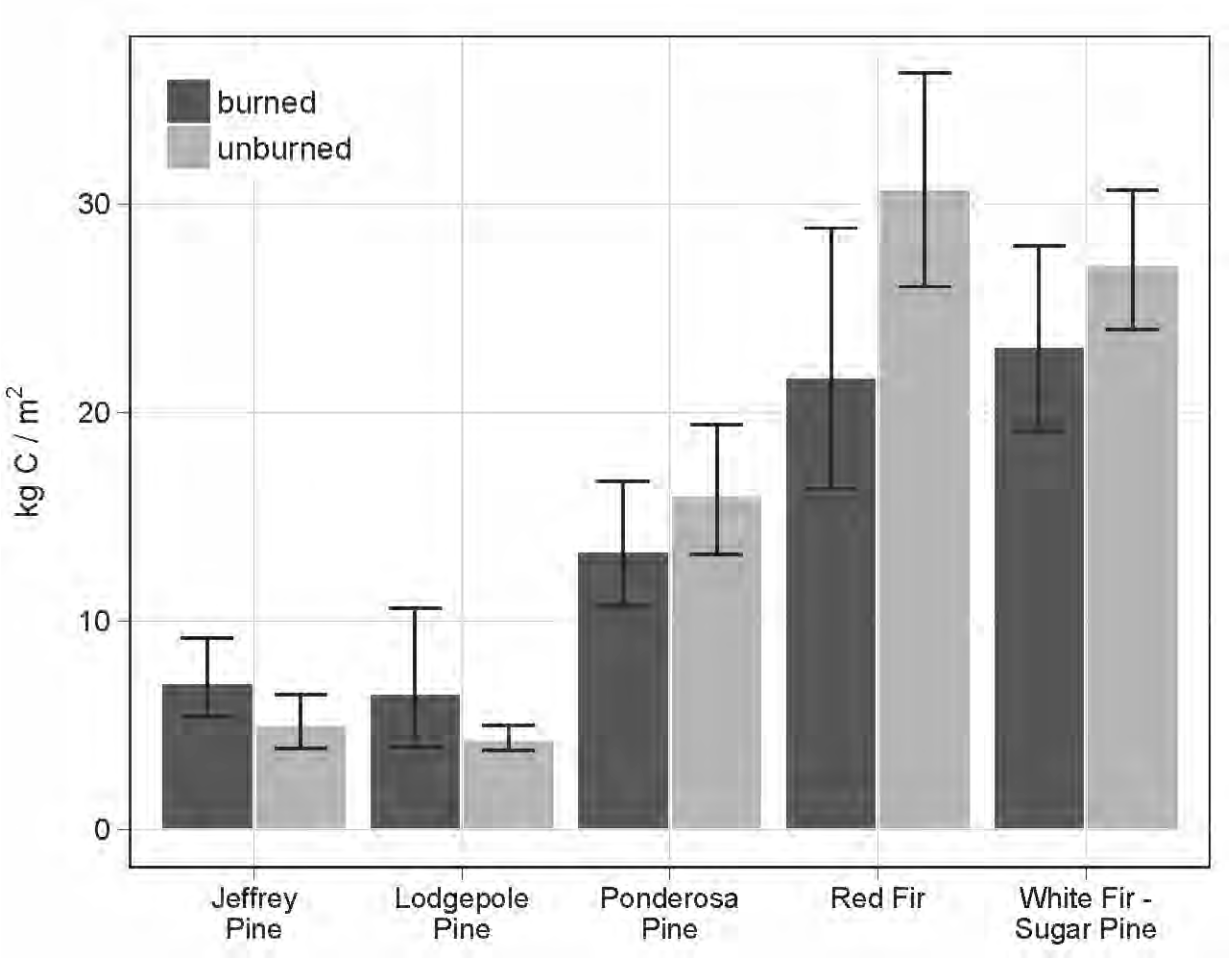


**Figure 7a**. Total tree carbon (95% CI) in burned and unburned plots stratified by vegetation type in Yosemite National Park and Sequoia & Kings Canyon National Parks combined.

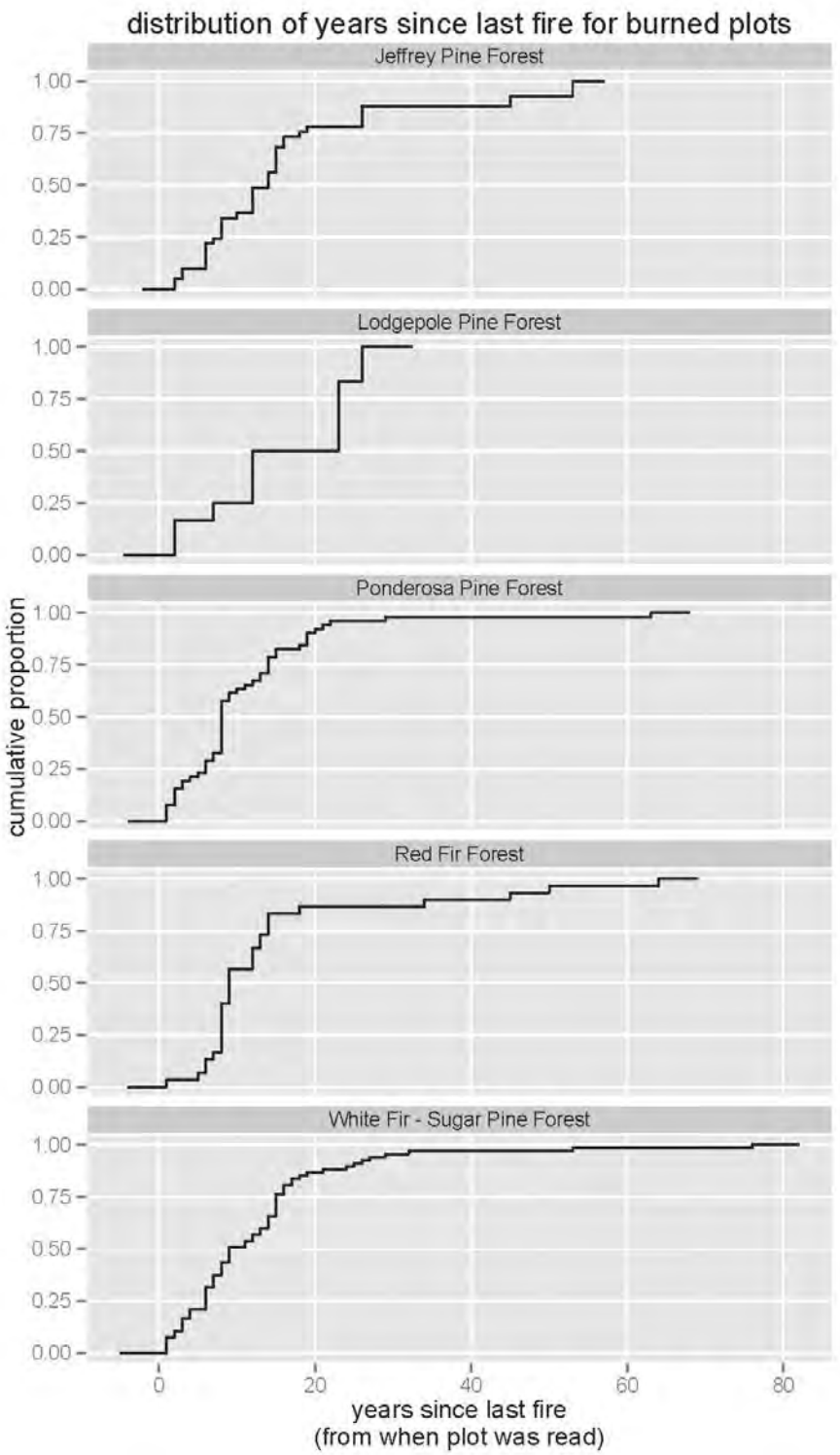


**Figure 7b**. Cumulative proportion of years since last fire for the plots used to calculate burned carbon within each of the 5 major forest types analyzed.

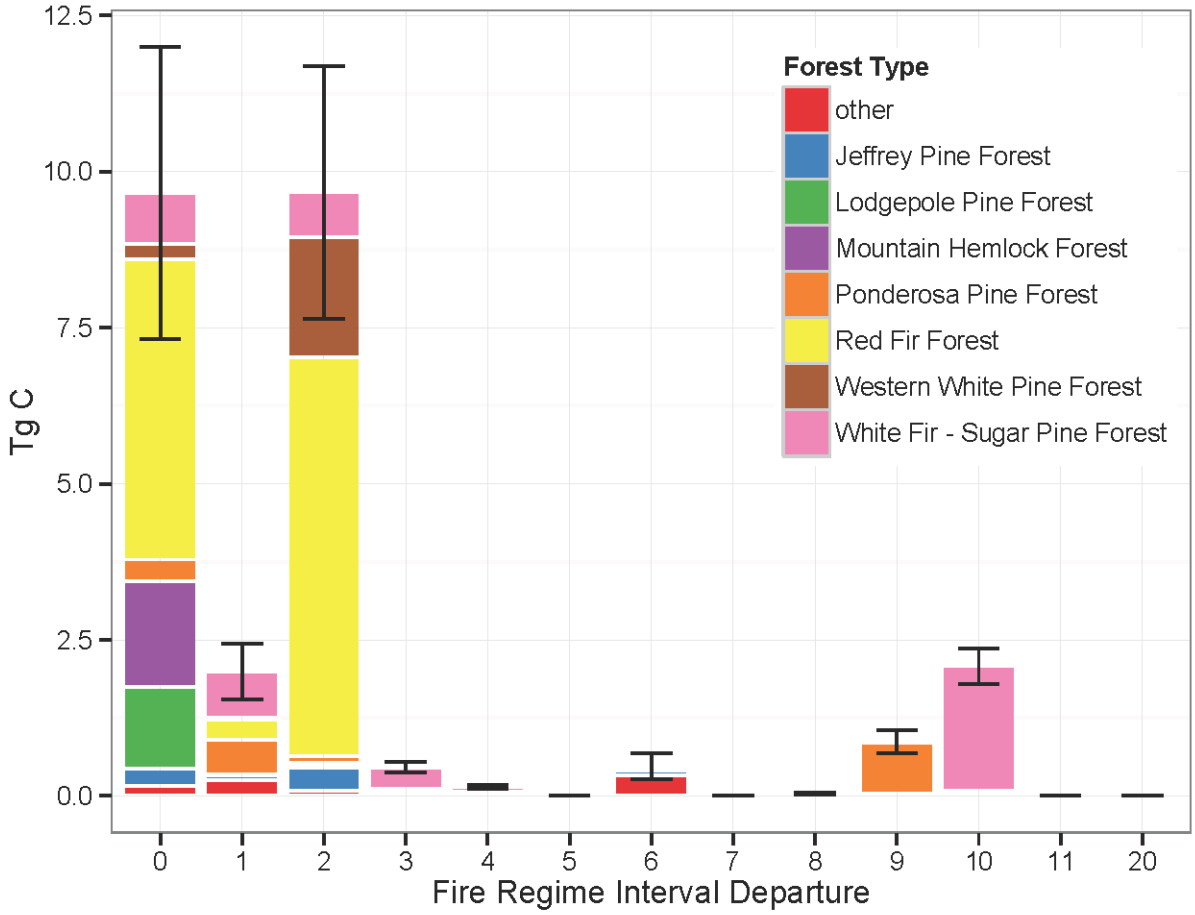


**Figure 8**. Relative stability of carbon (95% CI) within major vegetation types based on fire regime interval departure (FRID) within Yosemite National Park.

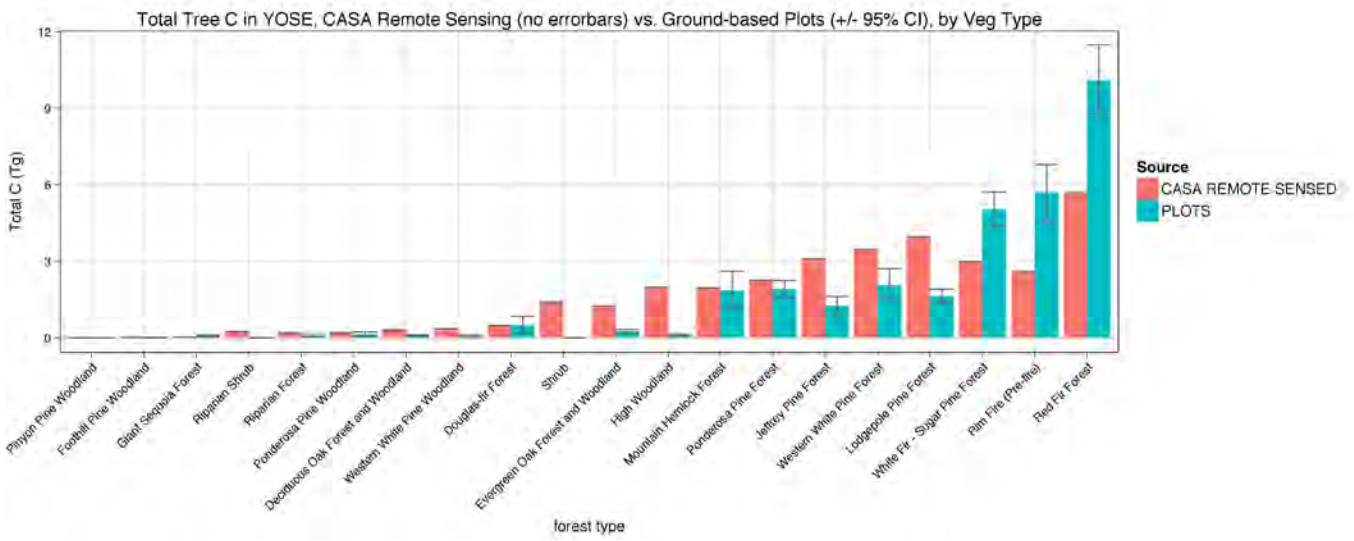


**Figure 9**.Comparison of total tree carbon (95% CI) in Yosemite National Park derived from CASA remote sensing and the ground-based plots used in the current study.

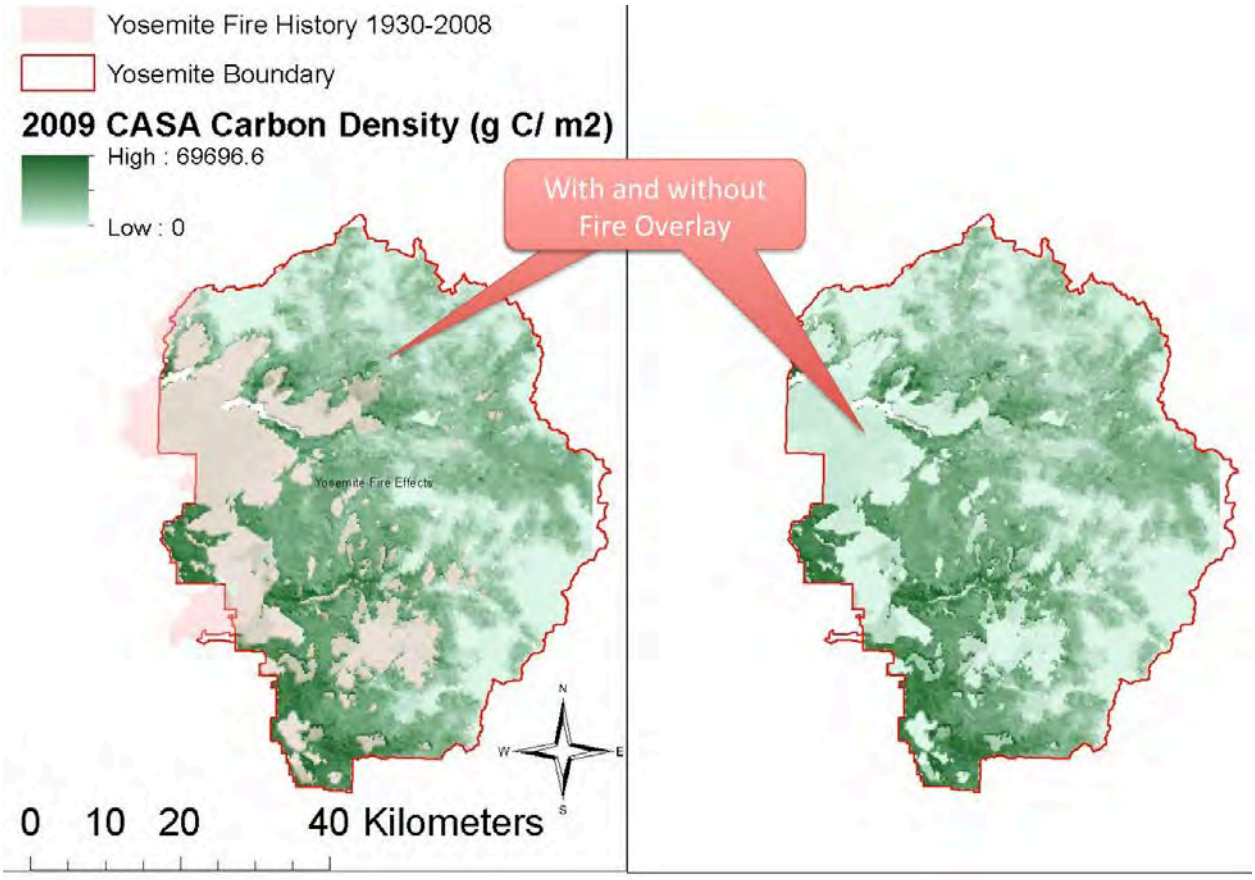


**Figure 10**. Total tree carbon in Yosemite National Park derived from CASA remote sensing and its relationship to fire history (1930-2008).

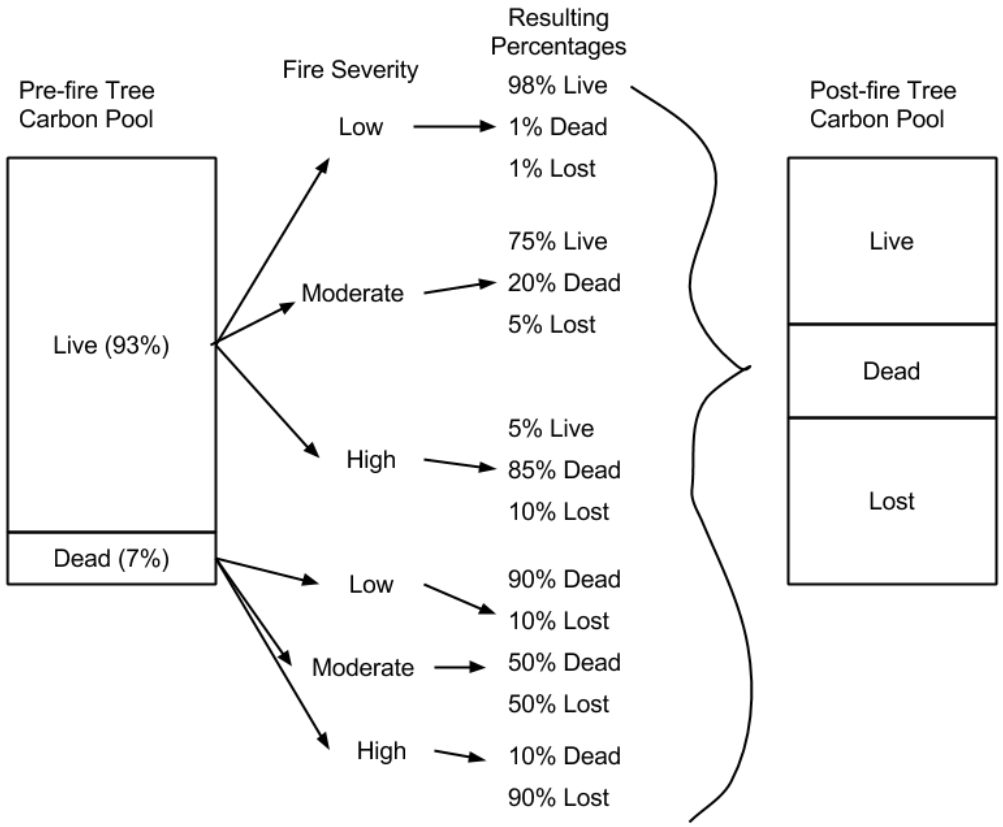


**Figure 11**. Fire severity and carbon dynamic conceptual model.

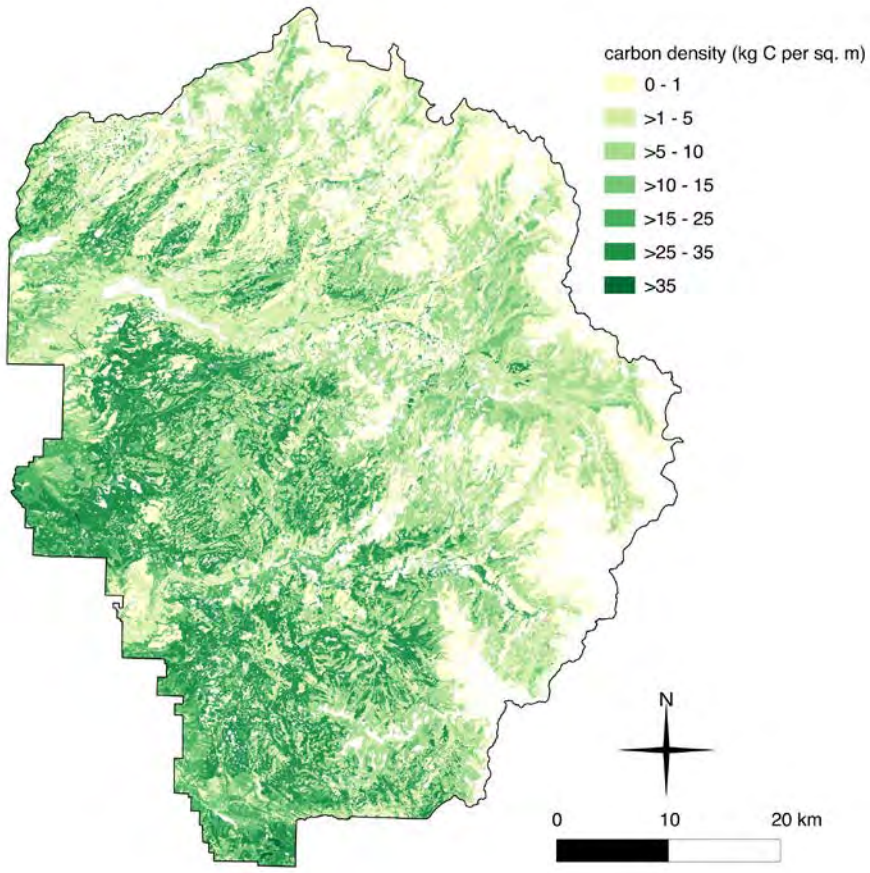


**Figure 12a**. Tree carbon density in Yosemite National Park.

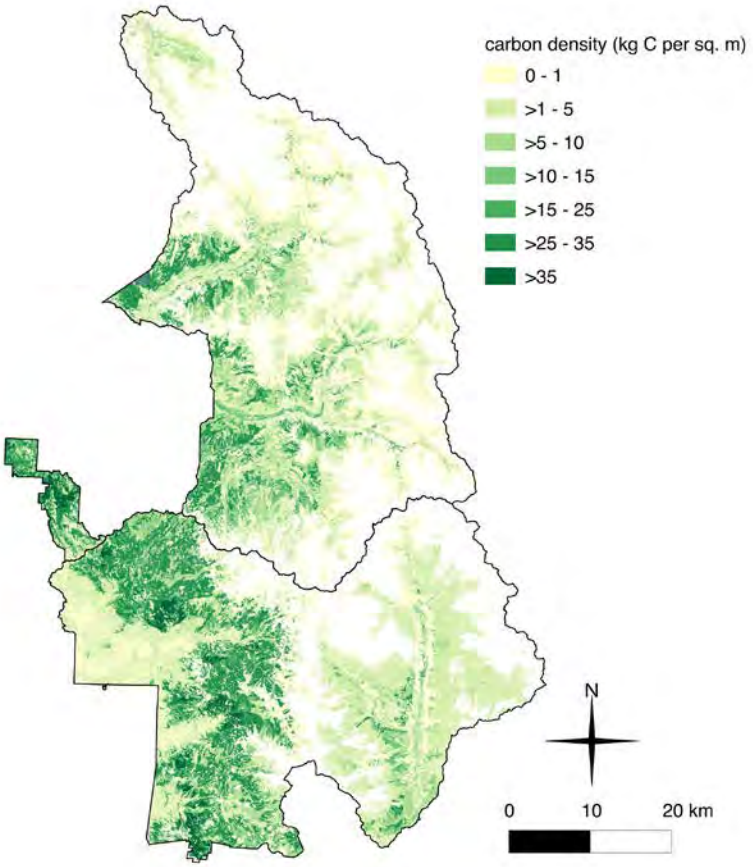


**Figure 12b**. Tree carbon density in Sequoia & Kings Canyon National Parks.

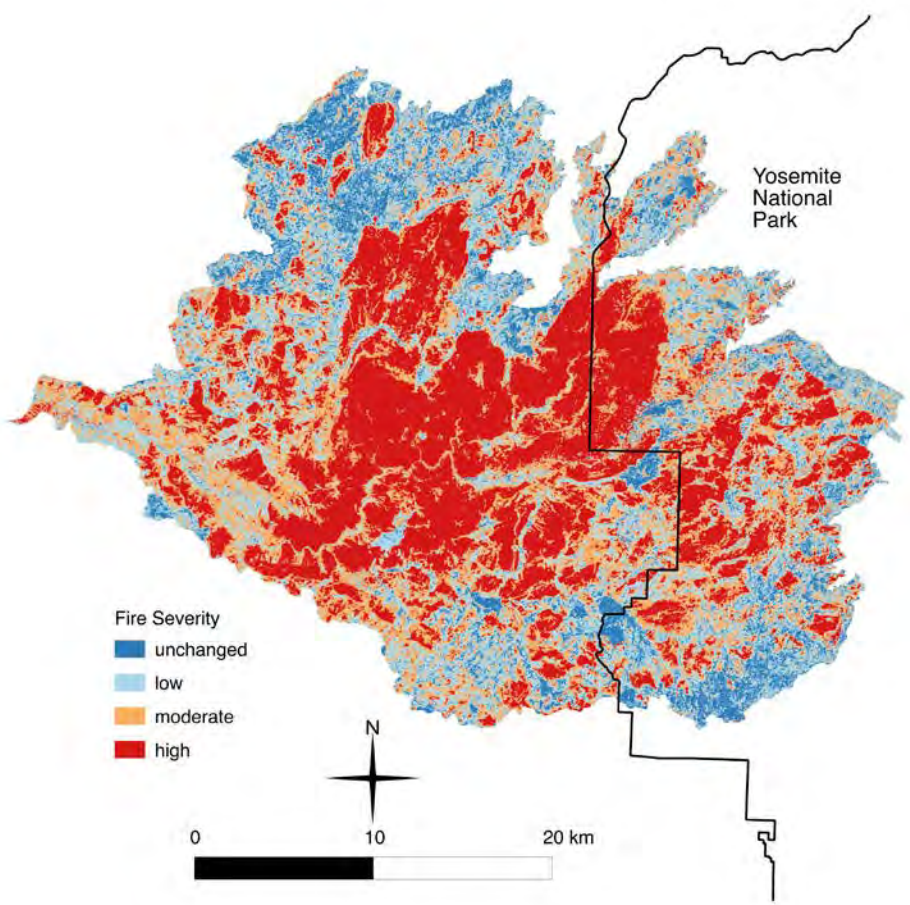


**Figure 13**. Initial fire severity for the 2013 Rim Fire.

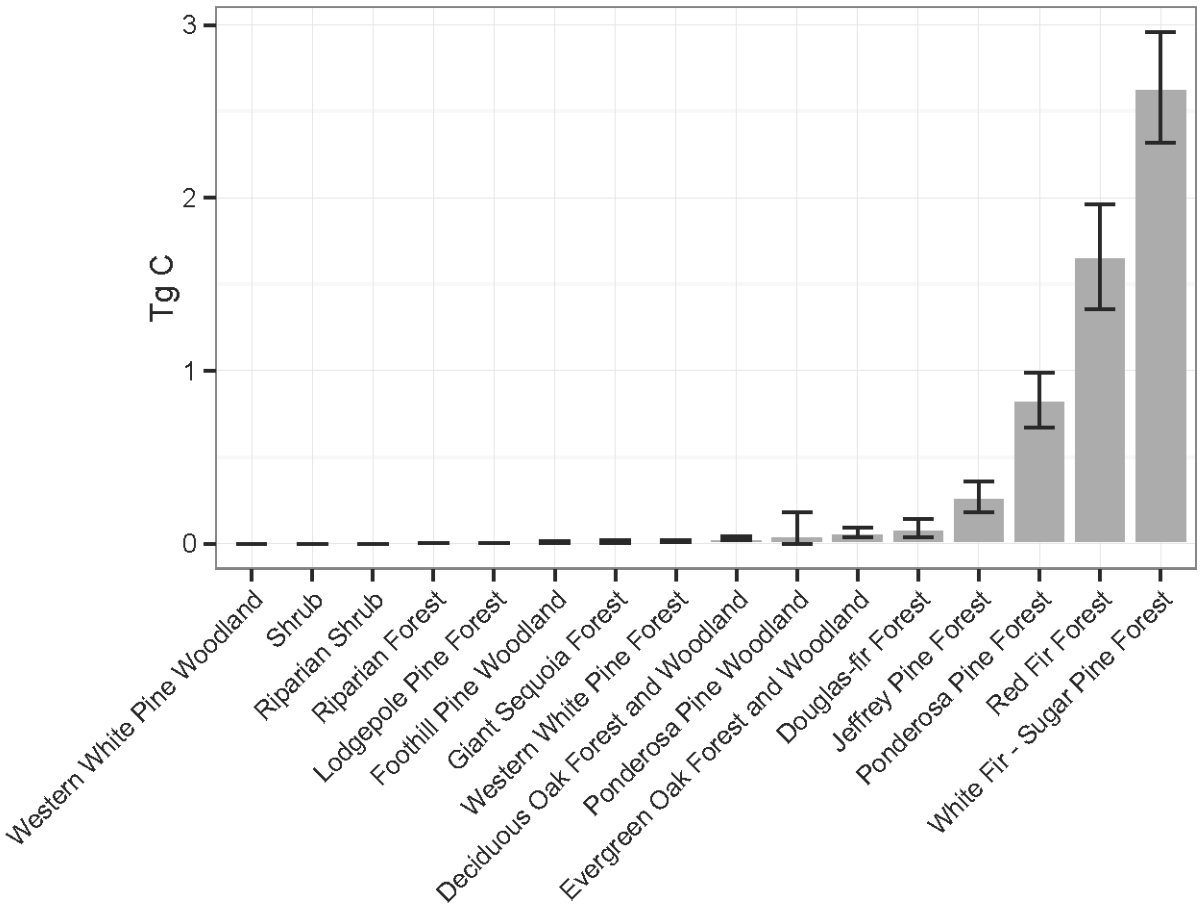


**Figure 14a.** Pre-fire carbon (95% CI) within the Rim fire perimeter, within Yosemite National Park (excludes areas burned outside the park boundaries).

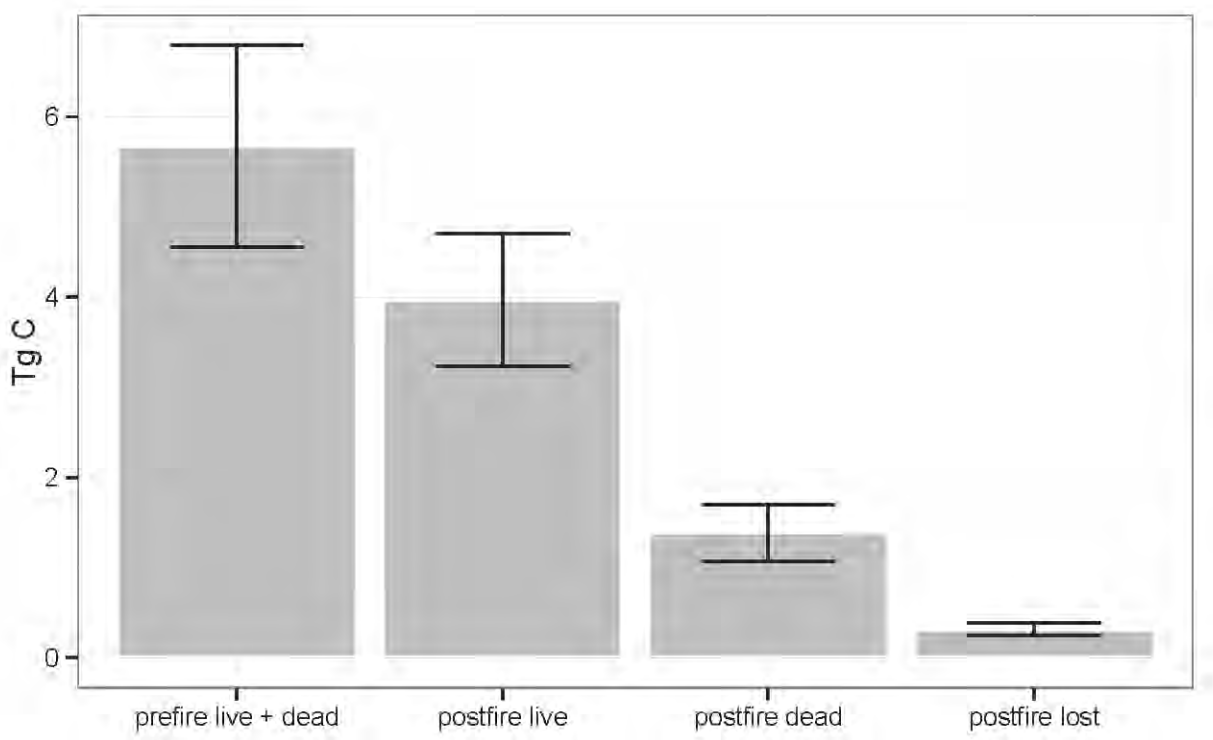


**Figure 14b**. Post-fire carbon (95% CI) within the Rim fire perimeter, within Yosemite National Park (excludes areas burned outside the park boundaries).

# Appendix A: Fire and Carbon Regime Categories Cross-walked to Mapped Vegetation Categories (Keeler-Wolf and Moore 2012)

| Mapped PI Code | Mapped Common Name | Mapped Vegetation Category | Fire and Carbon Regime Categories |
|---|---|---|---|
| 0 | none | | none |
| 100 | Alpine Talus Slope | No Biomass | Barren |
| 200 | Alpine Scree Slope | No Biomass | Barren |
| 300 | Alpine Snow Patch Communities | Herbaceous | Barren |
| 400 | Alpine Fell-field | No Biomass | Barren |
| 500 | Mesic Rock Outcrop | No Biomass | Barren |
| 700 | Boulder Field | No Biomass | Barren |
| 910 | Conifer Reproduction | Successional Conifer | Conifer Reproduction |
| 920 | Conifer Plantation | Successional Conifer | Ponderosa Pine |
| 940 | Sparsely Vegetated Undifferentiated | No Biomass | Barren |
| 941 | Sparsely Vegetated Riverine Flat | Herbaceous | Barren |
| 950 | Non-alpine Talus | No Biomass | Barren |
| 961 | Sparsely Vegetated to Non-vegetated Exposed Rock | No Biomass | Barren |
| 963 | Dome | No Biomass | Barren |
| 964 | Fissured Rock Outcrop | No Biomass | Barren |
| 965 | Sparsely Vegetated Rocky Streambed | No Biomass | Barren |
| 970 | Alpine Permanent Snowfield/Glacier | No Biomass | Barren |
| 980 | Water | No Biomass | Water |
| 981 | Permanently Flooded, Emergent, or Floating Vegetation Mapping Unit | No Biomass | Water |
| 990 | Urban/Developed | No Biomass | Barren |
| 1020 | Canyon Live Oak Forest Alliance | EVER-OAK Forest and Woodland | Live Oak |
| 1021 | Canyon Live Oak/Birchleaf Mountain Mahogany Forest Mapping Unit | EVER-OAK Forest and Woodland | Live Oak |
| 1022 | Canyon Live Oak/Whiteleaf Manzanita Forest Association | EVER-OAK Forest and Woodland | Live Oak |
| 1023 | Canyon Live Oak-(Ponderosa Pine-Incense-cedar) Forest Superassociation | EVER-OAK Forest and Woodland | Live Oak |
| 1024 | Canyon Live Oak-California Laurel Forest Superassociation | EVER-OAK Forest and Woodland | Live Oak |
| 1026 | Canyon Live Oak-Foothill Pine Forest Association | EVER-OAK Forest and Woodland | Live Oak |
| 1029 | Canyon live oak/Greenleaf Manzanita Forest Association | EVER-OAK Forest and Woodland | Live Oak |
| 1040 | Interior Live Oak Woodland Alliance | EVER-OAK Forest and | Live Oak |

| | | | |
|---|---|---|---|
| | | Woodland | |
| 1043 | Interior Live Oak-Canyon Live Oak Woodland Association | EVER-OAK Forest and Woodland | Live Oak |
| 1044 | Interior Live Oak-California Buckeye/Birchleaf Mountain Mahogany-California Redbud Forest Association | EVER-OAK Forest and Woodland | Live Oak |
| 1510 | Canyon Live Oak/California Buckeye Woodland & Interior Live Oak-California Buckeye S | EVER-OAK Forest and Woodland | Live Oak |
| 1520 | Blue Oak-(Interior Live Oak-Foothill Pine/Buckbrush/Annual Grass) Woodland Mapping U | EVER-OAK Forest and Woodland | Oak Woodland |
| 1530 | Interior Live Oak Woodland & Shrubland Superalliance | EVER-OAK Forest and Woodland | Live Oak |
| 2010 | Quaking Aspen Forest Alliance | Riparian Forest | Quaking Aspen |
| 2011 | Quaking Aspen/California False Hellebore Forest Association | Riparian Forest | Quaking Aspen |
| 2013 | Quaking Aspen/Willow spp. Forest Mapping Unit | Riparian Forest | Quaking Aspen |
| 2014 | Quaking Aspen/Willow spp. Talus Mapping Unit | Riparian Forest | Quaking Aspen |
| 2015 | Quaking Aspen-Jeffrey Pine/(Big Sagebrush) Forest Association | Riparian Forest | Quaking Aspen |
| 2016 | Quaking Aspen/Big Sagebrush Forest Superassociation | Riparian Forest | Quaking Aspen |
| 2017 | Quaking Aspen/Meadow Mapping Unit | Riparian Forest | Quaking Aspen |
| 2020 | California Black Oak Forest Alliance | DECID-OAK Forest and Woodland | Black Oak |
| 2021 | California Black Oak/Greenleaf Manzanita Forest Association | DECID-OAK Forest and Woodland | Black Oak |
| 2022 | California Black Oak-Incense-cedar Forest Association | EVER-OAK Forest and Woodland | Black Oak |
| 2025 | California Black Oak/(Bracken Fern) Forest Mapping Unit | DECID-OAK Forest and Woodland | Black Oak |
| 2030 | Blue Oak Woodland Alliance | DECID-OAK Forest and Woodland | Oak Woodland |
| 2033 | Blue Oak/Brome spp.-American Wild Carrot Woodland Association | DECID-OAK Forest and Woodland | Oak Woodland |
| 2034 | Blue Oak-Interior Live Oak/Brome spp.-American Wild Carrot Woodland Association | DECID-OAK Forest and Woodland | Oak Woodland |
| 2038 | Blue Oak-California Buckeye-(Interior Live Oak) Woodland Mapping Unit | DECID-OAK Forest and Woodland | Oak Woodland |
| 2040 | Valley Oak Woodland Alliance | DECID-OAK Forest and Woodland | Oak Woodland |
| 2050 | Black Cottonwood Temporarily Flooded Forest Alliance | Riparian Forest | Riparian |
| 2052 | Black Cottonwood-Quaking Aspen-(Jeffrey Pine)/Willow spp. Mapping Unit | Riparian Forest | Riparian |
| 2053 | Black Cottonwood Forest Association | Riparian Forest | Riparian |
| 2060 | White Alder Temporarily Flooded Forest Alliance | Riparian Shrub | Riparian |

| | | | |
|---|---|---|---|
| 2061 | White Alder-Red willow-California Sycamore Forest Association | Riparian Shrub | Riparian |
| 2070 | Mountain Alder Mapping Unit | Shrub | Riparian |
| 2080 | Bigleaf Maple Forest Alliance | DECID Forest | Riparian |
| 2100 | California Sycamore Temporarily Flooded Woodland Alliance | Riparian Forest | Riparian |
| 2102 | California Sycamore-(Canyon Live Oak-Interior Live Oak) Forest Mapping Unit | Riparian Forest | Riparian |
| 2110 | California Buckeye Woodland Alliance | EVER-OAK Forest and Woodland | Oak Woodland |
| 2114 | California Buckeye-Canyon Live Oak Woodland Association | EVER-OAK Forest and Woodland | Live Oak |
| 2510 | Willow spp. Forest Mapping Unit | Riparian Shrub | Riparian |
| 2520 | White Alder & Bigleaf Maple Forest Superalliance | Riparian Forest | Riparian |
| 2530 | Montane Broadleaf Deciduous Trees Mapping Unit | DECID Forest | Black Oak |
| 3010 | Sierra Lodgepole Pine-Quaking Aspen-(Jeffrey Pine) Forest Alliance | PICO Forest | Lodgepole Pine |
| 3012 | Sierra Lodgepole Pine-Quaking Aspen/(Kentucky Bluegrass) Forest Mapping Unit | PICO Forest | Lodgepole Pine |
| 3020 | Sierra Lodgepole Pine Forest Alliance | PICO Forest | Lodgepole Pine |
| 3022 | Sierra Lodgepole Pine/(Bog Blueberry) Forest Mapping Unit | PICO Forest | Lodgepole Pine |
| 3026 | Sierra Lodgepole Pine Rocky Woodlands Superassociation | PICO Forest | Lodgepole Pine |
| 3027 | Sierra Lodgepole Pine/(Big Sagebrush-Roundleaf Snowberry-Currant-Red Mountainheather | PICO Forest | Lodgepole Pine |
| 3028 | Sierra Lodgepole Pine-(Whitebark Pine)/(Ross Sedge-Shorthair Sedge) Forest Superassociation | PICO Forest | Lodgepole Pine |
| 3034 | Sierra Lodgepole Pine/Big Sagebrush Forest Association | PICO Forest | Lodgepole Pine |
| 3047 | Sierra Lodgepole Pine/(Big Sagebrush)/(Kentucky Bluegrass) Forest Mapping Unit | PICO Forest | Lodgepole Pine |
| 3048 | Sierra Lodgepole Pine Mesic Forest Superassociation | PICO Forest | Lodgepole Pine |
| 3049 | Sierra Lodgepole Pine Xeric Forest Superassociation | PICO Forest | Lodgepole Pine |
| 3050 | Ponderosa Pine Woodland Alliance | PIPO Woodland | Ponderosa Pine |
| 3053 | Ponderosa Pine-California Black Oak/Whiteleaf Manzanita Woodland Association | PIPO Woodland | Ponderosa Pine |
| 3060 | Ponderosa Pine-Incense-cedar Forest Alliance | PIPO Forest | Ponderosa Pine |
| 3061 | Ponderosa Pine-Incense-cedar-Canyon Live Oak/Mountain Misery Forest Association | PIPO Forest | Ponderosa Pine |
| 3062 | Ponderosa Pine-Incense-cedar/Mountain Misery Forest Association | PIPO Forest | Ponderosa Pine |
| 3063 | Ponderosa Pine-Incense-cedar-California Black Oak Forest Association | PIPO Forest | Ponderosa Pine |
| 3066 | Ponderosa Pine-Incense-cedar-(California Black Oak-Canyon Live Oak) | PIPO Forest | Ponderosa Pine |
| 3070 | Jeffrey Pine Woodland Alliance | PIJE Woodland | Jeffrey Pine |
| 3072 | Jeffrey Pine/Greenleaf Manzanita Woodland Association | PIJE Woodland | Jeffrey Pine |
| 3073 | Jeffrey Pine/Whitethorn Ceanothus Woodland Association | PIJE Woodland | Jeffrey Pine |
| 3075 | Jeffrey Pine/Huckleberry Oak Woodland Association | PIJE Woodland | Jeffrey Pine Shrub |
| 3076 | Jeffrey Pine/Antelope Bitterbrush Woodland Association | PIJE Woodland | Jeffrey Pine Shrub |
| 3081 | Jeffrey Pine?Singleleaf Pinyon Pine Woodland Association | PIJE Woodland | Jeffrey Pine - Pinyon Pine Shrub |
| 3082 | Jeffrey Pine/Curl-leaf Mountain Mahogany Woodland Association | PIJE Woodland | Jeffrey Pine Shrub |

| | | | |
|---|---|---|---|
| 3083 | Jeffrey Pine-White Fir/Roundleaf Snowberry/Squirreltail Woodland Association | PIJE Woodland | Jeffrey Pine |
| 3084 | Jeffrey Pine-Canyon Live Oak/Whiteleaf Manzanita Woodland Association | PIJE Woodland | Jeffrey Pine |
| 3085 | Jeffrey Pine-California Red Fir Woodland Association | PIJE Woodland | Jeffrey Pine - Western White Pine |
| 3090 | Foothill Pine Woodland Alliance | LOW Woodland | Conifer Patches |
| 3097 | Foothill Pine-Interior Live Oak/(Whiteleaf Manzanita-Buckbrush-Chamise) Woodland Sup | LOW Woodland | Conifer Patches |
| 3101 | Knobcone Pine/Whiteleaf Manzanita Woodland Association | Shrub | Conifer Patches |
| 3102 | Knobcone Pine-Canyon Live Oak Woodland Mapping Unit | Shrub | Conifer Patches |
| 3105 | Knobcone Pine/Chamise Woodland Association | Shrub | Conifer Patches |
| 3110 | Single-leaf Pinyon Pine Woodland Alliance | LOW Woodland | Pinyon - Juniper |
| 3112 | Singleleaf Pinyon Pine/Curl-leaf Mountain Mahogany-Big Sagebrush-Antelope Bitterbrus | LOW Woodland | Pinyon Pine - Sierra Juniper Shrub |
| 3113 | Singleleaf Pinyon Pine/(Desert Gooseberry-Big Sagebrush/Squirreltail) Woodland Super | LOW Woodland | Pinyon Pine - Sierra Juniper Shrub |
| 3114 | Single-leaf Pinyon Pine-Canyon Live Oak/Whiteleaf Manzanita Woodland Association | LOW Woodland | Pinyon - Juniper |
| 3130 | Western White Pine Woodland Alliance | PIMO Woodland | Jeffrey Pine - Western White Pine |
| 3131 | Western White Pine/Western Needlegrass Woodland Mapping Unit | PIMO Woodland | Jeffrey Pine - Western White Pine |
| 3133 | Western White Pine/(Greenleaf Manzanita-Bush Chinquapin-Oceanspray) Woodland Mapping Unit | PIMO Woodland | Jeffrey Pine - Western White Pine |
| 3140 | Whitebark Pine Woodland Alliance | HIGH Woodland | Whitebark Pine - Mountain Hemlock |
| 3142 | Whitebark Pine/DavidsonÆs Penstemon Woodland Association | HIGH Woodland | Whitebark Pine - Mountain Hemlock |
| 3143 | Whitebark Pine/(Ross Sedge-Shorthair Sedge) Woodland Superassociation | HIGH Woodland | Whitebark Pine - Mountain Hemlock |
| 3144 | Whitebark Pine/Shorthair Sedge Woodland Association | HIGH Woodland | Whitebark Pine - Mountain Hemlock |
| 3147 | Whitebark Pine-Mountain Hemlock Woodland Association | HIGH Woodland | Whitebark Pine - Mountain Hemlock |
| 3148 | Whitebark Pine-Mountain Hemlock Woodland Association | HIGH Woodland | Whitebark Pine - Mountain Hemlock |
| 3149 | Whitebark Pine-(Sierra Lodgepole Pine-Mountain Hemlock) Krummholz Conifer Mapping Un | HIGH Woodland | Whitebark Pine - Mountain Hemlock |
| 3150 | Limber Pine Woodland Alliance | HIGH Woodland | Whitebark Pine - Mountain Hemlock |
| 3200 | Foxtail Pine Woodland Alliance | Foxtail Pine | Foxtail Pine |
| 3202 | Foxtail Pine/Bush Chinquapin Woodland Association | Foxtail Pine | Foxtail Pine |

| | | | |
|---|---|---|---|
| 3203 | Foxtail Pine Woodland Superassociation | Foxtail Pine | Foxtail Pine |
| 3204 | Foxtail Pine-Western White Pine Woodland Superassociation | Foxtail Pine | Foxtail Pine |
| 3205 | Dead Foxtail Pine Mapping Unit | Foxtail Pine | Foxtail Pine |
| 3520 | (Foxtail Pine-Sierra Lodgepole Pine-Whitebark Pine) Krummholz Woodland Mapping Unit | Foxtail Pine | Foxtail Pine |
| 3530 | Whitebark Pine-Foxtail Pine-Lodgepole Pine Woodland Superalliance | HIGH Woodland | Whitebark Pine - Mountain Hemlock |
| 3540 | Foxtail Pine-Lodgepole Pine Woodland Superalliance | Foxtail Pine | Foxtail Pine |
| 4012 | Douglas-fir-Canyon Live Oak Forest Association | Douglas-fir Forest | Live Oak |
| 4014 | Douglas-fir-White Alder Forest Association | Douglas-fir Forest | Riparian |
| 4020 | Giant Sequoia Forest Alliance | SEGI Forest | Giant Sequoia |
| 4021 | Giant Sequoia-Sugar Pine/Pacific Dogwood Forest Association | SEGI Forest | Giant Sequoia |
| 4023 | Giant Sequoia-White Fir-California Red Fir Forest Association | SEGI Forest | Giant Sequoia |
| 4030 | Mountain Hemlock Forest Alliance | TSME Forest | Whitebark Pine - Mountain Hemlock |
| 4033 | Mountain Hemlock-Western White Pine Forest Association | TSME Forest | Whitebark Pine - Mountain Hemlock |
| 4035 | Mountain Hemlock-(Western White Pine-Sierra Lodgepole Pine) Forest | TSME Forest | Whitebark Pine - Mountain Hemlock |
| 4041 | Mountain Hemlock-Sierra Lodgepole Pine Forest Association | TSME Forest | Whitebark Pine - Mountain Hemlock |
| 4042 | Mountain Hemlock-Sierra Lodgepole Pine-Whitebark Pine Forest Mapping Unit | TSME Forest | Whitebark Pine - Mountain Hemlock |
| 4043 | Mountain Hemlock-Sierra Lodgepole Pine-Western White Pine Forest Association | TSME Forest | Whitebark Pine - Mountain Hemlock |
| 4050 | California Red Fir Forest Alliance | ABMA Forest | Red Fir |
| 4051 | California Red Fir Forest Association | ABMA Forest | Red Fir |
| 4056 | California Red Fir-(Sierra Lodgepole Pine) Forest Superassociation | ABMA Forest | Red Fir |
| 4057 | California Red Fir-Western White Pine Forest Association | ABMA Forest | Red Fir |
| 4063 | California Red Fir-Sierra Lodgepole Pine/Whiteflower Hawkweed Forest Mapping Unit | ABMA Forest | Red Fir |
| 4064 | California Red Fir-(Western White Pine)/(Pinemat Manzanita-Bush Chinquapin) Forest Mapping Unit | ABMA Forest | Red Fir |
| 4069 | California Red Fir-(Western White Pine)/(Bush Chinquapin-Huckleberry Oak-Pinemat Man | ABMA Forest | Red Fir |
| 4070 | California Red Fir-White Fir Forest Alliance | ABMA Forest | Red Fir |
| 4080 | White Fir -Sugar Pine Forest Alliance | ABCO-PILA Forest | White Fir |
| 4081 | White Fir Forest Mapping Unit | ABCO-PILA Forest | White Fir |
| 4082 | White Fir Mature Even-age Stands Mapping Unit | ABCO-PILA Forest | White Fir |
| 4084 | White Fir-(California Red Fir-Sugar Pine-Jeffrey Pine)/Whitethorn Ceanothus-(Greenleaf Manzanita) Forest Mapping Unit | ABCO-PILA Forest | White Fir |
| 4085 | White Fir East Side Mapping Unit | PIJE Woodland | White Fir |

| | | | |
|---|---|---|---|
| 4094 | White Fir-Sugar Pine-Incense-cedar Forest Superassociation | ABCO-PILA Forest | White Fir |
| 4095 | White Fir-Sugar Pine/Greenleaf Manzanita-Whitethorn Ceanothus Forest Mapping Unit | ABCO-PILA Forest | White Fir |
| 4100 | Sierra Juniper Woodland Alliance | HIGH Woodland | Sierra Juniper |
| 4101 | Sierra Juniper/(Oceanspray) Woodland Superassociation | HIGH Woodland | Sierra Juniper |
| 4107 | Sierra Juniper/Curl-leaf Mountain Mahogany-Big Sagebrush Woodland Association | HIGH Woodland | Sierra Juniper |
| 4108 | Sierra Juniper Woodland Association | HIGH Woodland | Sierra Juniper |
| 4109 | Sierra Juniper/(Oceanspray-Big Sagebrush) Woodland Superassociation | HIGH Woodland | Sierra Juniper |
| 4111 | Incense-cedar-White Alder Forest Association | Successional Conifer | Riparian |
| 4510 | Western White Pine-(California Red Fir-Sierra Lodgepole Pine) Forest Superalliance | PIMO Forest | Jeffrey Pine - Western White Pine |
| 4520 | White Fir-(California Red Fir-Sugar Pine-Jeffrey Pine)/(Pinemat Manzanita-Whitethorn | ABCO-PILA Forest | White Fir Shrub |
| 4530 | White Fir-Sugar Pine-(Incense-cedar-Jeffrey Pine) Forest Mapping Unit | ABCO-PILA Forest | White Fir |
| 4540 | Western White Pine-Sierra Lodgepole Pine-(California Red Fir) Woodland Superassociation | PIMO Woodland | Lodgepole Pine |
| 4550 | Douglas-fir-(White Fir-Incense-cedar-Ponderosa Pine) Forest Mapping Unit | Douglas-fir Forest | White Fir |
| 5010 | Birchleaf Mountain Mahogany Shrubland Alliance | Shrub | Lower Montane Chaparral |
| 5011 | Birchleaf Mountain Mahogany-California Redbud-California Flannelbush Shrubland Association | Shrub | Lower Montane Chaparral |
| 5012 | Birchleaf Mountain Mahogany-Whiteleaf Manzanita Shrubland Association | Shrub | Lower Montane Chaparral |
| 5020 | Chamise Shrubland Alliance | Shrub | Foothill Chaparral |
| 5021 | Chamise Shrubland Association | Shrub | Foothill Chaparral |
| 5022 | Chamise-Whiteleaf Manzanita Shrubland Association | Shrub | Foothill Chaparral |
| 5023 | Chamise-Chaparral Yucca Shrubland Association | Shrub | Foothill Chaparral |
| 5025 | Chamise-California Yerba Santa Shrubland Association | Shrub | Foothill Chaparral |
| 5031 | Chamise-Buckbrush Shrubland Association | Shrub | Foothill Chaparral |
| 5041 | Interior Live Oak-California Buckeye Shrubland Association | Shrub | Live Oak |
| 5050 | Buckbrush Shrubland Alliance | Shrub | Foothill Chaparral |
| 5060 | Chaparral Whitethorn Shrubland Alliance | Shrub | Foothill Chaparral |
| 5070 | Whiteleaf Manzanita Shrubland Alliance | Shrub | Lower Montane Chaparral |
| 5090 | Greenleaf Manzanita Shrubland Alliance | Shrub | Upper Montane Chaparral |
| 5110 | Whitethorn Ceanothus Shrubland Alliance | Shrub | Upper Montane Chaparral |
| 5120 | Tobacco Brush Shrubland Alliance | Shrub | Eastside Chaparral |
| 5130 | Mountain Misery Dwarf-shrubland Alliance | Shrub | Upper Montane Chaparral |
| 5131 | Mountain Misery-Manzanita spp. Mapping Unit | Shrub | Lower Montane Chaparral |
| 5140 | Indian Manzanita Shrubland Alliance | Shrub | Lower Montane Chaparral |
| 5160 | Big Sagebrush Shrubland Alliance | Shrub | Eastside Chaparral |

| | | | |
|---|---|---|---|
| 5200 | Timberline Sagebrush Shrubland Alliance | Shrub | Eastside Chaparral |
| 5210 | Low Sagebrush Dwarf-shrubland Alliance | Shrub | Eastside Chaparral |
| 5230 | Curl-leaf Mountain Mahogany Woodland Alliance | Shrub | Eastside Chaparral |
| 5240 | Antelope Bitterbrush Shrubland Alliance | Shrub | Eastside Chaparral |
| 5250 | (Silver Lupine)/Brome spp. Shrubland Mapping Unit | Herbaceous | Oak Woodland |
| 5260 | Big Sagebrush-(Silver Sagebrush) Shrubland Mapping Unit | Shrub | Eastside Chaparral |
| 5270 | Chaparral Yucca Shrubland Alliance | Shrub | Lower Montane Chaparral |
| 5280 | Pinemat Manzanita Dwarf-shrubland Alliance | Shrub | Upper Montane Chaparral |
| 5300 | Water Birch Shrubland Alliance | Shrub | Riparian |
| 5510 | Mountain Big Sagebrush & Timberline Sagebrush & Oceanspray & Red Mountainheather Shrubland Superalliance | Shrub | Eastside Chaparral |
| 5530 | Bitter Cherry-Gooseberry spp.-(Mountain Maple) Shrubland Mapping Unit | Shrub | Upper Montane Chaparral |
| 5550 | Red Mountainheather Dwarf-shrubland Alliance | Shrub | Eastside Chaparral |
| 5560 | Chamise-(Buckbrush-Whiteleaf Manzanita) Shrubland Mapping Unit | Shrub | Foothill Chaparral |
| 5570 | Greenleaf Manzanita & Bush Chinquapin & Huckleberry Oak Shrubland Superalliance | Shrub | Upper Montane Chaparral |
| 5580 | Birchleaf Mountain Mahogany & Buckbrush & Whiteleaf Manzanita Shrubland Superallianc | Shrub | Lower Montane Chaparral |
| 5590 | Greenleaf Manzanita-Bush Chinquapin-Whitethorn Ceanothus Shrubland Superalliance | Shrub | Upper Montane Chaparral |
| 6010 | Deerbrush Shrubland Alliance | Shrub | Upper Montane Chaparral |
| 6012 | Deerbrush-Whiteleaf Manzanita Shrubland Association | Shrub | Lower Montane Chaparral |
| 6020 | Oregon White Oak Shrubland Alliance | Shrub | Upper Montane Chaparral |
| 6022 | Oregon White Oak-Birchleaf Mountain Mahogany Shrubland Association | Shrub | Upper Montane Chaparral |
| 6030 | California Grape Association | Shrub | Riparian |
| 6110 | Sierra Willow/Swamp Onion Seasonally Flooded Shrubland Alliance | Shrub | Riparian |
| 6210 | Oceanspray Shrubland Alliance | Shrub | Eastside Chaparral |
| 6300 | Bitter Cherry Shrubland Alliance | Shrub | Upper Montane Chaparral |
| 6500 | Willow spp./Meadow Shrubland Mapping Unit | Riparian Shrub | Riparian |
| 6600 | Willow spp. Riparian Shrubland Mapping Unit | Riparian Shrub | Riparian |
| 6700 | Willow spp. Talus Shrubland Mapping Unit | Riparian Shrub | Riparian |
| 6900 | Mesic Montane Shrubland Mapping Unit | Shrub | Upper Montane Chaparral |
| 7000 | Upland Herbaceous | Herbaceous | Meadow |
| 7120 | Shorthair Sedge Herbaceous Alliance | Herbaceous | Meadow |
| 7260 | California Annual Grassland/Herbland Superalliance | Herbaceous | Oak Woodland |
| 7550 | Upland herbaceous | Herbaceous | Meadow |
| 7701 | Post-clearcut Shrub/Herbaceous Mapping Unit | Herbaceous | Lower Montane |

| | | | |
|---|---|---|---|
| | | | Chaparral |
| 7702 | Mesic Post Fire Herbaceous Mapping Unit | Herbaceous | Meadow |
| 7703 | Post Fire Shrub/Herbaceous Mapping Unit | Shrub | Lower Montane Chaparral |
| 8000 | Intermittently to Seasonally Flooded Meadow | Herbaceous | Meadow |
| 9000 | Semi-permanent to Permanently Flooded Meadow | Herbaceous | Meadow |
| 9030 | Bullrush-Cattail Mapping Unit | Herbaceous | Meadow |

# Appendix B: Allometric Equations and Citations

| code | scientific name | minumum applied DBH | maximum applied DBH | ceiling DBH | component | equation species | a | b | SEE | citation ID |
|---|---|---|---|---|---|---|---|---|---|---|
| ABCO | Abies concolor | 0 | 6.9999 | 1000 | tree | small conifer | -1.8516 | 2.3701 | 0.1191 | 15 |
| ABCO | Abies concolor | 7 | 98 | 1000 | tree | Abies concolor | -2.5521 | 2.5043 | 0.16805 | 2 |
| ABCO | Abies concolor | 98.0001 | 1000 | 1000 | bole | Abies procera | -3.0319 | 2.5812 | 0.1841 | 4 |
| ABCO | Abies concolor | 98.0001 | 1000 | 111 | branch live | Abies pooled | -4.9318 | 2.5585 | 0.454 | 8 |
| ABCO | Abies concolor | 98.0001 | 1000 | 111 | foliage | Abies pooled | -3.5458 | 1.9278 | 0.399 | 8 |
| ABIES | Abies | 0 | 27.5 | 1000 | tree | small conifer | -1.8516 | 2.3701 | 0.1191 | 15 |
| ABIES | Abies | 27.5001 | 100 | 1000 | tree | Abies magnifica | -4.3136 | 2.9121 | 0.22074 | 2 |
| ABIES | Abies | 100.0001 | 1000 | 1000 | bole | Abies procera | -3.0319 | 2.5812 | 0.1841 | 4 |
| ABIES | Abies | 100.0001 | 1000 | 111 | branch live | Abies pooled | -4.9318 | 2.5585 | 0.454 | 8 |
| ABIES | Abies | 100.0001 | 1000 | 111 | foliage | Abies pooled | -3.5458 | 1.9278 | 0.399 | 8 |
| ABMA | Abies magnifica | 0 | 27.5 | 1000 | tree | small conifer | -1.8516 | 2.3701 | 0.1191 | 15 |
| ABMA | Abies magnifica | 27.5001 | 100 | 1000 | tree | Abies magnifica | -4.3136 | 2.9121 | 0.22074 | 2 |
| ABMA | Abies magnifica | 100.0001 | 1000 | 1000 | bole | Abies procera | -3.0319 | 2.5812 | 0.1841 | 4 |
| ABMA | Abies magnifica | 100.0001 | 1000 | 111 | branch live | Abies pooled | -4.9318 | 2.5585 | 0.454 | 8 |
| ABMA | Abies magnifica | 100.0001 | 1000 | 111 | foliage | Abies pooled | -3.5458 | 1.9278 | 0.399 | 8 |
| ABMAM | Abies magnifica var. magnifica | 0 | 27.5 | 1000 | tree | small conifer | -1.8516 | 2.3701 | 0.1191 | 15 |
| ABMAM | Abies magnifica var. magnifica | 27.5001 | 100 | 1000 | tree | Abies magnifica | -4.3136 | 2.9121 | 0.22074 | 2 |
| ABMAM | Abies magnifica var. magnifica | 100.0001 | 1000 | 1000 | bole | Abies procera | -3.0319 | 2.5812 | 0.1841 | 4 |
| ABMAM | Abies magnifica var. magnifica | 100.0001 | 1000 | 111 | branch live | Abies pooled | -4.9318 | 2.5585 | 0.454 | 8 |
| ABMAM | Abies magnifica var. magnifica | 100.0001 | 1000 | 111 | foliage | Abies pooled | -3.5458 | 1.9278 | 0.399 | 8 |
| ABMAS | Abies magnifica var. shastensis | 0 | 27.5 | 1000 | tree | small conifer | -1.8516 | 2.3701 | 0.1191 | 15 |
| ABMAS | Abies magnifica var. shastensis | 27.5001 | 100 | 1000 | tree | Abies magnifica | -4.3136 | 2.9121 | 0.22074 | 2 |
| ABMAS | Abies magnifica var. shastensis | 100.0001 | 1000 | 1000 | bole | Abies procera | -3.0319 | 2.5812 | 0.1841 | 4 |
| ABMAS | Abies magnifica var. shastensis | 100.0001 | 1000 | 111 | branch live | Abies pooled | -4.9318 | 2.5585 | 0.454 | 8 |
| ABMAS | Abies magnifica var. shastensis | 100.0001 | 1000 | 111 | foliage | Abies pooled | -3.5458 | 1.9278 | 0.399 | 8 |
| ACMA3 | Acer macrophyllum | 0 | 7.5999 | 1000 | tree | soft maple/birch | -2.0332 | 2.3651 | 0.491685 | 16 |
| ACMA3 | Acer macrophyllum | 7.6 | 1000 | 1000 | bole bark | Acer macrophyllum | -4.5757 | 2.574 | 0.058 | 7 |
| ACMA3 | Acer macrophyllum | 7.6 | 1000 | 1000 | bole wood | Acer macrophyllum | -3.4931 | 2.723 | 0.014 | 7 |
| ACMA3 | Acer macrophyllum | 7.6 | 1000 | 1000 | branch dead | Acer macrophyllum | -3.8495 | 1.092 | 1.862 | 7 |

| | | | | | | | | | | |
|---|---|---|---|---|---|---|---|---|---|---|
| ACMA3 | Acer macrophyllum | 7.6 | 1000 | 1000 | branch live | Acer macrophyllum | -4.2613 | 2.43 | 0.225 | 7 |
| ACMA3 | Acer macrophyllum | 7.6 | 1000 | 1000 | foliage | Acer macrophyllum | -3.7701 | 1.617 | 0.101 | 7 |
| AECA | Aesculus californica | 0 | 1000 | 1000 | tree | mixed hardwood | -2.545 | 2.4835 | 0.360458 | 16 |
| ALRH2 | Alnus rhombifolia | 0 | 1000 | 1000 | tree | aspen/alder/cottonwood/willow | -2.3381 | 2.3867 | 0.507441 | 16 |
| ARVI4 | Arctostaphylos viscida | 0 | 1000 | 1000 | tree | mixed hardwood | -2.545 | 2.4835 | 0.360458 | 16 |
| ARVIV | Arctostaphylos viscida ssp. viscida | 0 | 1000 | 1000 | tree | mixed hardwood | -2.545 | 2.4835 | 0.360458 | 16 |
| BEOC2 | Betula occidentalis | 0 | 1000 | 1000 | tree | soft maple/birch | -2.0332 | 2.3651 | 0.491685 | 16 |
| CADE27 | Calocedrus decurrens | 0 | 1000 | 1000 | tree | cedar/larch | -2.077 | 2.2592 | 0.294574 | 16 |
| CEBEx | Cercocarpus betuloides | 0 | 1000 | 1000 | tree | mixed hardwood | -2.545 | 2.4835 | 0.360458 | 16 |
| CELE3 | Cercocarpus ledifolius | 0 | 1000 | 1000 | tree | mixed hardwood | -2.545 | 2.4835 | 0.360458 | 16 |
| CEOC3 | Cercis occidentalis | 0 | 1000 | 1000 | tree | mixed hardwood | -2.545 | 2.4835 | 0.360458 | 16 |
| COCOC | Corylus cornuta var. californica | 0 | 1000 | 1000 | tree | mixed hardwood | -2.545 | 2.4835 | 0.360458 | 16 |
| CONU4 | Cornus nuttallii | 0 | 1000 | 1000 | tree | mixed hardwood | -2.545 | 2.4835 | 0.360458 | 16 |
| FRDI2 | Fraxinus dipetala | 0 | 1000 | 1000 | tree | mixed hardwood | -2.545 | 2.4835 | 0.360458 | 16 |
| FRLA | Fraxinus latifolia | 0 | 1000 | 1000 | tree | mixed hardwood | -2.545 | 2.4835 | 0.360458 | 16 |
| FRVE2 | Fraxinus velutina | 0 | 1000 | 1000 | tree | mixed hardwood | -2.545 | 2.4835 | 0.360458 | 16 |
| jimUNKN | Jim Unknown | 0 | 15.8999 | 1000 | bole | small conifer | -1.915 | 2.348 | 0.1302 | 15 |
| jimUNKN | Jim Unknown | 15.9 | 1000 | 1000 | bole | Abies procera | -3.0319 | 2.5812 | 0.1841 | 4 |
| JUOC | Juniperus occidentalis | 0 | 1000 | 1000 | tree | Juniperus occidentalis | -5.6604 | 2.2462 | 0.1433 | 8 |
| JUOCA | Juniperus occidentalis var. australis | 0 | 1000 | 1000 | tree | Juniperus occidentalis | -5.6604 | 2.2462 | 0.1433 | 8 |
| JUOS | Juniperus osteosperma | 0 | 1000 | 1000 | tree | Juniperus occidentalis | -5.6604 | 2.2462 | 0.1433 | 8 |
| MALUS | Malus | 0 | 1000 | 1000 | tree | mixed hardwood | -2.545 | 2.4835 | 0.360458 | 16 |
| PIAL | Pinus albicaulis | 0 | 10 | 1000 | tree | Pinus albicaulis | -0.389 | 1.1585 | 0.4045 | 3 |
| PIAL | Pinus albicaulis | 10.0001 | 20 | 1000 | bole | Juniperus occidentalis | -8.3826 | 2.6378 | 0.159 | 8 |
| PIAL | Pinus albicaulis | 10.0001 | 20 | 1000 | canopy | Pinus albicaulis | -1.3017 | 1.2991 | 0.483 | 3 |
| PIAL | Pinus albicaulis | 20.0001 | 1000 | 1000 | tree | Juniperus occidentalis | -5.6604 | 2.2462 | 0.1433 | 8 |
| PIAT | Pinus attenuata | 0 | 1000 | 1000 | tree | pine | -2.5678 | 2.4349 | 0.253781 | 16 |
| PIBAA | Pinus balfouriana ssp. austrina | 0 | 10 | 1000 | tree | Pinus albicaulis | -0.389 | 1.1585 | 0.4045 | 3 |
| PIBAA | Pinus balfouriana ssp. austrina | 10.0001 | 20 | 1000 | bole | Juniperus occidentalis | -8.3826 | 2.6378 | 0.159 | 8 |
| PIBAA | Pinus balfouriana ssp. austrina | 10.0001 | 20 | 1000 | canopy | Pinus albicaulis | -1.3017 | 1.2991 | 0.483 | 3 |
| PIBAA | Pinus balfouriana ssp. austrina | 20.0001 | 1000 | 1000 | tree | Juniperus occidentalis | -5.6604 | 2.2462 | 0.1433 | 8 |
| PICOM | Pinus contorta var. murrayana | 0 | 19.9999 | 1000 | tree | Pinus contorta | -2.095 | 2.3909 | 0.4786 | 26 |
| PICOM | Pinus contorta var. murrayana | 20 | 1000 | 1000 | tree | Pinus contorta | -1.0386 | 1.9294 | 0.3205 | 1 |
| PIJE | Pinus jeffreyi | 0 | 22.3999 | 1000 | tree | small conifer | -1.8516 | 2.3701 | 0.1191 | 15 |
| PIJE | Pinus jeffreyi | 22.4 | 133.1 | 1000 | bole | Pinus jeffereyi | -5.1108 | 2.952 | 0.204834 | 4 |

| | | | | | | | | | | |
|---|---|---|---|---|---|---|---|---|---|---|
| PIJE | Pinus jeffreyi | 22.4 | 1000 | 162 | branches dead | Pseudotsuga menziesii | -3.794 | 1.7503 | 0.728 | 8 |
| PIJE | Pinus jeffreyi | 22.4 | 1000 | 162 | branches live | Pseudotsuga menziesii | -3.8938 | 2.1382 | 0.632 | 8 |
| PIJE | Pinus jeffreyi | 22.4 | 1000 | 162 | foliage | Pseudotsuga menziesii | -3.0877 | 1.7009 | 0.695 | 8 |
| PIJE | Pinus jeffreyi | 133.1001 | 1000 | 1000 | bole | Pseudotsuga menziesii | -2.2765 | 2.4247 | 0.2415 | 4 |
| PILA | Pinus lambertiana | 0 | 8.6999 | 1000 | tree | small conifer | -1.8516 | 2.3701 | 0.1191 | 15 |
| PILA | Pinus lambertiana | 8.7 | 179.6 | 1000 | bole | Pinus lambertiana | -3.6973 | 2.6863 | 0.193513 | 4 |
| PILA | Pinus lambertiana | 8.7 | 1000 | 162 | branches dead | Pseudotsuga menziesii | -3.794 | 1.7503 | 0.728 | 8 |
| PILA | Pinus lambertiana | 8.7 | 1000 | 162 | branches live | Pseudotsuga menziesii | -3.8938 | 2.1382 | 0.632 | 8 |
| PILA | Pinus lambertiana | 8.7 | 1000 | 162 | foliage | Pseudotsuga menziesii | -3.0877 | 1.7009 | 0.695 | 8 |
| PILA | Pinus lambertiana | 179.6001 | 1000 | 1000 | bole | Pseudotsuga menziesii | -2.2765 | 2.4247 | 0.2415 | 4 |
| PIMO | Pinus monophylla | 0 | 1000 | 1000 | tree | pine | -2.5678 | 2.4349 | 0.253781 | 16 |
| PIMO3 | Pinus monticola | 0 | 19.9999 | 1000 | tree | Pinus contorta | -2.095 | 2.3909 | 0.4786 | 26 |
| PIMO3 | Pinus monticola | 20 | 1000 | 1000 | tree | Pinus contorta | -1.0386 | 1.9294 | 0.3205 | 1 |
| PINUS | Pinus | 0 | 1000 | 1000 | tree | pine | -2.5678 | 2.4349 | 0.253781 | 16 |
| PIPO | Pinus ponderosa | 0 | 15.4999 | 1000 | tree | small conifer | -1.8516 | 2.3701 | 0.1191 | 15 |
| PIPO | Pinus ponderosa | 15.5 | 79.5 | 1000 | tree | Pinus ponderosa | -3.2673 | 2.582 | 0.1266 | 8 |
| PIPO | Pinus ponderosa | 79.5001 | 1000 | 1000 | bole | Pseudotsuga menziesii | -2.2765 | 2.4247 | 0.2415 | 4 |
| PIPO | Pinus ponderosa | 79.5001 | 1000 | 162 | branches dead | Pseudotsuga menziesii | -3.794 | 1.7503 | 0.728 | 8 |
| PIPO | Pinus ponderosa | 79.5001 | 1000 | 162 | branches live | Pseudotsuga menziesii | -3.8938 | 2.1382 | 0.632 | 8 |
| PIPO | Pinus ponderosa | 79.5001 | 1000 | 162 | foliage | Pseudotsuga menziesii | -3.0877 | 1.7009 | 0.695 | 8 |
| PISA2 | Pinus sabiniana | 0 | 1000 | 1000 | tree | pine | -2.5678 | 2.4349 | 0.253781 | 16 |
| PLRA | Platanus racemosa | 0 | 1000 | 1000 | tree | mixed hardwood | -2.545 | 2.4835 | 0.360458 | 16 |
| POBA2 | Populus balsamifera | 0 | 1000 | 1000 | tree | aspen/alder/cottonwood/willow | -2.3381 | 2.3867 | 0.507441 | 16 |
| POBAT | Populus balsamifera ssp. trichocarpa | 0 | 1000 | 1000 | tree | aspen/alder/cottonwood/willow | -2.3381 | 2.3867 | 0.507441 | 16 |
| POTR5 | Populus tremuloides | 0 | 36 | 1000 | tree | Populus tremuloides | -2.1461 | 2.242 | 0.3205 | 11 |
| POTR5 | Populus tremuloides | 36.0001 | 1000 | 1000 | tree | aspen/alder/cottonwood/willow | -2.3381 | 2.3867 | 0.507441 | 16 |
| PREM | Prunus emarginata | 0 | 1000 | 1000 | tree | mixed hardwood | -2.545 | 2.4835 | 0.360458 | 16 |
| PRVID | Prunus virginiana var. demissa | 0 | 1000 | 1000 | tree | mixed hardwood | -2.545 | 2.4835 | 0.360458 | 16 |
| PSME | Pseudotsuga menziesii | 0 | 1000 | 1000 | tree | Pseudotsuga menziesii | -2.2543 | 2.4435 | 0.218712 | 16 |
| QUCH2 | Quercus chrysolepis | 0 | 1000 | 1000 | tree | hard maple/oak/hickory/beech | -2.0407 | 2.4342 | 0.236483 | 16 |
| QUDO | Quercus douglasii | 0 | 1000 | 1000 | tree | hard maple/oak/hickory/beech | -2.0407 | 2.4342 | 0.236483 | 16 |

| | | | | | | | | | | |
|---|---|---|---|---|---|---|---|---|---|---|
| QUKE | Quercus kelloggii | 0 | 1000 | 1000 | tree | hard maple/oak/hickory/beech | -2.0407 | 2.4342 | 0.236483 | 16 |
| QULO | Quercus lobata | 0 | 1000 | 1000 | tree | hard maple/oak/hickory/beech | -2.0407 | 2.4342 | 0.236483 | 16 |
| QUMO2 | Quercus x moreha | 0 | 1000 | 1000 | tree | hard maple/oak/hickory/beech | -2.0407 | 2.4342 | 0.236483 | 16 |
| QUWI2 | Quercus wislizeni | 0 | 1000 | 1000 | tree | hard maple/oak/hickory/beech | -2.0407 | 2.4342 | 0.236483 | 16 |
| QUWIW | Quercus wislizeni var. wislizeni | 0 | 1000 | 1000 | tree | hard maple/oak/hickory/beech | -2.0407 | 2.4342 | 0.236483 | 16 |
| RHCA | Rhamnus californica | 0 | 1000 | 1000 | tree | mixed hardwood | -2.545 | 2.4835 | 0.360458 | 16 |
| RHIL | Rhamnus ilicifolia | 0 | 1000 | 1000 | tree | mixed hardwood | -2.545 | 2.4835 | 0.360458 | 16 |
| SALA3 | Salix laevigata | 0 | 1000 | 1000 | tree | aspen/alder/cottonwood/willow | -2.3381 | 2.3867 | 0.507441 | 16 |
| SALA6 | Salix lasiolepis | 0 | 1000 | 1000 | tree | aspen/alder/cottonwood/willow | -2.3381 | 2.3867 | 0.507441 | 16 |
| SALIX | Salix | 0 | 1000 | 1000 | tree | aspen/alder/cottonwood/willow | -2.3381 | 2.3867 | 0.507441 | 16 |
| SALU | Salix lucida | 0 | 1000 | 1000 | tree | aspen/alder/cottonwood/willow | -2.3381 | 2.3867 | 0.507441 | 16 |
| SALUL | Salix lucida ssp. lasiandra | 0 | 1000 | 1000 | tree | aspen/alder/cottonwood/willow | -2.3381 | 2.3867 | 0.507441 | 16 |
| SAME2 | Salix melanopsis | 0 | 1000 | 1000 | tree | aspen/alder/cottonwood/willow | -2.3381 | 2.3867 | 0.507441 | 16 |
| SASC | Salix scouleriana | 0 | 1000 | 1000 | tree | aspen/alder/cottonwood/willow | -2.3381 | 2.3867 | 0.507441 | 16 |
| SEGI2 | Sequoiadendron giganteum | 0 | 96.7999 | 1000 | tree | cedar/larch | -2.077 | 2.2592 | 0.294574 | 16 |
| SEGI2 | Sequoiadendron giganteum | 96.8 | 1000 | 1000 | bole | Sequoiadendron giganteum | -2.8134 | 2.4019 | 0.254442 | 4 |
| TOCA | Torreya californica | 0 | 1000 | 1000 | tree | mixed hardwood | -2.545 | 2.4835 | 0.360458 | 16 |
| treeDead | | 0 | 15.8999 | 1000 | bole | small conifer | -1.915 | 2.348 | 0.1302 | 15 |
| treeDead | | 15.9 | 1000 | 1000 | bole | Abies procera | -3.0319 | 2.5812 | 0.1841 | 4 |
| treeNone | | 0 | 1000 | 1000 | tree | none | 0 | 0 | 0 | 25 |
| treeUnk | generic tree species | 0 | 1000 | 1000 | tree | pine | -2.5678 | 2.4349 | 0.253781 | 16 |
| TSME | Tsuga mertensiana | 0 | 11.4999 | 1000 | tree | small conifer | -1.8516 | 2.3701 | 0.1191 | 15 |
| TSME | Tsuga mertensiana | 11.5 | 1000 | 1000 | bole | Tsuga mertensiana | -3.2801 | 2.5915 | 0.195028 | 4 |
| TSME | Tsuga mertensiana | 11.5 | 1000 | 1000 | branch live | Tsuga mertensiana | -5.2655 | 2.6045 | 0.122 | 8 |
| TSME | Tsuga mertensiana | 11.5 | 1000 | 1000 | branches dead | Tsuga mertensiana | -9.951 | 3.2845 | 0.11 | 8 |
| TSME | Tsuga mertensiana | 11.5 | 1000 | 1000 | foliage | Tsuga mertensiana | -3.8294 | 1.9756 | 0.158 | 8 |
| UMCA | Umbellularia californica | 0 | 1000 | 1000 | tree | Umbellularia californica | -2.1313 | 2.3996 | 0.2497 | 21 |

ID citation


1 Pearson JA, Fahey TJ, Knight DH (1984) Biomass and leaf area in contrasting lodgepole pine forests. Canadian Journal of Forest Resources 14:259-265

2 Westman WE (1987) Aboveground biomass, surface area, and production relations of red fir (Abies magnifica) and white fir (A. concolor). Canadian Journal of Forest Resources 17:311-319

3 Brown JK (1978) Weight and density of crowns of Rocky Mountain conifers. USFS Research Paper INT-197:56

4 Means JE, Hansen HA, Koerper GJ, Alaback PB, Klopsch MW (1994) Software for computing plant biomass--BIOPAK users guide. USFS Research Paper PNW-GTR-340

5 Jenkins JC, Chojnacky DC, Heath LS, Birdsey RA (2004) Comprehensive database of diameter-based biomass regressions for north american tree species. USFS Research Paper GTR NE-319

6 Ter-Mikaelian MT, Korzukhin MD (1997) Biomass equations for sixty-five North American tree species. Forest Ecology and Management 97:1-24

7 Grier CC, Logan RS (1977) Old-growth Pseudotsuga menziesii communities of a western Oregon watershed: biomass distribution and production budgets. Ecological Monographs 47:373-400

8 Gholz HL, Grier CC, Campbell AG, Brown AT (1979) Equations for estimating biomass and leaf area of plants in the Pacific Northwest. Oregon State University School of Forestry Research Paper 41:39

9 Chojnacky DC, Moisen GG (1993) Converting wood volume to biomass for pinyon and juniper. USFS Research Paper INT-411

10 Miller E, Meeuwig R, Budy J (1981) Biomass of singleleaf pinyon and Utah juniper. USFS Research Paper INT-273

11 Johnston RS, Bartos DL (1977) Summary of nutrient and biomass data from two aspen sites in western United States. USFS Research Paper INT-277:15

12 Perala DA, Alban DH (1994) Allometric biomass estimation for aspen-dominated ecosystems in the Upper Great Lakes. USFS Research Paper NC-134:38

13 Boerner REJ, Kost JA (1986) Biomass equations for flowering dogwood, Cornus florida L.. Castane 51:153-154

14 Helgerson O, Cromack K, Stafford S, Miller R, Slagle R (1988) Equations for estimating aboveground components of young Douglas-fir and red alder in a coastal Oregon plantation. Canadian Journal of Forest Research 18:1082-1085

15 Gower ST, Vogt KA, Grier CC (1992) Carbon dynamics of rocky mountain douglas-fir: Influence of water and nutrient availability. Ecological Monographs 62:43-65

16 Jenkins JC, Chojnacky DC, Heath LS, Birdsey RA (2003) National-scale biomass estimators for United States tree species. Forest Science 49:12-35

17 Lambert MC, Ung CH, Raulier F (2005) Canadian national tree aboveground biomass equations. Canadian Journal of Forest Research 35:1996-2018

18 Chojnacky DC (1984) Volume and biomass for curlleaf Cercocarpus in Nevada. USFS Research Paper INT-332

21 Coltrin WR (2010) Biomass quantification of live trees in a mixed evergreen forest using biomass diameter-based allometric equations. Master's Thesis, Humboldt State University 52 pp

22 Harmon M (1994) Mark Harmon, Forest Science Dept., Ore State Univ. fit the equation.. x x

23 Pastor J, Aber JD, Melillo JM (1984) Biomass prediction using generalized allometric regressions for some northeast tree species. Forest Ecology and Management 7:265-274

24 Halpern CB, Miller EA, Melora (1996) Equations for predicting above-ground biomass of plant species in early successional forests of the western cascade range, Oregon. Northwest Science 70:306-320

26 Gower ST, Grier CG, Vogt DJ, Vogt KA (1987) Allometric relations of deciduous (Larix occidentalis) and evergreen conifers (Pinus contorta and Pseudotsuga menziesii) of the Cascade Mountains in Central Washington. Canadian Journal of Forest Resources 17:63

# Appendix C: Carbon Summaries for Major Vegetation Types

Deciduous Oak Forest and Woodland (n = 88)

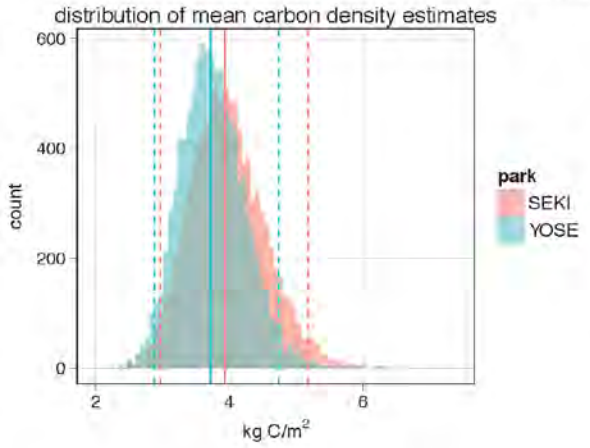


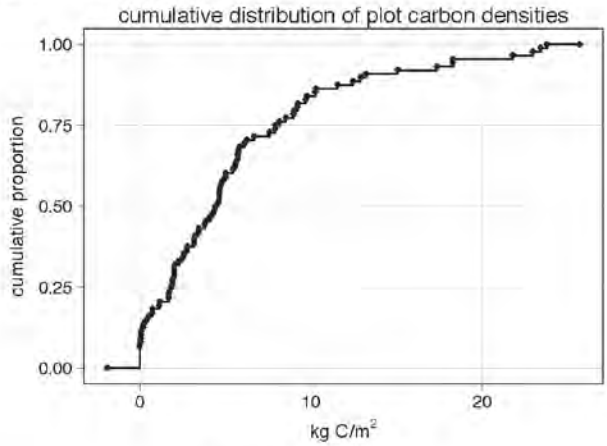


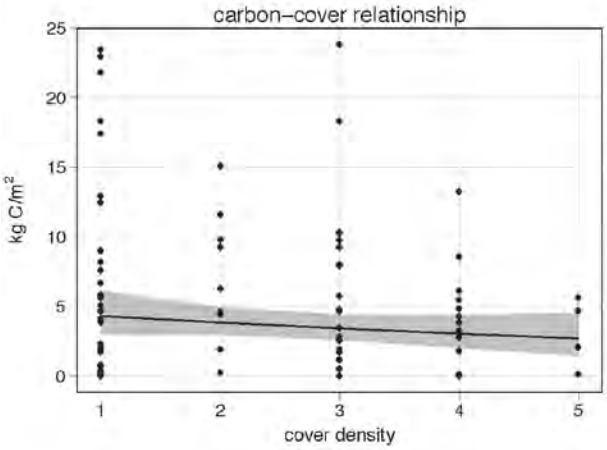


species composition

| code | carbon | nTrees | carbonPct | nTreesPct |
|---|---|---|---|---|
| QUKE | 169,908 | 848 | 35.6 | 31.9 |
| QUDO | 129,201 | 378 | 27 | 14.3 |
| CADE27 | 56,740 | 525 | 11.9 | 19.8 |
| QULO | 36,726 | 25 | 7.7 | 0.9 |
| ABCO | 21,665 | 179 | 4.5 | 6.8 |
| QUCH2 | 11,674 | 121 | 2.4 | 4.6 |
| treeDead | 9,640 | 186 | 2 | 7 |
| PIPO | 8,667 | 34 | 1.8 | 1.3 |
| AECA | 7,521 | 97 | 1.6 | 3.7 |
| QUWI | 7,883 | 111 | 1.6 | 4.2 |
| QUWI2 | 5,884 | 55 | 1.2 | 2.1 |
| PIJE | 4,096 | 3 | 0.9 | 0.1 |
| PILA | 2,999 | 26 | 0.6 | 1 |
| FRLA | 2,325 | 11 | 0.5 | 0.4 |
| PISA2 | 1,425 | 8 | 0.3 | 0.3 |
| ARVI4 | 379 | 10 | 0.1 | 0.4 |
| CEBEx | 413 | 5 | 0.1 | 0.2 |
| FRDI2 | 279 | 8 | 0.1 | 0.3 |
| CEOC3 | 71 | 4 | 0 | 0.2 |
| PSME | 219 | 1 | 0 | 0 |

Douglas–fir Forest (n = 7)

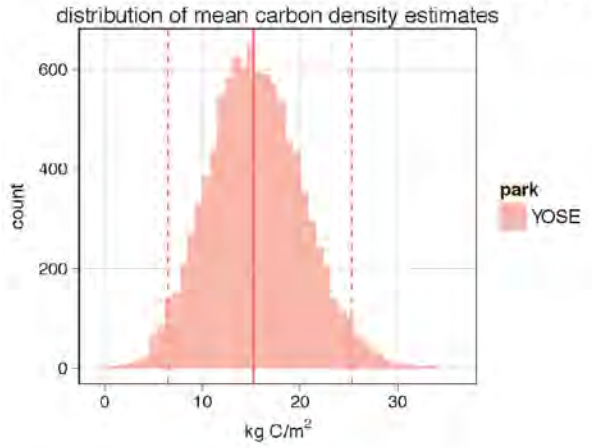


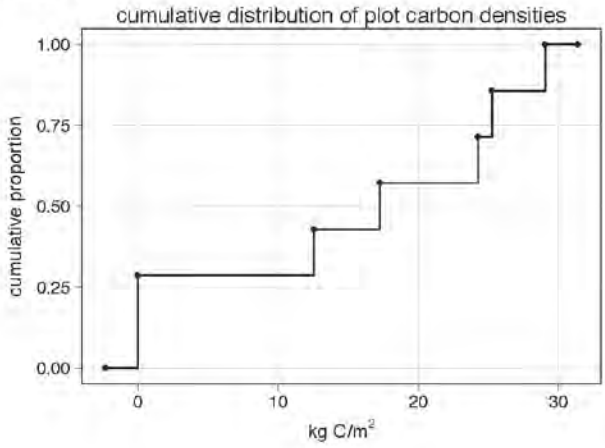


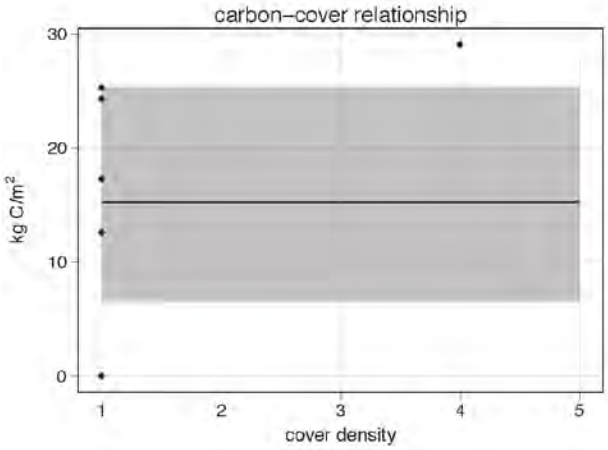


species composition

| code | carbon | nTrees | carbonPct | nTreesPct |
|---|---|---|---|---|
| PSME | 40,767 | 113 | 47.1 | 29.7 |
| CADE27 | 20,126 | 102 | 23.2 | 26.8 |
| PIPO | 8,423 | 13 | 9.7 | 3.4 |
| QUCH2 | 8,096 | 81 | 9.3 | 21.3 |
| ABCO | 4,812 | 21 | 5.6 | 5.5 |
| QUKE | 1,665 | 12 | 1.9 | 3.2 |
| ALRH2 | 1,202 | 7 | 1.4 | 1.8 |
| PILA | 502 | 3 | 0.6 | 0.8 |
| treeDead | 447 | 14 | 0.5 | 3.7 |
| ACMA3 | 333 | 2 | 0.4 | 0.5 |
| CONU4 | 213 | 10 | 0.2 | 2.6 |
| treeNone | 0 | 2 | 0.0 | 0.5 |

Evergreen Oak Forest and Woodland (n = 110)

distribution of mean carbon density estimates

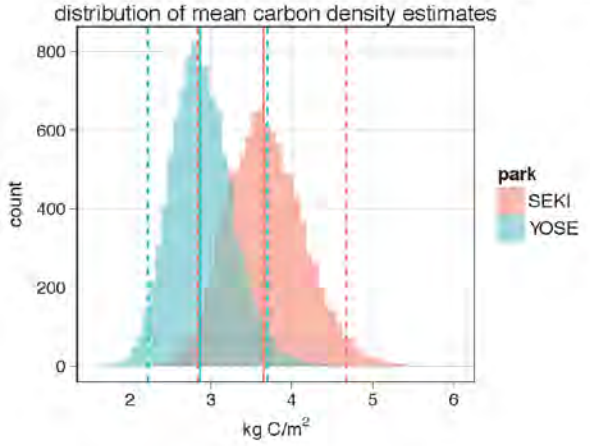


cumulative distribution of plot carbon densities

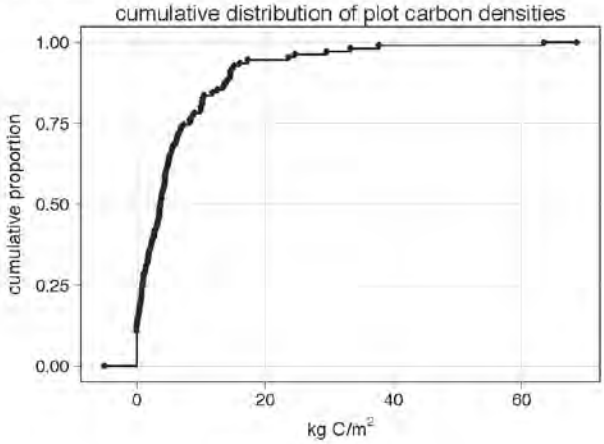


carbon–cover relationship

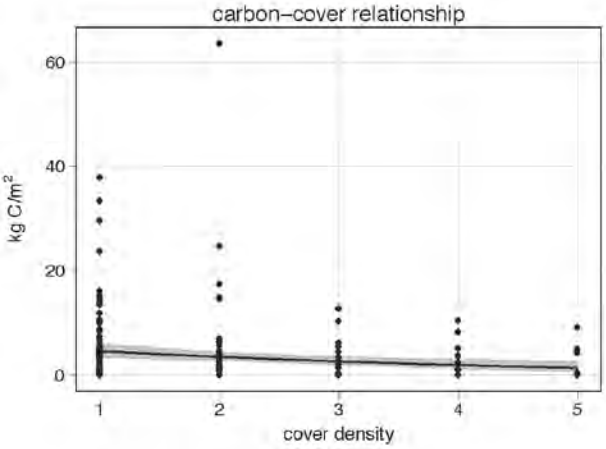


species composition

| code | carbon | nTrees | carbonPct | nTreesPct |
|---|---|---|---|---|
| QUCH2 | 286,176 | 1,754 | 50.8 | 45.4 |
| QUWIW | 82,351 | 348 | 14.6 | 9 |
| AECA | 37,330 | 258 | 6.6 | 6.7 |
| PIPO | 24,675 | 39 | 4.4 | 1 |
| QUWI2 | 20,179 | 185 | 3.6 | 4.8 |
| CADE27 | 18,224 | 118 | 3.2 | 3.1 |
| QUKE | 17,824 | 71 | 3.2 | 1.8 |
| treeDead | 16,223 | 156 | 2.9 | 4.1 |
| PISA2 | 11,702 | 19 | 2.1 | 0.5 |
| PSME | 12,045 | 20 | 2.1 | 0.5 |
| TOCA | 8,927 | 45 | 1.6 | 1.2 |
| UMCA | 7,945 | 676 | 1.4 | 17.5 |
| PLRA | 4,421 | 4 | 0.8 | 0.1 |
| PILA | 2,596 | 6 | 0.5 | 0.2 |
| ABCO | 1,608 | 14 | 0.3 | 0.4 |
| ALRH2 | 1,880 | 4 | 0.3 | 0.1 |
| FRLA | 1,581 | 6 | 0.3 | 0.2 |
| QUDO | 1,890 | 10 | 0.3 | 0.3 |
| ACMA3 | 1,297 | 5 | 0.2 | 0.1 |
| QUMO2 | 1,275 | 3 | 0.2 | 0.1 |

Foothill Pine Woodland (n = 11)

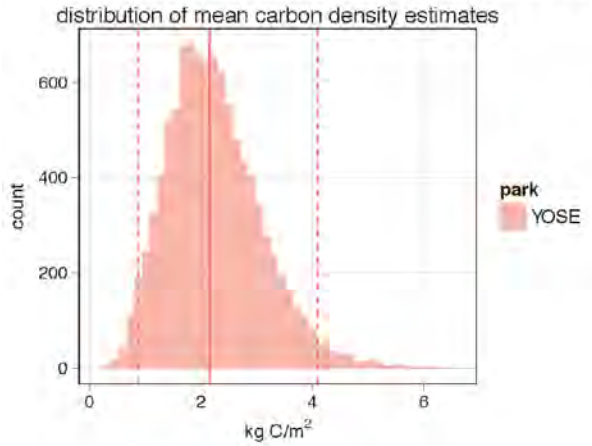


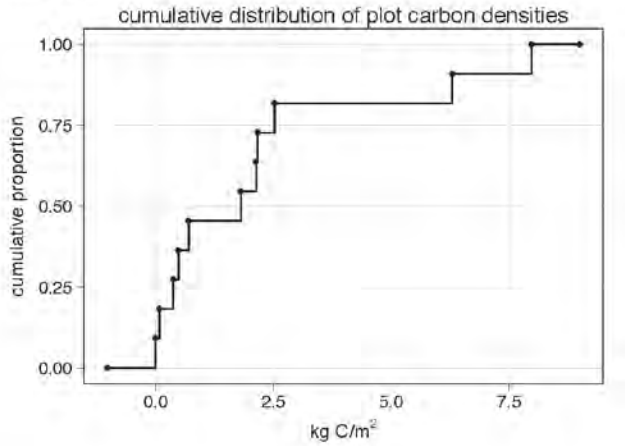


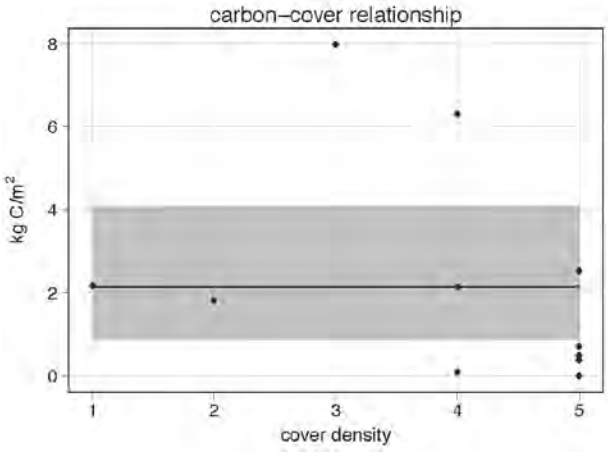


species composition

| code | carbon | nTrees | carbonPct | nTreesPct |
|---|---|---|---|---|
| PISA2 | 18,126 | 32 | 72.3 | 65.3 |
| QUWI2 | 2,949 | 7 | 11.8 | 14.3 |
| QUKE | 2,718 | 3 | 10.8 | 6.1 |
| QUCH2 | 964 | 3 | 3.8 | 6.1 |
| QULO | 242 | 1 | 1.0 | 2.0 |
| AECA | 48 | 1 | 0.2 | 2.0 |
| QUDO | 28 | 1 | 0.1 | 2.0 |
| treeNone | 0 | 1 | 0.0 | 2.0 |

Foxtail Pine Forest (n = 58)

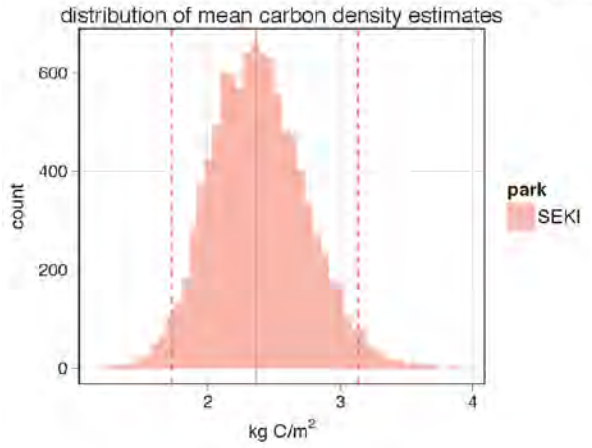


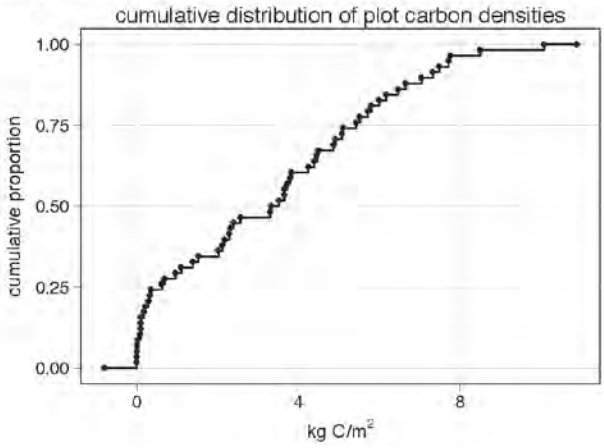


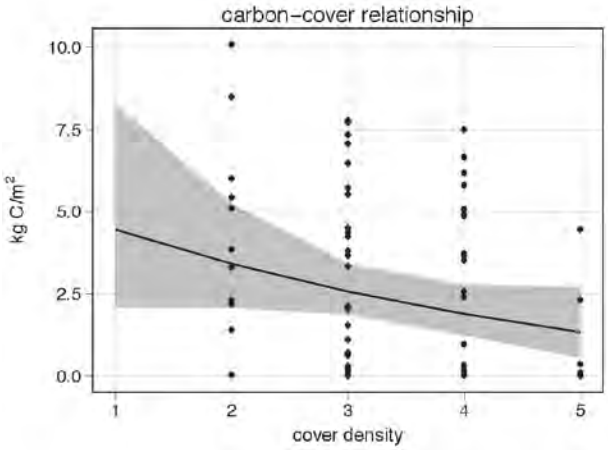


species composition

| code | carbon | nTrees | carbonPct | nTreesPct |
|---|---|---|---|---|
| PICOM | 94,106 | 731 | 46.4 | 46.0 |
| treeDead | 91,325 | 109 | 45.0 | 6.9 |
| PIBAA | 10,595 | 690 | 5.2 | 43.4 |
| PIMO3 | 6,661 | 22 | 3.3 | 1.4 |
| PIAL | 169 | 35 | 0.1 | 2.2 |
| ABMA | 46 | 1 | 0.0 | 0.1 |
| treeNone | 0 | 1 | 0.0 | 0.1 |

Giant Sequoia Forest (n = 42)

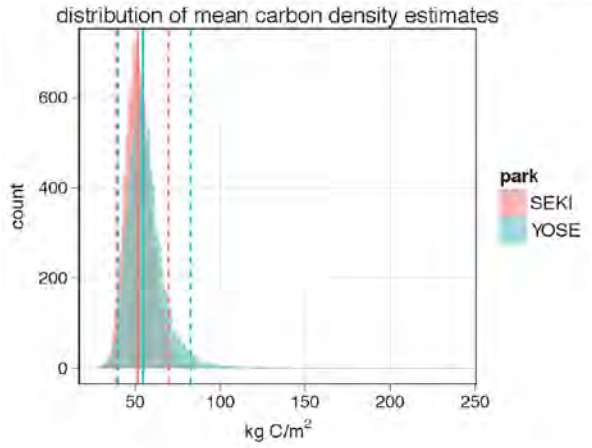


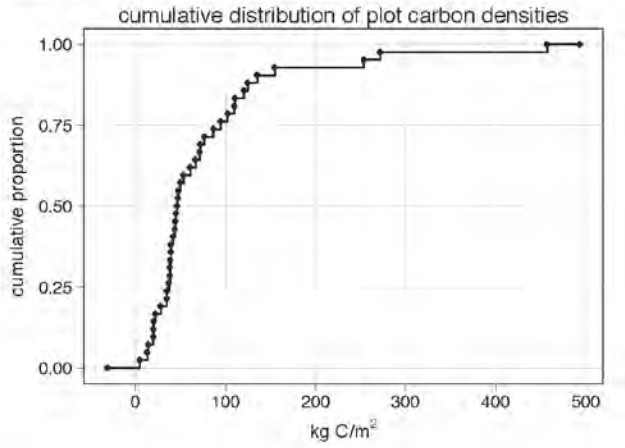


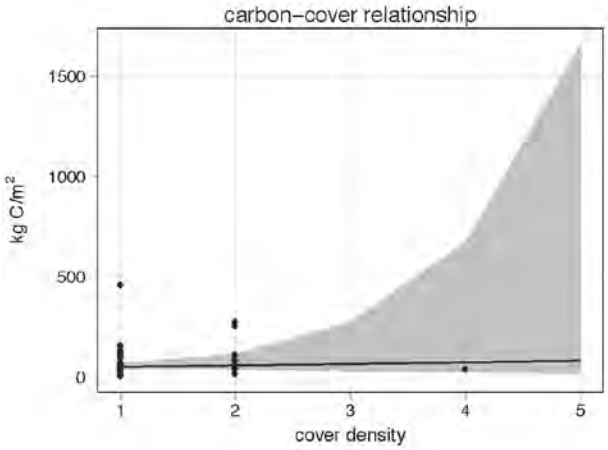


species composition

| code | carbon | nTrees | carbonPct | nTreesPct |
|---|---|---|---|---|
| SEGI2 | 2,442,130 | 197 | 73.1 | 7.0 |
| ABCO | 488,420 | 1,746 | 14.6 | 62.4 |
| treeDead | 185,832 | 341 | 5.6 | 12.2 |
| PILA | 114,900 | 251 | 3.4 | 9.0 |
| ABMAM | 57,362 | 48 | 1.7 | 1.7 |
| PIPO | 27,913 | 13 | 0.8 | 0.5 |
| CADE27 | 17,923 | 194 | 0.5 | 6.9 |
| PINUS | 7,486 | 1 | 0.2 | 0.0 |
| CONU4 | 37 | 7 | 0.0 | 0.2 |
| PIJE | 172 | 1 | 0.0 | 0.0 |
| QUKE | 18 | 1 | 0.0 | 0.0 |

High Woodland (n = 89)

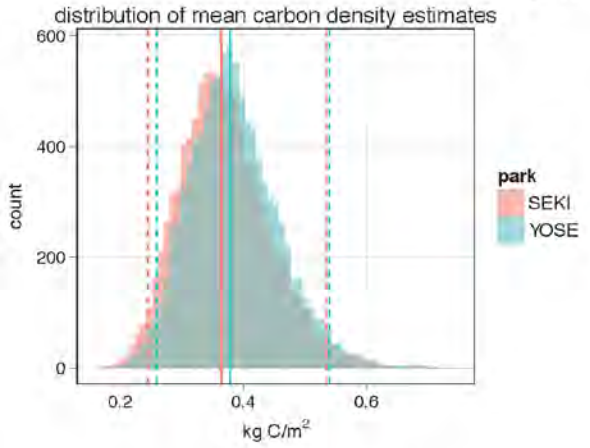


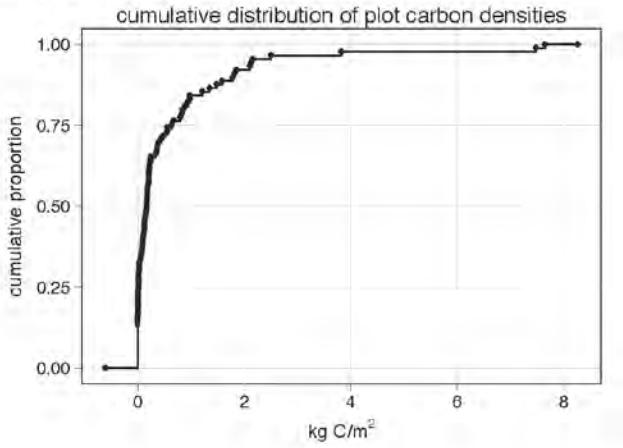


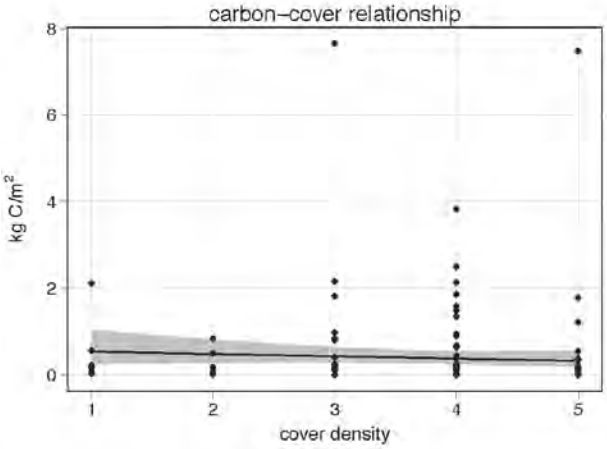


species composition

| code | carbon | nTrees | carbonPct | nTreesPct |
|---|---|---|---|---|
| PICOM | 14,939 | 227 | 33.6 | 11.0 |
| treeDead | 11,011 | 52 | 24.8 | 2.5 |
| PIAL | 6,126 | 1,552 | 13.8 | 75.2 |
| JUOC | 5,277 | 161 | 11.9 | 7.8 |
| PIJE | 2,125 | 18 | 4.8 | 0.9 |
| PIMO | 1,679 | 7 | 3.8 | 0.3 |
| TSME | 1,629 | 13 | 3.7 | 0.6 |
| PIMO3 | 1,160 | 2 | 2.6 | 0.1 |
| CADE27 | 324 | 13 | 0.7 | 0.6 |
| ABCO | 131 | 3 | 0.3 | 0.1 |
| PIBAA | 5 | 1 | 0.0 | 0.0 |
| QUKE | 14 | 1 | 0.0 | 0.0 |
| treeNone | 0 | 13 | 0.0 | 0.6 |

Jeffrey Pine Forest (n = 111)

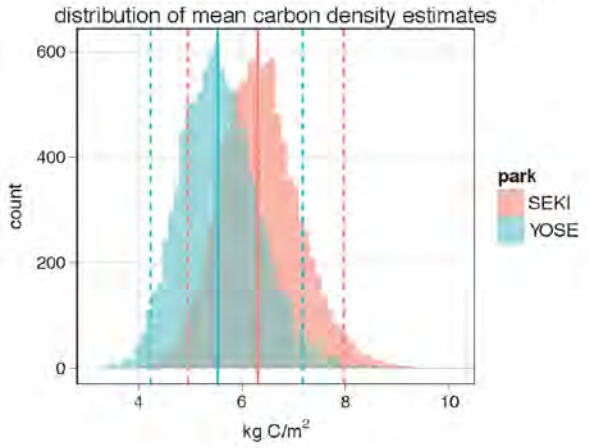


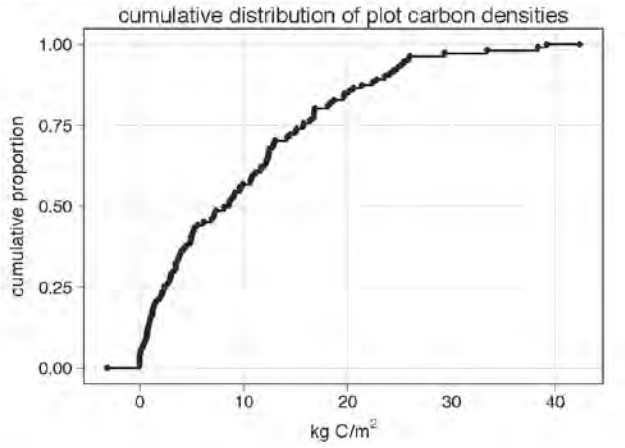


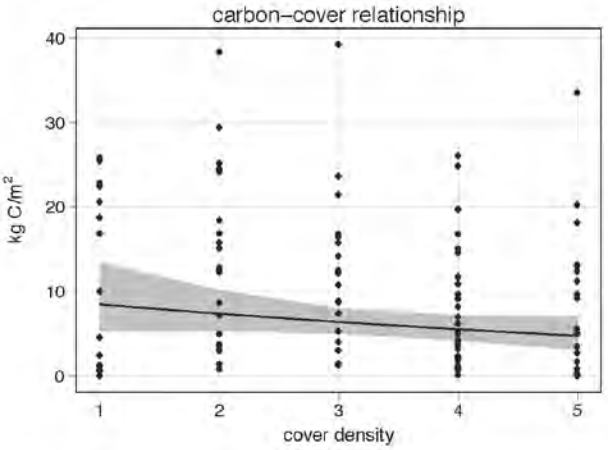


species composition

| code | carbon | nTrees | carbonPct | nTreesPct |
|---|---|---|---|---|
| PIJE | 862,498 | 855 | 65.3 | 38.9 |
| ABCO | 173,613 | 435 | 17.1 | 18.8 |
| treeDead | 65,430 | 179 | 6.4 | 7.7 |
| ABMA | 34,960 | 30 | 3.4 | 1.3 |
| CADE27 | 27,536 | 162 | 2.7 | 7 |
| PILA | 14,887 | 10 | 1.5 | 0.4 |
| QUCH2 | 10,800 | 200 | 1.1 | 8.6 |
| PICOM | 10,184 | 103 | 1 | 4.4 |
| QUKE | 4,216 | 88 | 0.4 | 3.8 |
| PIPO | 2,906 | 16 | 0.3 | 0.7 |
| CELE3 | 1,929 | 8 | 0.2 | 0.3 |
| PIMO | 2,203 | 17 | 0.2 | 0.7 |
| ABMAS | 1,281 | 20 | 0.1 | 0.9 |
| POBAT | 1,293 | 5 | 0.1 | 0.2 |
| BEOC2 | 231 | 6 | 0 | 0.3 |
| JUOC | 358 | 64 | 0 | 2.8 |
| JUCCA | 77 | 7 | 0 | 0.3 |
| PIMO3 | 4 | 2 | 0 | 0.1 |
| POBA2 | 176 | 5 | 0 | 0.2 |
| POTR5 | 484 | 9 | 0 | 0.4 |

Lodgepole Pine Forest (n = 190)

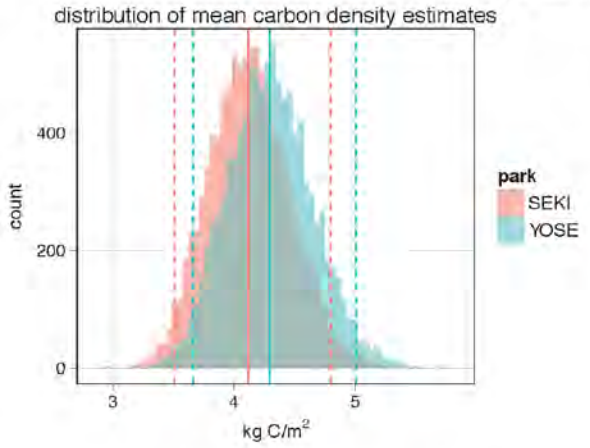


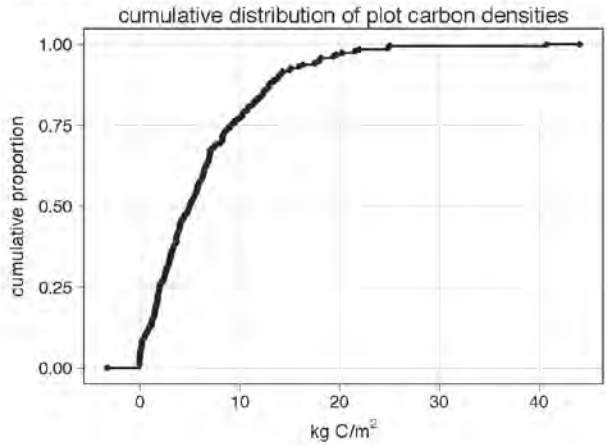


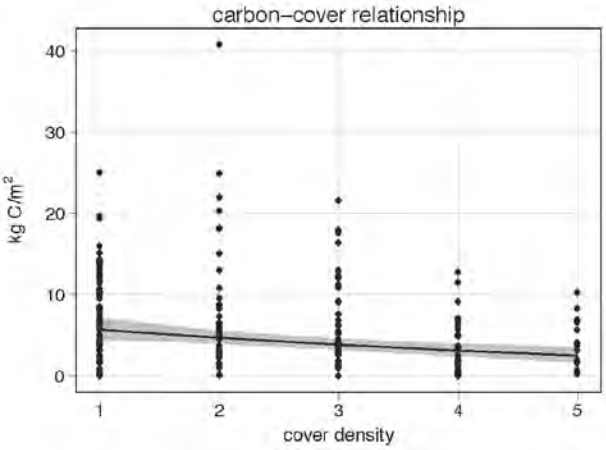


species composition

| code | carbon | nTrees | carbonPct | nTreesPct |
|---|---|---|---|---|
| PICOM | 603,220 | 6,773 | 73.7 | 75.7 |
| treeDead | 114,283 | 265 | 10.5 | 3.0 |
| ABMA | 99,628 | 735 | 9.1 | 8.3 |
| ABMAS | 22,410 | 89 | 2.1 | 1.0 |
| PIMO3 | 22,889 | 120 | 2.1 | 1.4 |
| PIJE | 8,085 | 22 | 0.7 | 0.2 |
| ABCO | 5,439 | 39 | 0.5 | 0.4 |
| POTR5 | 5,655 | 69 | 0.5 | 0.8 |
| TSME | 5,579 | 83 | 0.5 | 0.9 |
| PIAL | 2,140 | 598 | 0.2 | 6.8 |
| JUOC | 25 | 4 | 0.0 | 0.0 |
| PIBAA | 514 | 35 | 0.0 | 0.4 |
| POBAT | 436 | 2 | 0.0 | 0.0 |
| treeNone | 0 | 2 | 0.0 | 0.0 |

Mountain Hemlock Forest (n = 38)

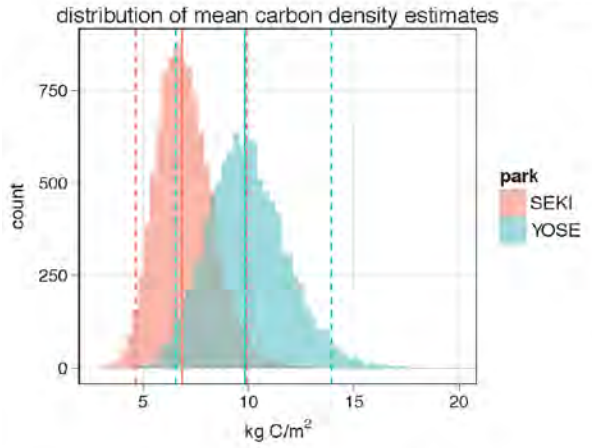


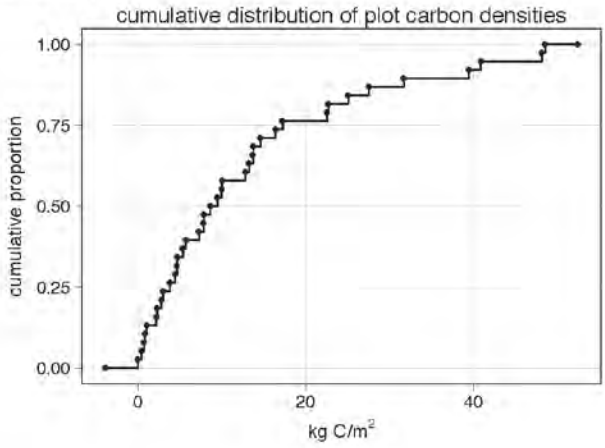


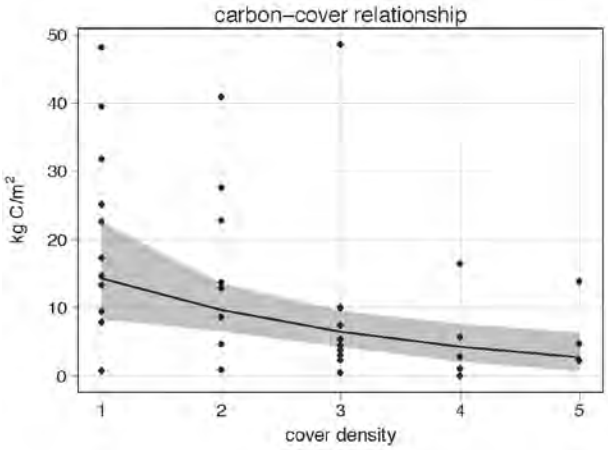


species composition

| code | carbon | nTrees | carbonPct | nTreesPct |
|---|---|---|---|---|
| TSME | 375,554 | 1,389 | 87.1 | 73.0 |
| PICOM | 18,043 | 338 | 4.2 | 17.8 |
| treeDead | 17,714 | 13 | 4.1 | 0.7 |
| PIMO3 | 11,131 | 58 | 2.6 | 3.0 |
| ABMA | 8,227 | 3 | 1.9 | 0.2 |
| PIAL | 400 | 102 | 0.1 | 5.4 |
| treeNone | 0 | 1 | 0.0 | 0.1 |

Pinyon Pine Woodland (n = 27)

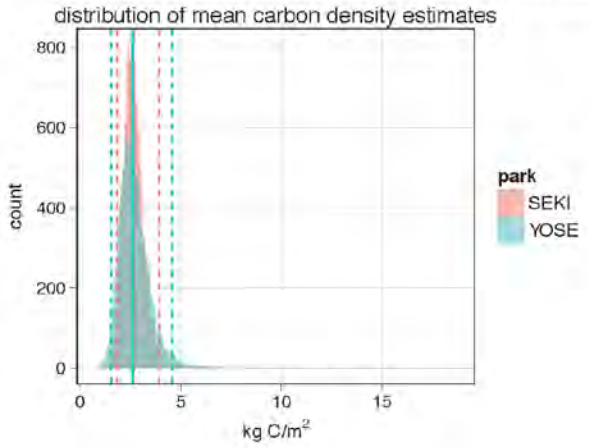


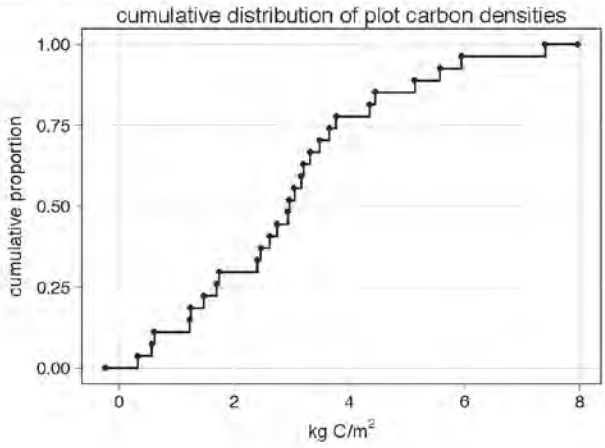


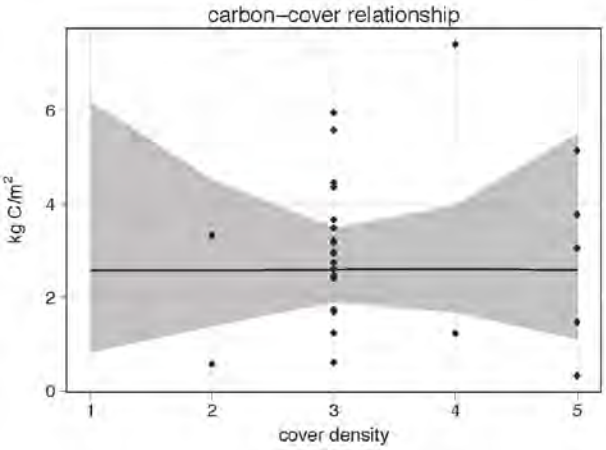


species composition

| code | carbon | nTrees | carbonPct | nTreesPct |
|---|---|---|---|---|
| PIMO | 54,971 | 355 | 80.4 | 71.4 |
| CUCH2 | 4,164 | 56 | 6.1 | 11.3 |
| CELE3 | 3,962 | 66 | 5.8 | 13.3 |
| CADE27 | 3,293 | 7 | 4.8 | 1.4 |
| PIJE | 1,389 | 4 | 2.0 | 0.8 |
| treeDead | 277 | 2 | 0.4 | 0.4 |
| JUOC | 200 | 5 | 0.3 | 1.0 |
| PIPO | 86 | 1 | 0.1 | 0.2 |
| QUKE | 34 | 1 | 0.1 | 0.2 |

Ponderosa Pine Forest (n = 123)

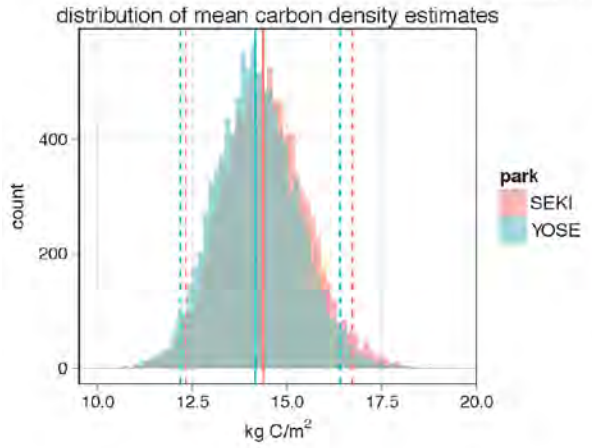


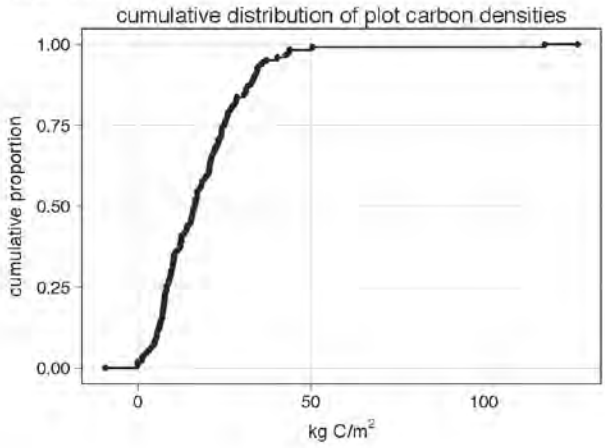


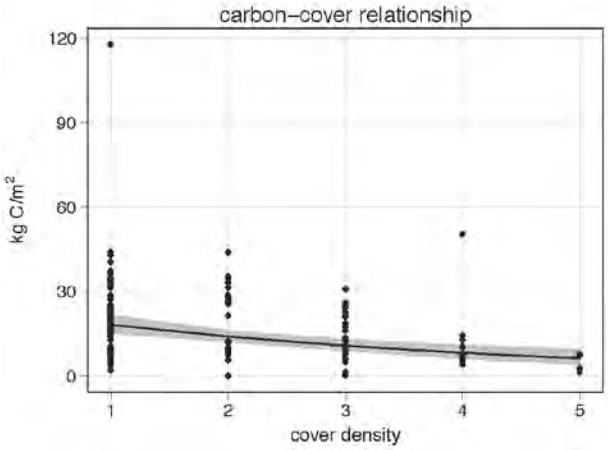


species composition

| code | carbon | nTrees | carbonPct | nTreesPct |
|---|---|---|---|---|
| PIPO | 1,058,437 | 1,827 | 49.6 | 23.2 |
| CADE27 | 410,747 | 2,878 | 19.2 | 36.6 |
| ABCO | 225,332 | 1,204 | 10.5 | 15.3 |
| treeDead | 177,104 | 820 | 8.3 | 10.4 |
| QUKE | 132,868 | 423 | 6.2 | 5.4 |
| PILA | 97,653 | 435 | 4.6 | 5.5 |
| QUCH2 | 15,315 | 178 | 0.7 | 2.3 |
| PIJE | 10,859 | 12 | 0.5 | 0.2 |
| PSME | 4,375 | 30 | 0.2 | 0.4 |
| ACMA3 | 918 | 8 | 0.0 | 0.1 |
| ALRH2 | 577 | 7 | 0.0 | 0.1 |
| CONU4 | 50 | 4 | 0.0 | 0.1 |
| PIAT | 1,008 | 6 | 0.0 | 0.1 |
| QUWI2 | 28 | 1 | 0.0 | 0.0 |
| treeNone | 0 | 1 | 0.0 | 0.0 |
| treeUnk | 39 | 1 | 0.0 | 0.0 |
| UMCA | 641 | 34 | 0.0 | 0.4 |

Ponderosa Pine Woodland (n = 13)

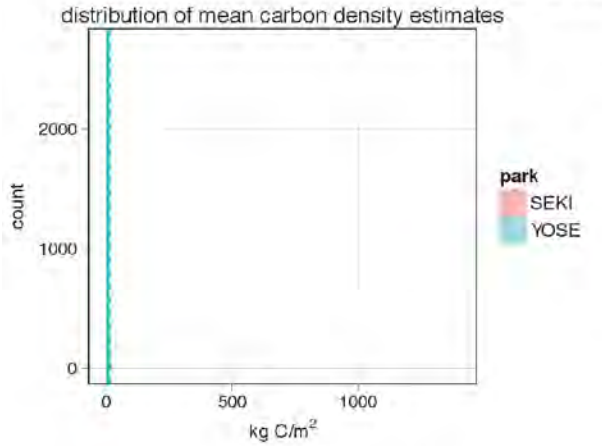


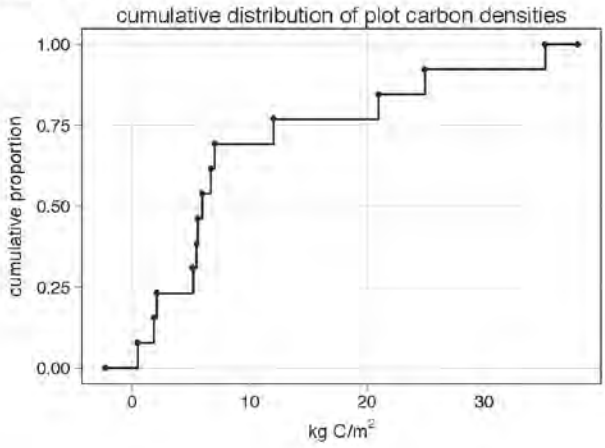


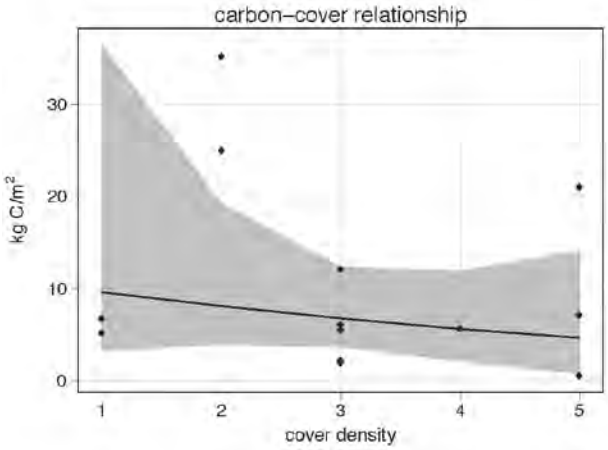


species composition

| code | carbon | nTrees | carbonPct | nTreesPct |
|---|---|---|---|---|
| QUKE | 60,719 | 87 | 51.8 | 19.7 |
| PIPO | 32,965 | 89 | 28.1 | 20.2 |
| CADE27 | 12,753 | 146 | 10.9 | 33.1 |
| treeDead | 7,497 | 59 | 6.4 | 13.4 |
| PSME | 985 | 13 | 0.8 | 2.9 |
| PILA | 589 | 11 | 0.5 | 2.5 |
| ABCO | 498 | 7 | 0.4 | 1.6 |
| AECA | 441 | 4 | 0.4 | 0.9 |
| ARVI4 | 335 | 15 | 0.3 | 3.4 |
| PIJE | 192 | 2 | 0.2 | 0.5 |
| ALRH2 | 119 | 1 | 0.1 | 0.2 |
| QUCH2 | 78 | 4 | 0.1 | 0.9 |
| PISA2 | 7 | 3 | 0.0 | 0.7 |

Red Fir Forest (n = 116)

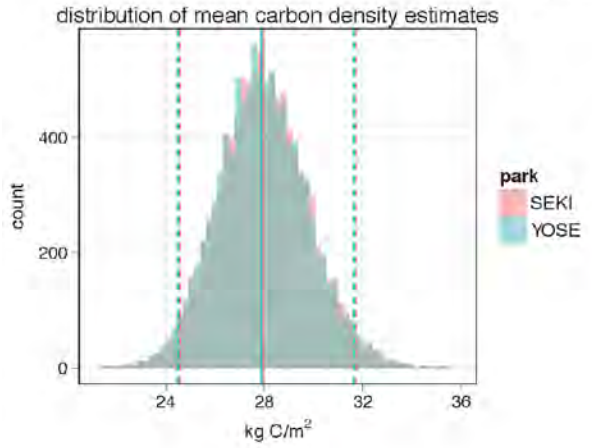


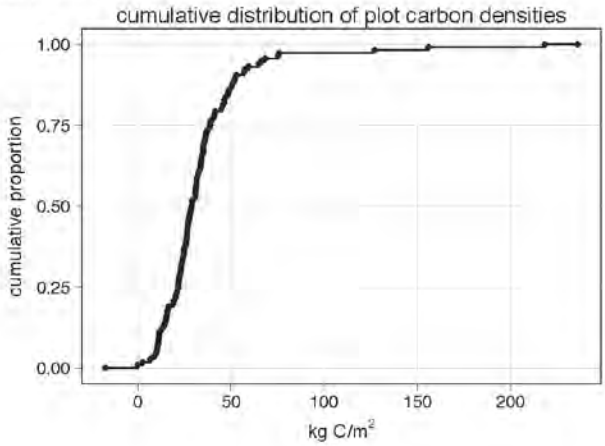


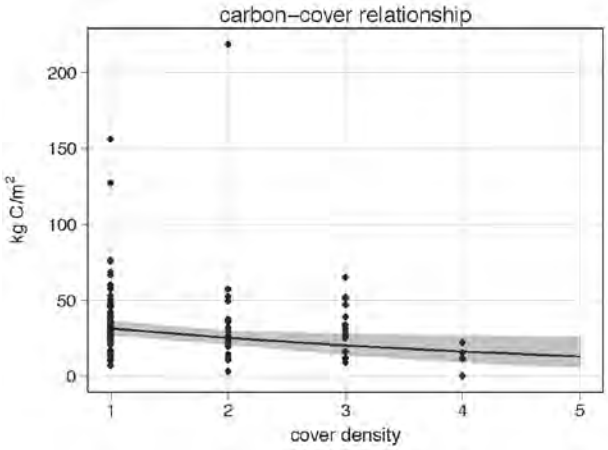


species composition

| code | carbon | nTrees | carbonPct | nTreesPct |
|---|---|---|---|---|
| ABMA | 1,911,434 | 1,600 | 52.7 | 29.0 |
| ABMAS | 537,531 | 1,213 | 14.8 | 22.0 |
| ABCO | 472,044 | 1,271 | 13.0 | 23.1 |
| treeDead | 280,782 | 372 | 7.7 | 6.7 |
| ABMAM | 215,955 | 369 | 5.9 | 6.7 |
| PIMO3 | 50,262 | 124 | 1.4 | 2.2 |
| PICOM | 46,917 | 361 | 1.3 | 6.5 |
| PILA | 42,209 | 47 | 1.2 | 0.9 |
| PIJE | 36,350 | 47 | 1.0 | 0.9 |
| PIMO | 27,134 | 33 | 0.7 | 0.6 |
| TSME | 6,420 | 42 | 0.2 | 0.8 |
| CADE27 | 1,158 | 7 | 0.0 | 0.1 |
| JUOC | 379 | 3 | 0.0 | 0.1 |
| PIBAA | 231 | 18 | 0.0 | 0.3 |
| SEGI2 | 797 | 7 | 0.0 | 0.1 |

Riparian Forest (n = 87)

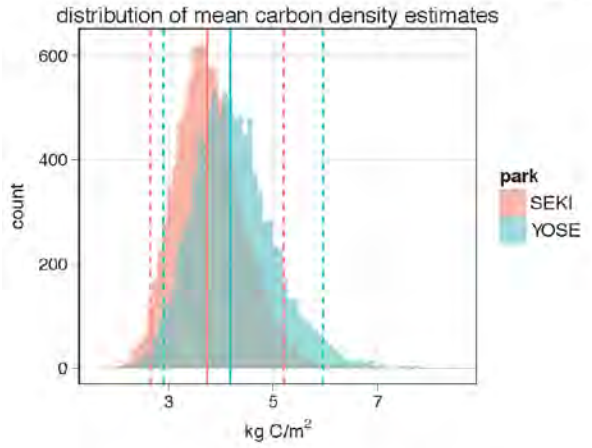


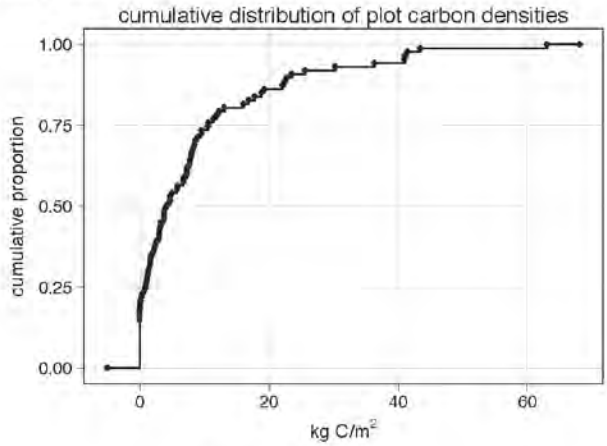


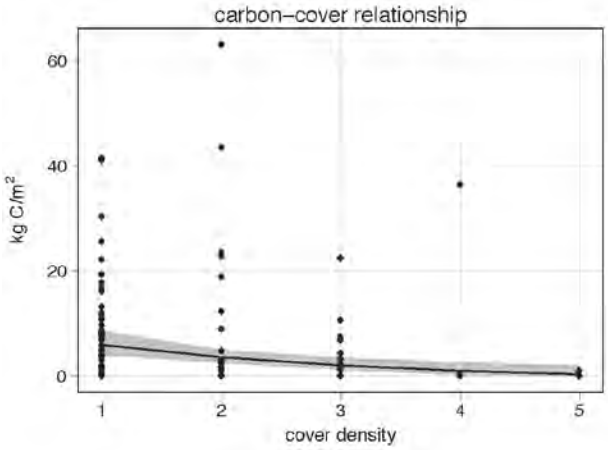


species composition

| code | carbon | nTrees | carbonPct | nTreesPct |
|---|---|---|---|---|
| ABCO | 72,250 | 78 | 17.7 | 5.1 |
| POBAT | 63,377 | 136 | 15.6 | 8.8 |
| ALRH2 | 53,730 | 344 | 13.2 | 22.4 |
| PIPO | 46,695 | 13 | 11.5 | 0.8 |
| CADE27 | 44,191 | 74 | 10.9 | 4.8 |
| POTR5 | 33,056 | 550 | 8.1 | 35.8 |
| PLRA | 27,596 | 35 | 6.8 | 2.3 |
| POBA2 | 16,383 | 25 | 4 | 1.6 |
| QUCH2 | 13,897 | 62 | 3.4 | 4 |
| treeDead | 9,635 | 27 | 2.4 | 1.8 |
| PICOM | 5,199 | 36 | 1.3 | 2.3 |
| PIJE | 4,913 | 16 | 1.2 | 1 |
| QUKE | 4,156 | 8 | 1 | 0.5 |
| CONU4 | 2,274 | 37 | 0.6 | 2.4 |
| PSME | 1,630 | 5 | 0.4 | 0.3 |
| SALIX | 1,459 | 19 | 0.4 | 1.2 |
| AECA | 1,249 | 13 | 0.3 | 0.8 |
| QUWIW | 1,117 | 3 | 0.3 | 0.2 |
| ACMA3 | 764 | 9 | 0.2 | 0.6 |
| PILA | 949 | 2 | 0.2 | 0.1 |

Riparian Shrub (n = 23)

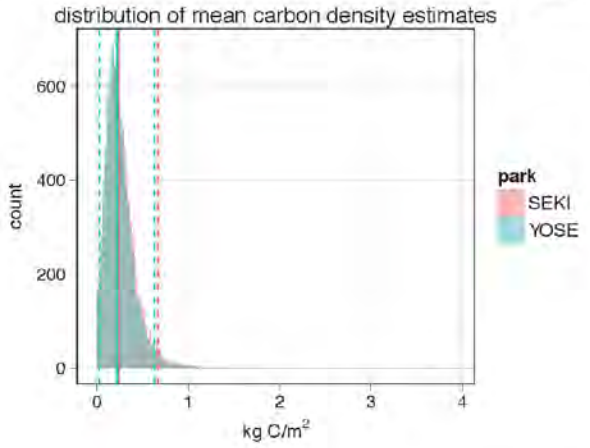


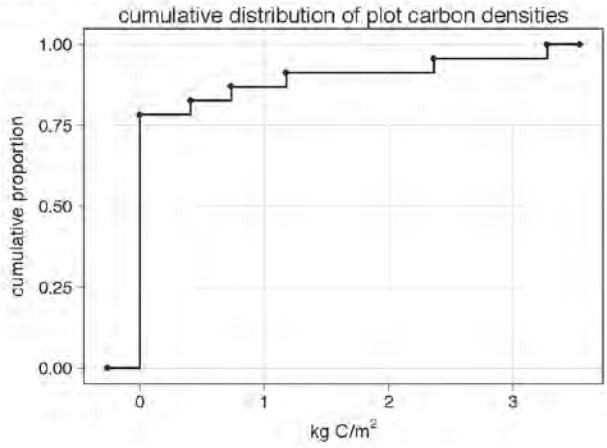


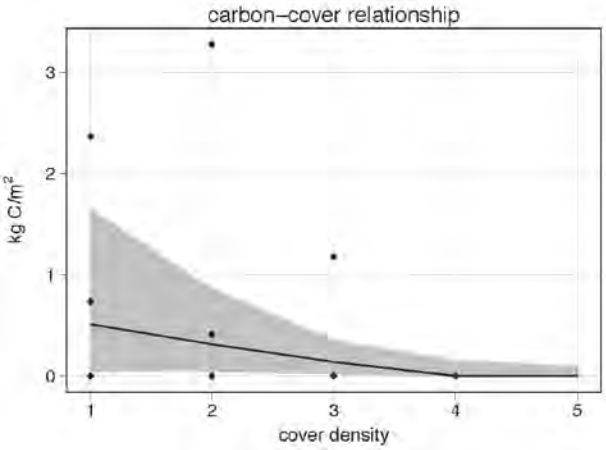


species composition

| code | carbon | nTrees | carbonPct | nTreesPct |
|---|---|---|---|---|
| SALA3 | 3,985 | 25 | 65.7 | 37.3 |
| SALA6 | 1,199 | 8 | 19.8 | 11.9 |
| SALUL | 473 | 9 | 7.8 | 13.4 |
| ACMA3 | 226 | 1 | 3.7 | 1.5 |
| ALRH2 | 97 | 3 | 1.6 | 4.5 |
| QUWI2 | 64 | 2 | 1.1 | 3.0 |
| PISA2 | 24 | 1 | 0.4 | 1.5 |
| treeNone | 0 | 18 | 0.0 | 26.9 |

Shrub (n = 258)

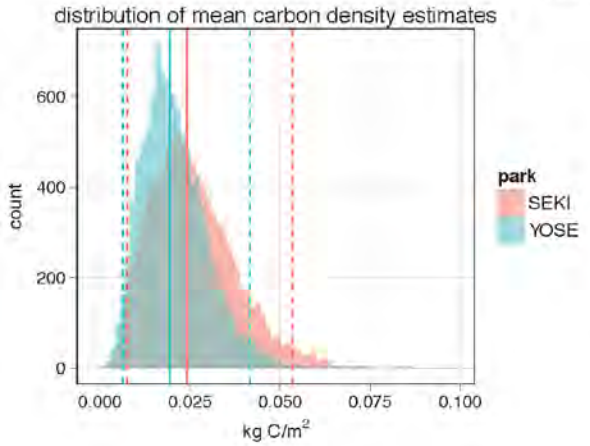


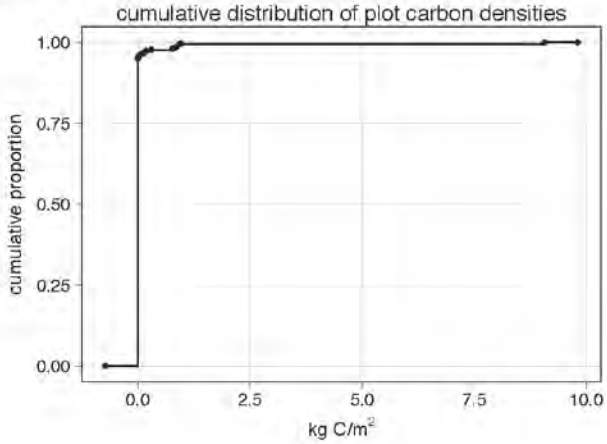


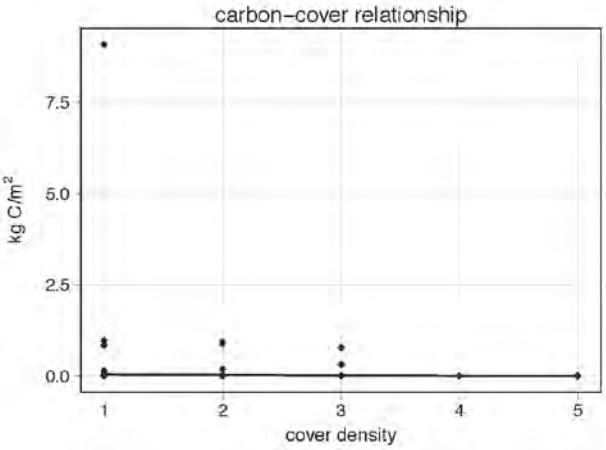


species composition

| code | carbon | nTrees | carbonPct | nTreesPct |
|---|---|---|---|---|
| treeDead | 9,258 | 33 | 71.9 | 9.3 |
| PIAT | 2,609 | 65 | 21.8 | 18.3 |
| CADE27 | 367 | 2 | 2.9 | 0.6 |
| ABCO | 166 | 1 | 1.3 | 0.3 |
| ABMA | 150 | 3 | 1.2 | 0.8 |
| QUCH2 | 120 | 3 | 0.9 | 0.8 |
| treeNone | 0 | 249 | 0.0 | 69.9 |

Western White Pine Forest (n = 27)

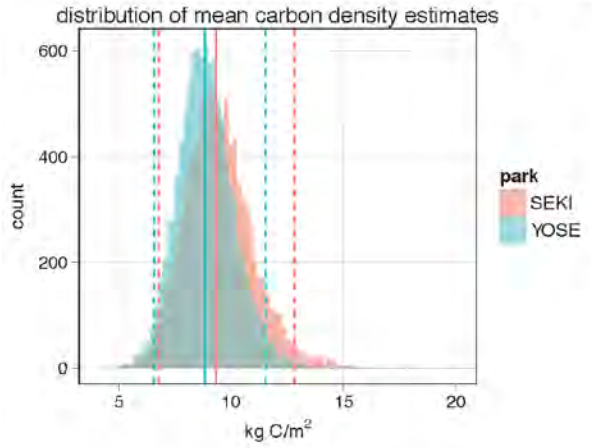


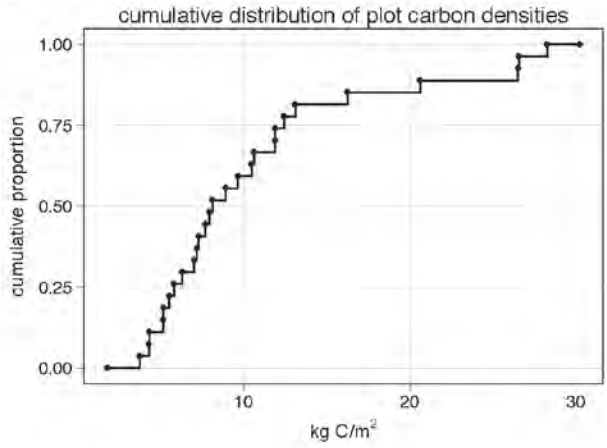


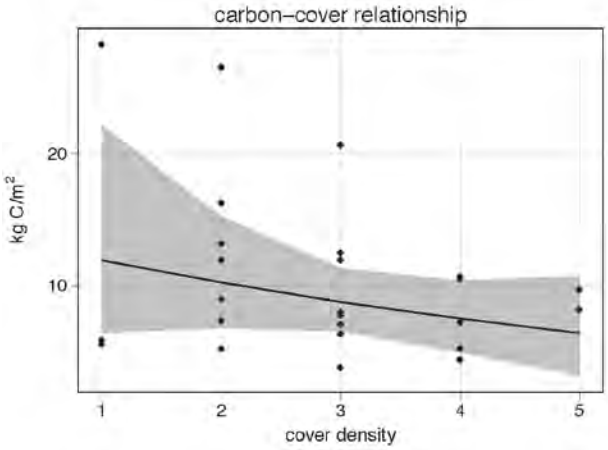


species composition

| code | carbon | nTrees | carbonPct | nTreesPct |
|---|---|---|---|---|
| PIMO3 | 129,158 | 138 | 53.9 | 43.6 |
| ABMA | 48,256 | 41 | 20.1 | 13.1 |
| TSME | 31,582 | 46 | 13.2 | 14.7 |
| treeDead | 16,572 | 14 | 6.9 | 4.5 |
| PICOM | 13,918 | 74 | 5.8 | 23.7 |
| PIJE | 181 | 1 | 0.1 | 0.3 |

Western White Pine Woodland (n = 4)

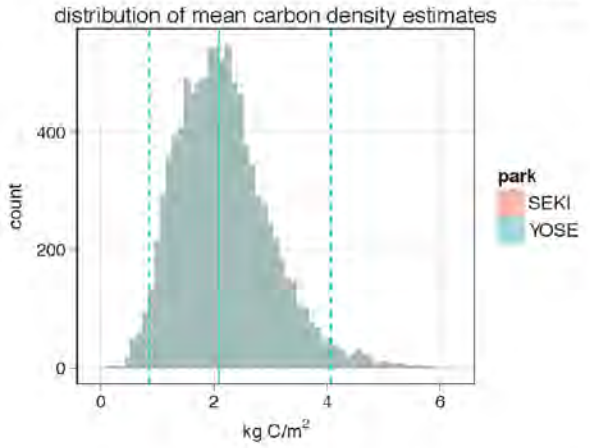


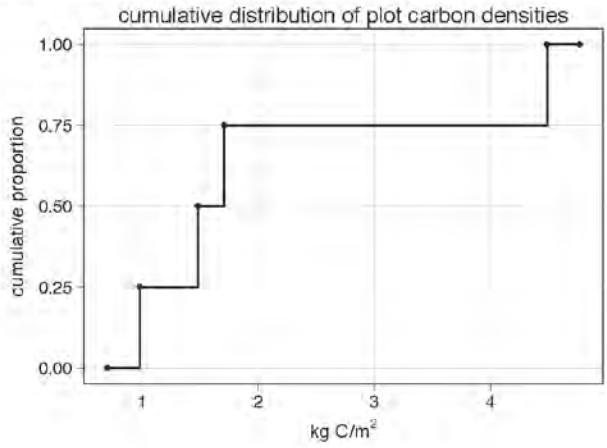


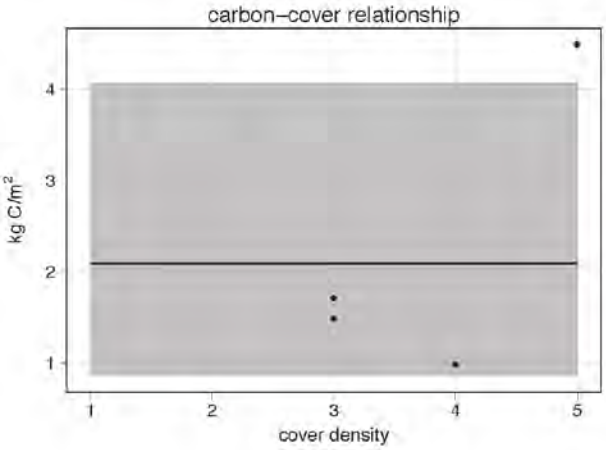


species composition

| code | carbon | nTrees | carbonPct | nTreesPct |
|---|---|---|---|---|
| PIMO3 | 6,392 | 53 | 64.3 | 80.3 |
| treeDead | 3,038 | 1 | 30.6 | 1.5 |
| PICOM | 358 | 8 | 3.6 | 12.1 |
| ABMA | 137 | 1 | 1.4 | 1.5 |
| ABMAS | 8 | 1 | 0.1 | 1.5 |
| PIAL | 3 | 2 | 0.0 | 3.0 |

White Fir – Sugar Pine Forest (n = 224)

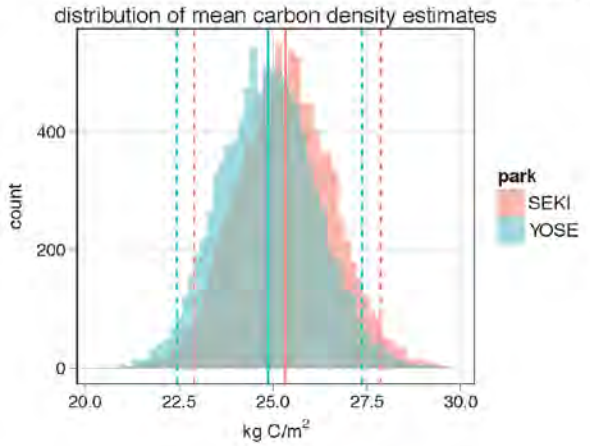


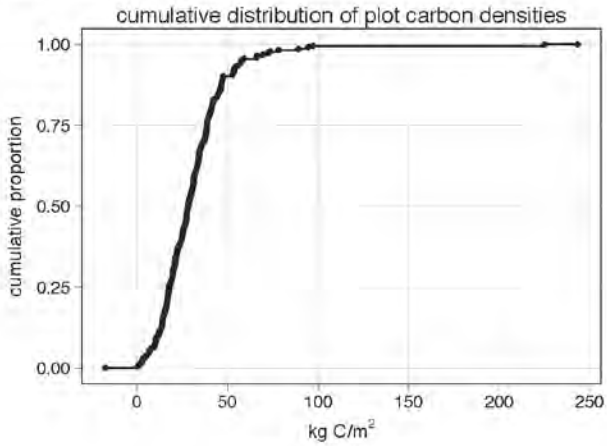


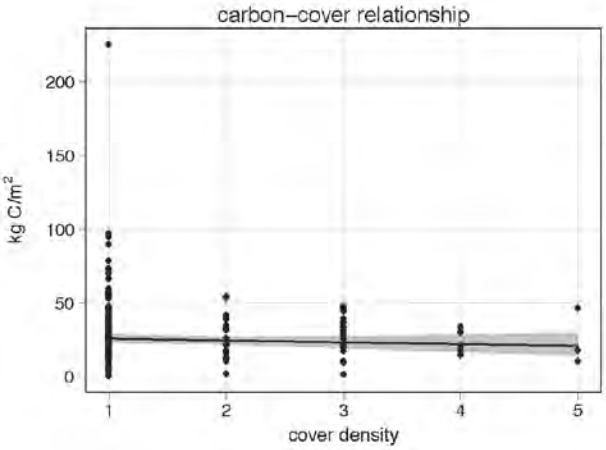


species composition

| code | carbon | nTrees | carbonPct | nTreesPct |
|---|---|---|---|---|
| ABCO | 3,331,974 | 8,376 | 50.6 | 56.6 |
| PILA | 1,631,938 | 1,069 | 24.8 | 7.2 |
| treeDead | 699,566 | 1,966 | 10.6 | 13.3 |
| CADE27 | 421,130 | 2,217 | 6.4 | 15 |
| PIPO | 195,055 | 219 | 3 | 1.5 |
| PIJE | 144,698 | 111 | 2.2 | 0.8 |
| QUKE | 59,170 | 282 | 0.9 | 1.9 |
| ABMA | 29,722 | 54 | 0.5 | 0.4 |
| SEGI2 | 29,959 | 24 | 0.5 | 0.2 |
| ABMAM | 8,504 | 16 | 0.1 | 0.1 |
| ABMAS | 6,402 | 81 | 0.1 | 0.5 |
| PICOM | 6,012 | 25 | 0.1 | 0.2 |
| POBAT | 5,757 | 6 | 0.1 | 0 |
| PSME | 5,342 | 13 | 0.1 | 0.1 |
| QUCH2 | 5,313 | 116 | 0.1 | 0.8 |
| ACMA3 | 959 | 25 | 0 | 0.2 |
| ALRH2 | 0 | 1 | 0 | 0 |
| COCOC | 0 | 3 | 0 | 0 |
| CONU4 | 1,226 | 130 | 0 | 0.9 |
| JUOC | 0 | 1 | 0 | 0 |

**The inside back cover should always occur on an odd-numbered page. This arrangement assures that there is no extra blank page at the end of printed copies of the document**

**Make sure to delete all explanatory text currently shown in orange font.**

The Department of the Interior protects and manages the nation's natural resources and cultural heritage; provides scientific and other information about those resources; and honors its special responsibilities to American Indians, Alaska Natives, and affiliated Island Communities.

NPS XXXXXX, Month Year

**National Park Service**
**U.S. Department of the Interior**

**Natural Resource Stewardship and Science**
1201 Oakridge Drive, Suite 150
Fort Collins, CO 80525

www.nature.nps.gov